75

MODELLING OF VOLTAGE COLLAPSE INCLUDING DYNAMIC PHENOMA

Task Force 38.02.10
of
Study Committee 38
(Power System Analysis and techniques)

Modelling of Voltage Collapse Including Dynamic Phenomena

prepared by
Task Force 38.02.10

edited by
Carson W. Taylor

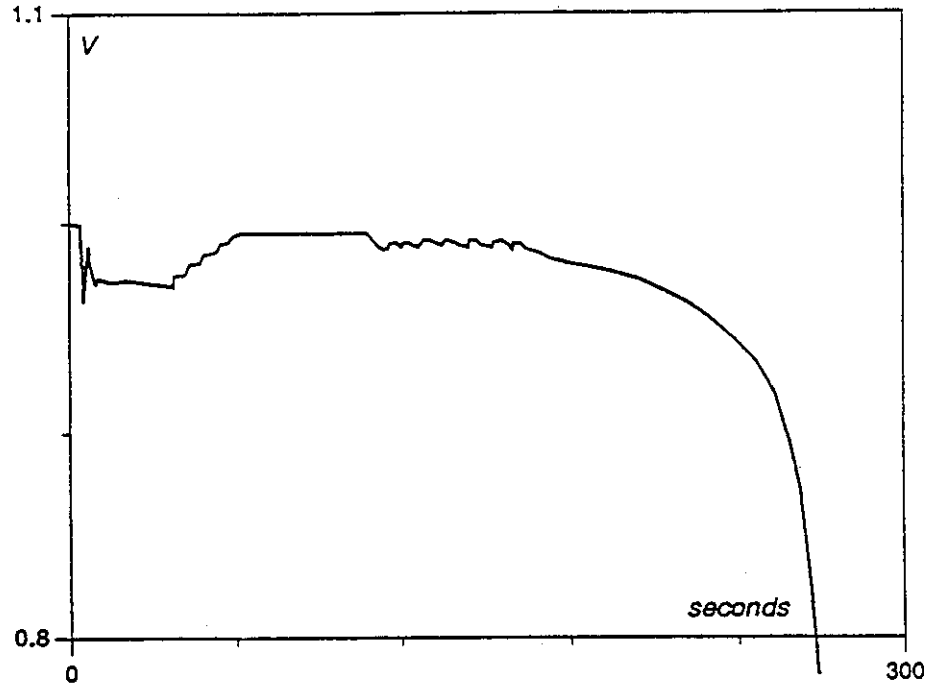

International Conference on Large High Voltage Electric Systems
Conférence Internationale des Grands Réseaux Electriques

cigré

CIGRÉ TF 38.02.10

Modelling of Voltage Collapse Including Dynamic Phenomena

Convenor: C. W. Taylor (USA)

List of members and contributors

F. Van de Meulebroeke (Belgium)*
S. Corsi (Italy)*
F. P. de Mello (USA)*
A. Hammad (Switzerland)*
K. R. Heggland (Norway)*
P. Hemon (Yugoslavia)*
R. Hirvonen (Finland)*
J. Y. Leost France)*
P. Kundur (Canada)*
P. O. Lindström (Sweden)*
R. W. McGee (United Kingdom)*
P. Modlitba (Czech Republic)*
T. K. Østrup (Denmark)*
C. Parker (Australia)*
F. Aboytes (Mexico)*
C. Vournas (Greece)*
H. Arakawa (Japan)**
M. Egàwa (Japan)*
R. B. Prada (Brazil)*
M. K. Hadingham (South Africa)*
D. Xia (China)*
N. W. Miller (USA)
W. W. Price (USA)
M. K. Pal (USA)
C. Concordia (USA)
W. Lachs (Australia)

*member, **past member

Modelling of Voltage Collapse Including Dynamic Phenomena

prepared by
Task Force 38.02.10

edited by
C. W. Taylor

presented at the request of
Chairman of Study Committee 38
J. Falck Christensen

Chairman of Working Group 38.02
N. Flatabø

Preface

This report is intended as an application guide for modelling in static and dynamic simulation studies of voltage collapse. It also provides an overview of voltage collapse and voltage instability phenomena.

Based on several incidents that have been experienced, the electric power industry has become increasingly concerned with voltage instability and collapse. There is a recognized need to expand the analysis of voltage collapse to include dynamic phenomena.

Dynamic analysis is clearly required for fast forms of voltage collapse. Fast or transient voltage collapse usually involves induction motor loads, and motor stalling (or reacceleration difficulty) following faults.

Longer-term voltage collapse has most frequently been studied via power flow simulation. Longer-term voltage collapse can be approximated by "snapshot" power flows at tens of seconds or minutes following a major outage. Dynamic simulation, however, is valuable in determining and demonstrating the time sequence of control and protection actions. Longer-term simulation can confirm results from less computational intensive static analysis.

Voltage collapse modelling involves generation, transmission, and distribution/load equipment of electric power systems. The analyst must have a good understanding of the equipment, and of modelling and simulation techniques. This report, hopefully, significantly contributes to the growing body of knowledge available on the subject of voltage collapse.

Modelling of Voltage Collapse Including Dynamic Phenomena

Table of Contents

Chapter 1

Introduction

1.1 The Voltage Collapse Problem

The electric power industry—world-wide—has become increasingly concerned with voltage instability and collapse. This concern is based on several incidents that have been experienced. As described in the next section, CIGRÉ has previously studied voltage collapse and the related problems of reactive power planning and management. The previous work has mainly involved steady-state analysis of voltage problems. There is a recognized need, however, to expand the analysis of voltage collapse to include dynamic phenomena. *This report, and a companion report,* will emphasize dynamic phenomena.* Voltage collapse is ultimately a dynamic phenomenon.

This report describes modelling and simulation techniques for voltage stability analysis.

Many voltage collapse incidents are described in a recent IEEE report [1]. These, and a few other incidents, are tabulated in Appendix VIII. For further information, you should refer to the IEEE report or the Appendix VIII references. See also Section 3.5.

Voltage collapse has most frequently been studied via power flow simulation (i.e., steady-state analysis). Longer-term voltage collapse can be approximated by "snapshot" power flows at tens of seconds or minutes following major outages. Dynamic analysis is clearly required for fast forms of voltage collapse. Fast or transient voltage collapse often involves induction motor loads, and motor stalling (or reacceleration difficulty) following faults. Conventional transient stability programs and models are satisfactory, but motors must be modeled as dynamic loads. The voltage dependence of static loads should be correctly modelled.

Longer-term dynamic simulation is valuable for determining and demonstrating the time sequence of control and protection actions. Tap changers in series, undervoltage load shedding, and shunt capacitor bank insertion hierarchy are difficult to simulate with power flow type programs. Longer-term simulation can confirm results from less computationally intensive static analysis.

Large-scale, longer-term simulation programs are available, or are becoming available. Transient stability program models are supplemented with models for equipment such as on-load tap changers, overexcitation limiters and overexcitation protection, thermostatically-controlled loads, automatic generation control, and energy supply systems. Modelling of these slower devices are

* TF 38-02-11, *Indices for Prediction of Voltage Collapse Including Dynamic Phenomena.*

described in this report. Representation of the composite effects of loads, including subtransmission and distribution systems, are critical to proper simulation of voltage collapse.

The longer-term simulation programs must be efficient so that run time is within computer resources. The programs should be able to efficiently simulate slow phenomena during quiescent periods, and fast phenomena during transient periods.

Static analysis can be effectively used to determine security margins and identify network limitations. Static analysis can also be used to examine a wide range of system conditions and contingencies. Static and dynamic analyses can complement each other.

1.2 Past and Current CIGRÉ Work

1.2.1 Joint CIGRÉ TF 14.07/IEEE WG 15.05.05, *Guide for Planning DC Links Terminating at AC Locations Having Low Short Circuit Capacities, Part I: AC/DC System Interaction Phenomena*, June 1992

This work classifies the strength of the ac/dc system and provides information about interactions between ac and dc systems, including voltage/power stability and effects of control schemes.

1.2.2 TF 38-01-02, *Static VAr Compensators*, 1986

This 125 page book provides comprehensive guidance for application of static var compensators. Included are chapters on modelling and on control to improve power system performance.

1.2.3 *Electra* report "Planning Against Voltage Collapse" (March 1987) and extensive version (October 1986)

The report provides basic explanation of voltage collapse and recommendations for steady-state analysis. Practical guidelines for planners are provided.

1.2.4 TF 38-01-03, *Reactive Power Compensation Analysis and Planning Procedures* (summary in March 1989 Electra)

This brochure provides description of system equipment as regards reactive power and recommends planning procedures.

1.2.5 TF 38-02-05, "Load Modelling and Dynamics," *Electra*, May 1990

The report summarizes approaches to load modelling for the various types of steady-state and dynamic simulation studies.

1.2.6 TF 38-02-03, "Improvements in Voltage Control" *Electra*, April 1991

The report discusses practices and trends in voltage control over various time frames and for the hierarchy of control actions.

1.2.7 TF 39-04-18 "Coordination of Protective Relays and Controls of Generating Sets under Abnormal Voltage Conditions on the Network" (Symposium on Electric Power System Reliability, Montréal, 16–18 September 1991).

The report describes problems in coordination of protection and control during disturbances. Several incidents are analyzed.

1.2.8 TF 38-05-04, Analysis and Optimization of SVC Use in Transmission Systems

The report includes steady-state voltage control and stability, and transient

stability improvement.

1.2.9 TF 38-05-05, AC System Aspects of AC/DC Interactions

The report (in preparation) will include HVDC capability charts, HVDC converter use for voltage control, limitations and comparisons with other sources for voltage control, models for system investigations, and transient phenomena in context of switching operations and faults.

1.2.10 TF 38-06-01, Expert Systems Applied to Voltage and VAr Control

An international survey of conventional and expert systems solutions to voltage and reactive power control has been completed, and a report has been approved. The Task Force is considering a comparison of classical methods with the expert system approach using a test system provided by WG 38-02.

1.2.11 TF 38-02-08, Long Term Dynamics

The second phase of this work involves simulation techniques similar to those used for the longer-term types of voltage stability.

1.2.12 TF 38-02-11, Indices of Prediction of Voltage Collapse, Including Dynamic Phenomena

TF 38-02-11 is providing a companion report on methods to predict proximity to voltage collapse.

1.3 Other Industry Work

This section briefly describes IEEE work and several major simulation programs. The necessary features of simulation programs are described in more detail in Chapter 7, and in the Task Force 38-02-08 report.

1.3.1 IEEE report, *Voltage Stability of Power Systems: Concepts, Analytical Tools, and Industry Experience*

This report was completed in 1990 [1]. It consists of three parts:

- Part 1: Definitions and Basic Concepts
- Part 2: Analytical Tools
- Part 3: Industry Experiences, Practices, and Needs.

The first part of the report provides information basic to an understanding of voltage stability phenomenon. Theoretical analysis of simple and generic systems is presented to gain insight into the problem and factors influencing it. The following formal definition of terms related to voltage stability are given:

- *Voltage Stability* is the ability of a system to maintain voltage so that when load admittance is increased, load power will increase, and so both power and voltage are controllable.
- *Voltage Collapse* is the process by which voltage instability leads to loss of voltage in a significant part of the system. (Voltage may be lost due to "angle instability" as well, and sometimes only a careful post-incident analysis can discover the primary cause.)
- *Voltage Security* is the ability of a system, not only to operate stably, but also to remain stable (as far as the maintenance of system voltage is concerned) following any reasonably credible contingency or adverse system change.

A system enters a state of *voltage instability* when a disturbance, increase

in load, or system change causes voltage to drop quickly or drift downward, and operators and automatic system controls fail to halt the decay. The voltage decay may take just a few seconds or ten to twenty minutes. If the decay continues unabated, steady-state angular instability or *voltage collapse* will occur.

The second part to the report explains the general mathematical formulation of the problem and describes four special algorithms published in the literature for analysis of voltage stability. The results of applying these algorithms to a thirty bus test system are presented.

In the third part, several selected voltage collapse incidents are reviewed in detail and possible lessons that can be learned are identified. In addition, criteria and special practices used by some utilities are described. Industry needs to effectively deal with voltage stability related problems are also identified; these include analytical tools, planning and operating guidelines, and protection schemes for prevention of voltage collapse.

1.3.2 IEEE report, "Static Var Compensator Models for Power Flow and Dynamic Performance Simulation"

This report, accepted for presentation at the 1993 IEEE/PES winter meeting, describes SVC models for power flow, transient stability, and longer-term dynamic computer programs.

1.3.3 EPRI VSTAB simulation program

The main objective is to develop software capable of performing voltage stability/security analysis of large power systems. The project, in which Ontario Hydro is the contractor, addressed the following four main tasks:

Task 1, Voltage Stability Analysis. Examination of current methods of voltage stability analysis, review industry requirements, and development of a production grade program for the assessment of voltage stability.

Task 2, Contingency Evaluation. Development of software for contingency analysis and ranking based on thermal overloads, voltage decline, and impact on voltage stability.

Task 3, Transient State Approximation. Examination of the concept of steady state approximations to the intermediate transient states of a system following a disturbance. Development of software to determine post-fault snapshots of the transient system trajectory associated with excitation system action, tap changer action, governor response, AGC, and economic dispatch.

Task 4, On-Line Security Assessment. Review industry requirements for on-line security assessment and development of software to meet those needs.

A production grade program has been developed which is designed as a platform for a variety of *static* voltage stability analysis techniques. The program includes *P–V* curve and *V–Q* curves, together with a fast power flow for contingency analysis and transient "snapshot" capabilities. Emphasis has been on identifying and implementing device models for voltage stability analysis. The models, suitable for use in power flow studies, include generator field current limiters, generator armature current limiters, induction machines, static var compensators, and voltage-dependent loads. Research efforts have lead to the

development of new voltage stability analysis techniques, including a modal analysis approach described in Chapter 8.

1.3.4 EPRI ETMSP simulation program

The Extended Transient/Midterm Stability Program (ETMSP), developed by Ontario Hydro, has been enhanced to meet the modelling requirements for dynamic analysis of voltage stability. These include representation of transformer LTC* action, generator field current limits, dynamic loads, constant energy loads, special relaying, and undervoltage load shedding.

1.3.5 EUROSTAG simulation program

The EUROSTAG program, jointly developed by TRACTEBEL and EdF covers the domains of transient, mid-term, and long-term stability by means of a continuously variable stepsize integration algorithm. It allows a complete simulation of voltage stability phenomena and includes models for transformer under load tap changing, dynamic loads, rotor current limiters, SVCs, protective relays, etc. EUROSTAG also has an interactive capability to compute the eigenvalues of the system for any operating point during the simulation.

1.3.6 PTI simulation program

The PSS/E, Power System Simulation Program, has new options for the study of longer term phenomena. Conversion of the entire PSS/E equipment model library to use implicit (trapezoidal) integration allows use of time steps in the order of 0.1 seconds with a speed advantage of 6 to 8 times over the usual stability simulation with 0.00833 or 0.01 second time step. At the small time step the extended term version yields essentially identical results to those of the standard PSS/E program using explicit integration. With the longer time step higher frequency effects are filtered out. The solution step can be switched back and forth from small to large at the user's discretion. The extended term version also has the facility to switch to the simulation mode where all units follow a common global frequency, with elimination of intermachine swing effects. New models include boiler dynamics, automatic generation control, tap changer, and load restoration effects. Dimensions are the same as PSS/E (12000 busses, 4000 machines, and over 100 equipment models).

1.3.7 General Electric/Tokyo Electric Power Company simulation program

The EXSTAB program, jointly developed by TEPCO and GE, allows for dynamic simulation over an extended range of time domain. The program includes detailed models of AGC with frequency and interchange control, power plants, dynamic and thermostatically controlled loads, LTCs, and many protective functions, as well as a full complement of transient stability models. Simulation modes allow for automatic continuously variable time-step integration, as well as a fast algebraic quasi-steady state mode for slowly varying system conditions. State matrices are available for eigenanalysis before and during time simulations.

---

* The terms LTC (Load Tap Changing), ULTC (Under-load Tap Changing), and OLTC (On-Load Tap Changing) are widely used. We use "LTC" since it is the term specified in *IEEE Standard Dictionary of Electrical and Electronic Terms*, ANSI/IEEE Std 100-1988.

Chapter 2

Definitions and Relation to Other Phenomena

2.1 Voltage Collapse and Voltage Stability

Although we will provide precise definitions, the terms *voltage collapse* and *voltage instability* are often used interchangeably. Other terms used are: *voltage security, voltage control* or controllability, *power stability* or controllability, *maximum power transfer capability, tap-changer stability, load stability, static bifurcation, dynamic bifurcation,* and *motor stability.* CIGRÉ and IEEE HVDC committees have debated the *power instability* versus *voltage instability* issue—an increase in direct current may reduce power (abnormal) and voltage (normal).

Chapter 1 quotes the IEEE Working Group definitions for voltage stability, voltage collapse, and voltage security. There is some dissatisfaction with the IEEE voltage stability definition. Voltage instability is for a load greater than the *maximum power transfer capability* of the network (i.e., for a simple system the magnitude of the load impedance is less than the magnitude of the source impedance). IEEE-defined voltage instability can be described as being on the underside of an equivalent P–V curve where increase in load causes reduction in load power. Power is no longer controllable by devices such as thermostats. (Voltage falls for an increase in load, just as on the upper side of a P–V curve.) For loads whose voltages are regulated, operation on the underside of a P–V curve implies tap changer (and voltage) instability. Tap changing regulators at limits or thermostatically-controlled loads fully on results in voltage sensitive loads that may be stable on the underside of a P–V curve.

With voltage-sensitive static loads, stable (but usually not acceptable) operation is possible with the IEEE-defined voltage instability. This stable operation could be considered partial voltage collapse. The partial voltage collapse in Western France on January 12, 1987 [1] demonstrates that a power system can operate stably for extended time at voltages as low as 0.5 per unit.

A power system is a dynamic system. The following section presents definitions that overcome objections to the IEEE definitions. The definitions are closely related to other definitions for stability of general linearized and nonlinear dynamic systems.

Voltage instability and collapse is almost always caused by large disturbances, including large load increases or buildup. Linearized analysis around an operating point is useful, however, in assessing the degree of stability.

2.2 Definitions

Power system voltage stability is a subset of overall power system stability. Voltage instability generally results in aperiodic decreasing (or increasing) voltages. Maladjusted control or protection induced oscillations (hunting) are excluded from the definitions.

Based on reference 3, and influenced by references 4– 6, we provide the following formal definitions. The voltage stability definitions follow established definitions for stability of dynamic systems.

2.2.1. Small-disturbance voltage stability definition

A power system at a given operating state is *small-disturbance voltage stable* if, following any small disturbance, voltages near loads are identical or close to the pre-disturbance values.

(Small-disturbance voltage stability corresponds to a related linearized dynamic model with eigenvalues having negative real parts. For analysis, discontinuous models for tap changers may have to be replaced with equivalent continuous models.)

2.2.2 Voltage stability definition

A power system at a given operating state and subject to a given disturbance is *voltage stable* if voltages near loads approach post-disturbance equilibrium values. The disturbed state is within the region of attraction of the stable post-disturbance equilibrium.

2.2.3 Voltage collapse definition

Following voltage instability, a power system undergoes *voltage collapse* if the post-disturbance equilibrium voltages near loads are below acceptable limits. Voltage collapse may be *total* (blackout) or *partial*.

2.2.4 Voltage instability

Voltage instability is the absence of voltage stability, and results in progressive voltage decrease (or increase). Destabilizing controls reaching limits, or other control actions (e.g., load disconnection), however, may establish global stability.

2.2.5 Additional terminology

In several editions of a popular textbook, voltage stability is called *load stability* [7].

Stable operation due to voltage sensitive loads on the underside of a *P–V* curve is partial voltage collapse with *power uncontrollability.*

The term *maximum power transfer capability* has been discussed in Section 2.1. The term *maximum loadability* has the same meaning.

We make an important distinction between load power at nominal (or pre-disturbance) voltage and frequency, and load power actually served or consumed. The terms *nominal load power* and *consumed load power* are used in this report.

There is a distinction between voltage stability or voltage collapse definitions, and corresponding indices or criteria for system operation or planning.

As described in Chapter 3, there are several forms of voltage instability and col-

lapse. Time frame terminology such as short term or long term have been used. Time frame terminologies adopted in Chapter 3 are *transient voltage stability*, and *longer-term voltage stability*.

The concepts and definitions are clarified by simulation examples provided in Chapter 8 and related appendices.

2.3 Relation to Rotor Angle Stability

While voltage collapse may be associated with the process of rotor angles going out-of-step, voltage collapse phenomena may also occur where rotor angle stability is not an issue.

The gradual pulling out-of-step of machines or groups of machines would result in a very low voltage at some intermediate points in the network. Voltages would oscillate from low back to normal through every slip cycle. This condition is normally detected in the first slip cycle and system separation is effected. The loss of small disturbance stability could be a gradual process, with the long term characteristics of load versus voltage as a contributing factor.

Systems with a large content of industrial loads can have a substantial induction motor load component. Voltage collapse and loss of synchronism can then be caused by the drastic change in motor load admittance as the motor slips increase due to voltage depression following a system contingency.

Another effect that can cause voltage collapse and/or loss of synchronism is the behavior of synchronous machines with excitation under manual control or under current limiting action. Although, following a disturbance, machine flux is transiently maintained by field and damper winding currents, a phenomenon which has been traditionally visualized as a machine exhibiting an internal reactance approaching transient reactance, the maintenance of flux by these induced rotor currents disappears within a few seconds with the machine behaving as a source behind a much higher equivalent reactance.

For decades power system planners have accepted synchronous machine performance integral with AVRs, hence the phenomenon of lack of synchronizing capability due to high synchronous reactance is usually academic. A more common concern is oscillatory instability caused by AVR control of excitation.

Field current limiters are provided to protect the rotor windings against overheating over relatively long periods of time, and to protect the thyristor bridges of static exciters which have short thermal time constants. Field current limiters may permit short periods of field forcing, for example during rapid power swings, but generator reactive power output is limited over the period of interest for voltage stability analysis. As the load area voltage decreases through the load increase brought about by tap-changer operation, generators may reach reactive power output limits. Once reactive power control is lost at the source, voltage collapse at the load may follow.

Voltage collapse can also occur where rotor angle stability is not involved, for instance in the case of a single plant or closely-knit generation system supplying a heavy load radially through a weak transmission system. Without adequate voltage support near the load areas, a point can be reached where the constant power versus voltage nature of the load, exhibited in the long term due to tap-changer operation, cannot be satisfied. The increased stress on such

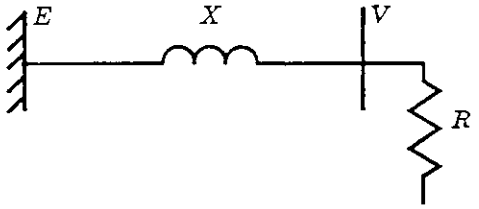

Fig. 2-1. Simple radial system.

a system could be as a result of a weakening of the transmission system through line outages or by gradually increased load. The result would be a gradual voltage decay as tap-changer operation unsuccessfully compensates for sagging transmission voltage. In this case there is no loss of synchronism between machines, but rather a condition of unsatisfactory load voltage. Total collapse on such heavily loaded systems may be forestalled due to tap-changers reaching the limit of their range. In some cases of heavy industrial load with large motor content, motor stalling could result.

This latter type of voltage collapse can be explained with the help of a simple analysis of the radial system of Figure 2-1.

The power delivered to the load with resistance R from a constant voltage source E through a transmission system with reactance X. (Shunt compensation or line capacitance can be included in the thévenin equivalent.) Increasing load reaches a maximum when $R = X$. Starting with a load resistance greater than X, increasing load brought about by decreasing R will cause decreasing voltage at the load and increasing power consumption up to the point $R = X$. Further decrease in R will continue to cause decreasing voltage but the power consumption will drop.

Another example of voltage instability where rotor angle stability is not necessarily involved is the case of an HVDC inverter terminal operating at fixed extinction angle and supplying constant power to a weak ac system [35,36]. Voltage instability can occur during the recovery of the dc power following a severe disturbance, or when attempting to increase the dc power beyond its critical level.

Chapter 3

Relevant Phenomena and Mechanisms

3.1 Time Domains for Voltage Collapse Phenomena

Voltage collapse dynamics span a range in time from a fraction of a second to tens of minutes. Time frame charts have been used to describe dynamic phenomena [8]. Figure 3-1 shows time responses for equipment which may be involved in voltage collapse [9]. Also shown are two time frames for voltage stability: transient and longer-term. There is almost always a clear separation between these time frames.

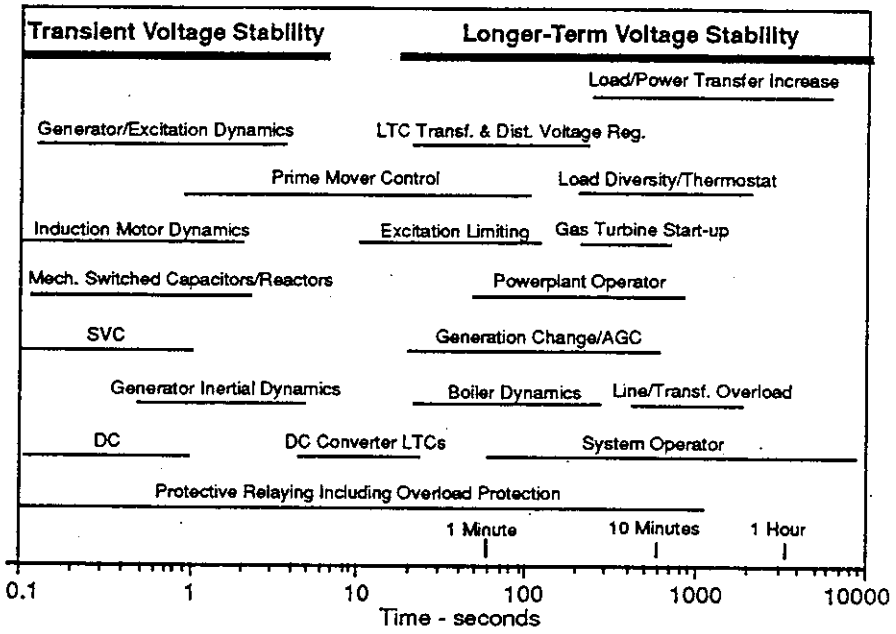

Fig. 3-1. Time frames for voltage stability phenomena.

The main characteristics of the two time domains are:

- Transient voltage collapse involves a large disturbance, and unfavorable loads having rapid response such as induction motors or HVDC converters (note both motors and converters may be heavily shunt capacitor compensated). Motor dynamics (reacceleration) following a fault is often the main concern. The time frame is one to several seconds.

- Longer-term voltage collapse involves a large disturbance and/or load increase or power transfer increase. Voltage collapse involves slow load restoration by tap changing or thermostats, and generator/synchronous condenser and static var compensator current limiting. Manual actions by system operators or consumers may also be important. The time frame is usually 0.5–30 minutes.

As slower forms of voltage collapse progress, faster phenomena will become important. There are many interactions among the various phenomena. For instance, maximum excitation limiters or overexcitation protection prevent automatic voltage regulation. As another example, on-load tap changer regulation of load-side voltage prevents loss of load diversity by thermostat controls.

3.2 Mechanism of Voltage Collapse

Voltage collapse is closely connected to lack of reactive power reserves in the network. Therefore the mechanisms of voltage collapse is clarified by describing the reactive power balance in the network when the voltage becomes low.

It's possible to look at the different network components separately because longer-term voltage collapse is a rather slow process where static equations can be used to approximate the state of the system at a given time.

3.2.1 Generators

It is common to show the performance of a generator using a capability chart also called a P–Q diagram. However, to show the important characteristics in case of voltage problems it is more convenient to use a Q–V diagram. Such diagrams can be constructed from a series of P–Q diagrams for different network voltages, V. The diagram is for the generator plus the step-up transformer. The Q–V diagram is valid for a single active power output P. This is also what is of interest for voltage collapse investigations where the active power is normally held constant while the reactive power and the voltage varies.

Figure 3-2 shows a typical Q–V diagram for a generator. Curves for constant terminal voltage U are shown. If the reference value for the terminal voltage U is given and the network voltage V is given, the reactive output from the generator can be found from the figure. (The sign of the reactive power in the diagram has been chosen according to the common convention for shunt elements.)

When the generator is clear of all limits, the curves for constant U are very flat, indicating that a large change in reactive power output is obtained for a small change in the network voltage. In this state the generator keeps a nearly constant voltage in the network, thus preventing voltage collapse.

However, if the network voltage becomes sufficiently low either the field current limit or the armature current limit of the generator is reached. This drastically changes the characteristics of the generator. The slope of the field current limiter curve is nearly vertical, meaning that voltage support from the generator is lost when this limit is reached.

Even worse conditions occur if the armature current limit is reached. In this case the reactive output from the generator decreases fast if the network voltage is further lowered which easily leads to unstable situations.

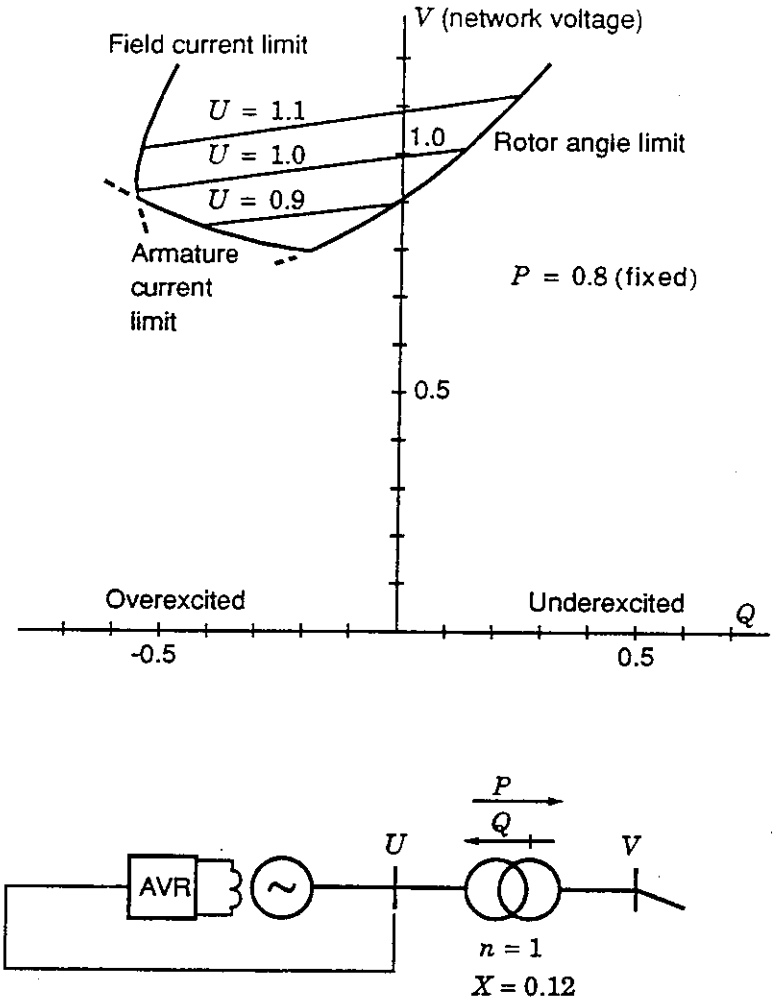

Fig. 3-2. Generator Q–V diagram for constant value of active power. In many cases the rotor angle limit, which is not of concern for voltage stability, may be less restrictive.

Therefore, voltage collapse will accelerate if generators begin to reach current limits. Further, there will be a tendency for the current limiting to spread among the generators. Lowering the active power output of critical generators has been suggested to avoid reaching one of the current limiters. However, as the reason for the development of a voltage collapse is normally too large an active power transfer into or through the area where these generators are located, lowering active power may further increase the problems. An exception is when power is reduced at generators serving heavily loaded lines and the power is increased at generators serving lightly loaded lines into the same load area.

Figure 3-3 shows similar information in the form of a capability polyhedron for a 1330 MVA generator.

3.2.2 Transmission lines

Figure 3-4 shows P–U curves for a single transmission line, where the voltage

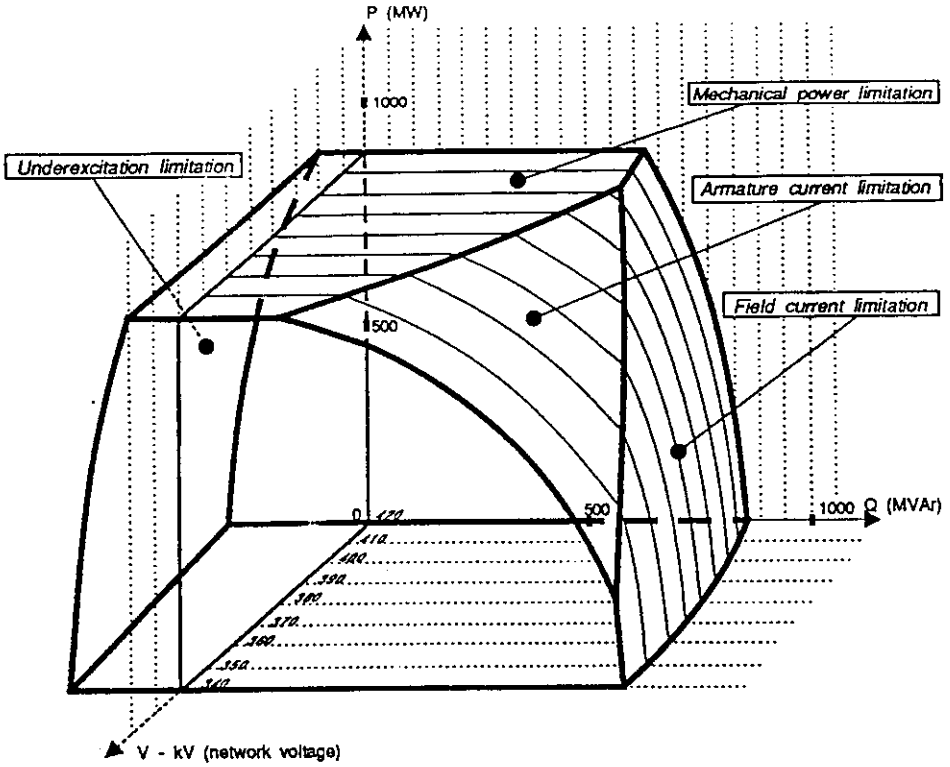

Fig. 3-3. Capability polyhedron of a 1330-MVA generator.

can be kept constant at the midpoint by changing the voltage at the sending end up to a certain limit. These P–U curves are composed by two different curves, with a sharp transition between them at the point where the fixed midpoint voltage can no longer be maintained. Besides reducing the maximum power transfer, the sudden disappearance of the voltage support reduces the margin between the point where a threatening voltage collapse becomes clear and the point where the final breakdown occurs. In this and subsequent figures, the power is normalized by the short circuit capacity, E^2/X.

When the voltage decreases, the transmission line reactive power consumption increases, and the reactive power production from line shunt capacitance decreases. The reactive power drawn from neighboring parts of the network will increase. However, the first two quantities are dependent on the square of the voltage, while the last one is proportional to the voltage. Therefore, if the voltage becomes sufficiently low in an area, the voltage will become unstable if only passive constant loads are present. This is illustrated on Figure 3-5 where U–Q curves are shown for a single line connecting a load to an infinite bus. The curves show the necessary reactive power input at the load bus in order to maintain a given voltage. The U–Q curves have a minimum and all operating points to the left of the minimum are unstable. The minimums can be located at rather high voltages if the network is stressed. (Since passive constant loads are non-physical loads, conclusions drawn from static analysis for loads with fast dynamics should be confirmed by dynamic analysis [5].)

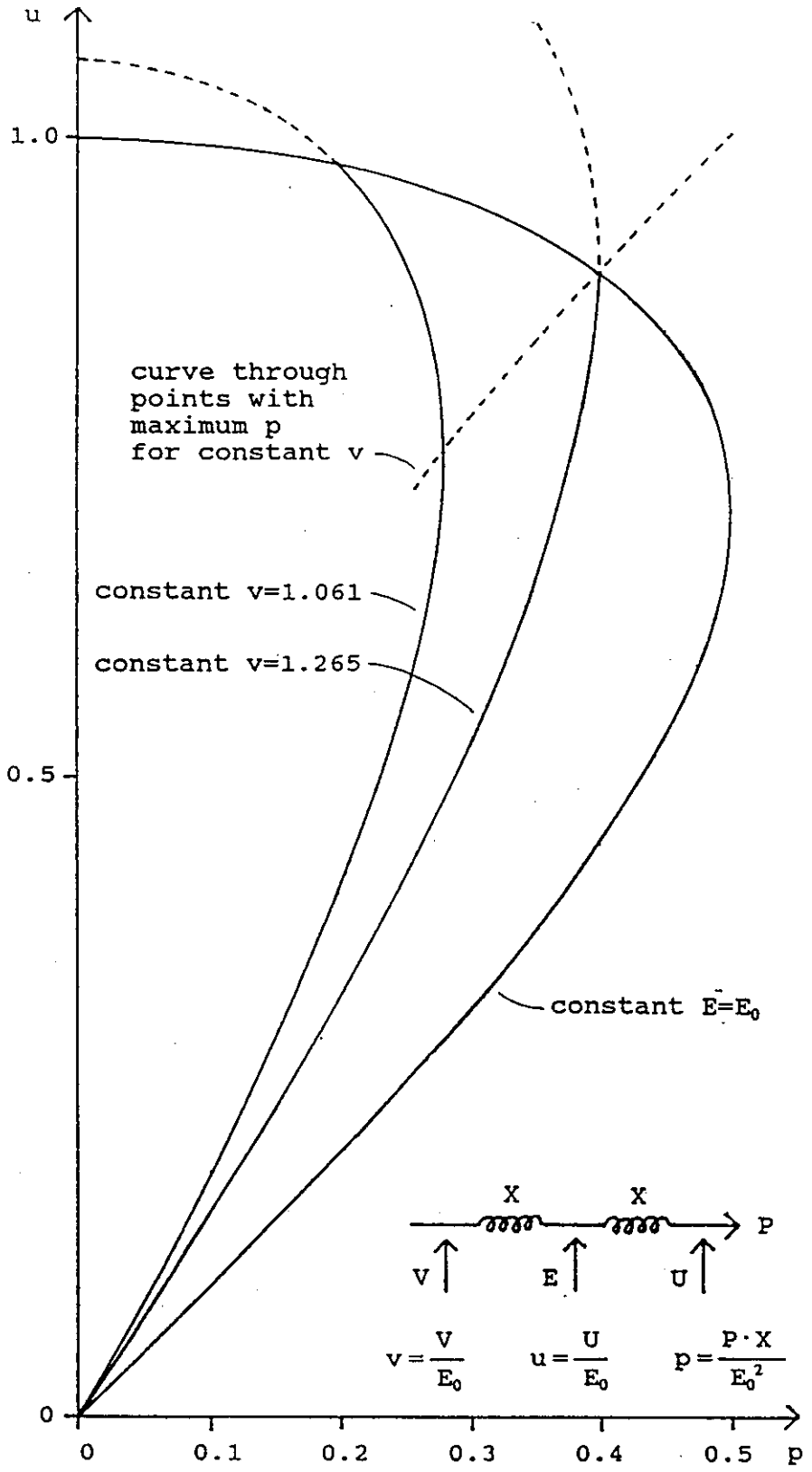

Fig. 3-4. *P–U* curves for a single transmission line where the midpoint voltage is kept constant by increasing V until the sending end voltage reaches a given upper limit.

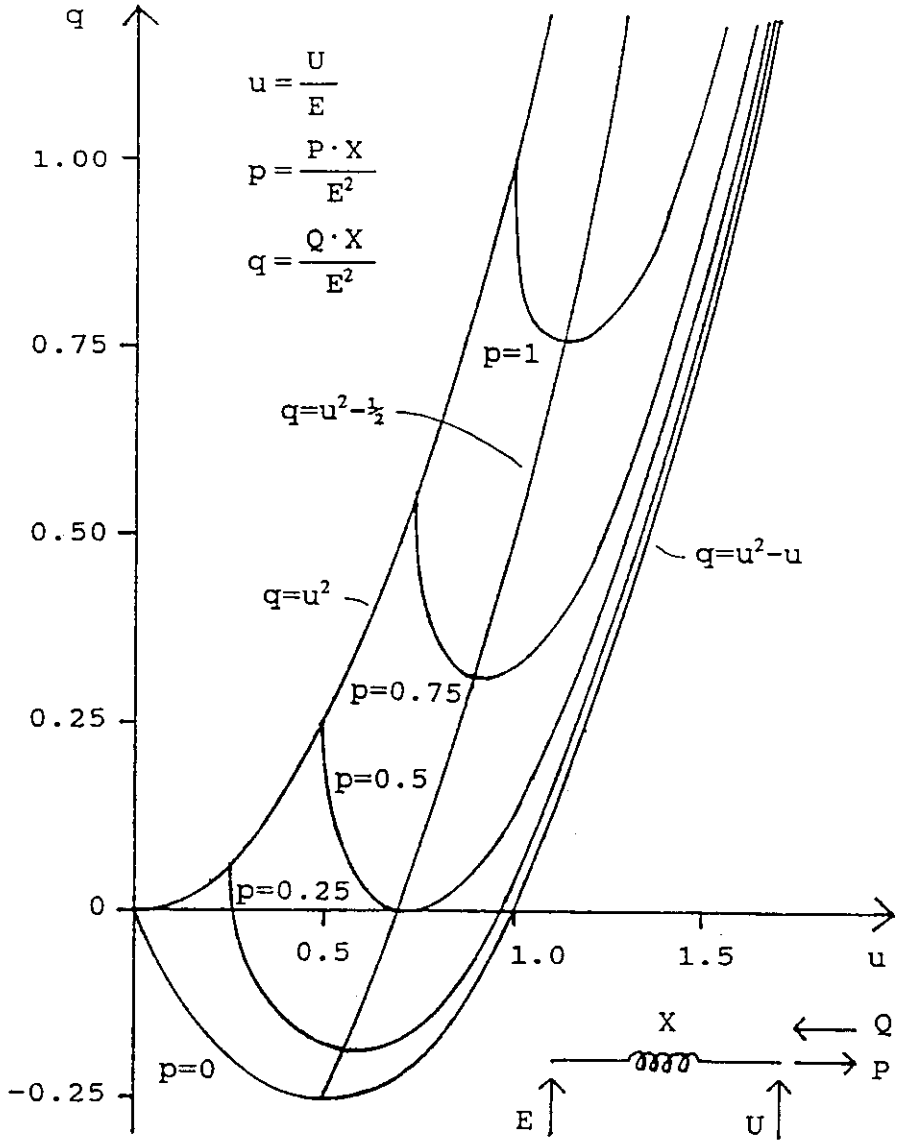

Fig. 3-5. Generalized *U–Q* curves for a single line connecting a load to an infinite bus.

Further discussion of this subject can be found in references 10 and 11.

3.2.3 Shunt components

The reactive power output of passive capacitors and reactors are proportional to the square of the voltage. For low voltages, it is the capacitors which are of interest, and unfortunately, the reactive power characteristic can increase the risk of a voltage collapse.

A static var compensators (SVC) acts as a controllable source of reactive power and will normally have a characteristic similar to that of a generator (Figure 3-2) in the active range of the SVC. This is shown on Figure 3-6. If the SVC reaches its limit, however, it acts as a passive shunt. In the capacitive range, the slope of the characteristic changes sign, which is bad for voltage stability.

3.2.4 Transformers

The impedance of transformers has the same influence on a voltage collapse as a line impedance, but a very important factor for the development of a voltage collapse is automatic tap changing.

Normally automatic tap changes are used to keep the voltage at the consumers constant. After an event causing low voltages, the taps are adjusted with certain time delays to restore the loads to the pre-fault level. When the voltage at the consumers gets low, the loads decrease, which makes the system less stressed, helping to counteract the voltage decrease. However, the changing of the taps in some minutes removes this stabilizing effect. The automatic tap changing can therefore lead to a rather slowly decreasing transmission voltage which is typical for a voltage collapse.

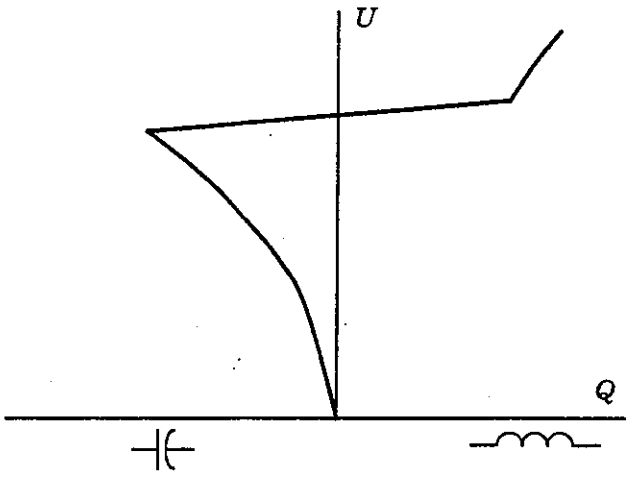

Fig. 3-6. Steady-state characteristic of static var compensator. Characteristic is for transmission side bus.

An example of the influence from the tap changers on the load is shown on Figure 3-7. The recording is from a Danish 10-kV substation where an automatic tap changer fails and moves to the upper limit at a speed of one step per minute. A load peak corresponding to the voltage peak created is clearly seen. (The sensitivity of the MW load to the slow voltage changes is in this case 1.8 per unit/per unit).

3.2.5 Relays

Once a voltage collapse is in progress the line currents will increase as the voltage drops. If line current becomes so large that a protective relay trips a line, parallel lines will be further overloaded. This will create a risk of cascading of line tripping which will accelerate the voltage collapse.

3.2.6 Loads

The voltage dependency of the loads will normally help to stabilize the situation after an event leading to low voltages. However, as already mentioned, automatic tap changers can eliminate this effect.

Thyristor controlled loads tend to act as constant loads and will therefore not

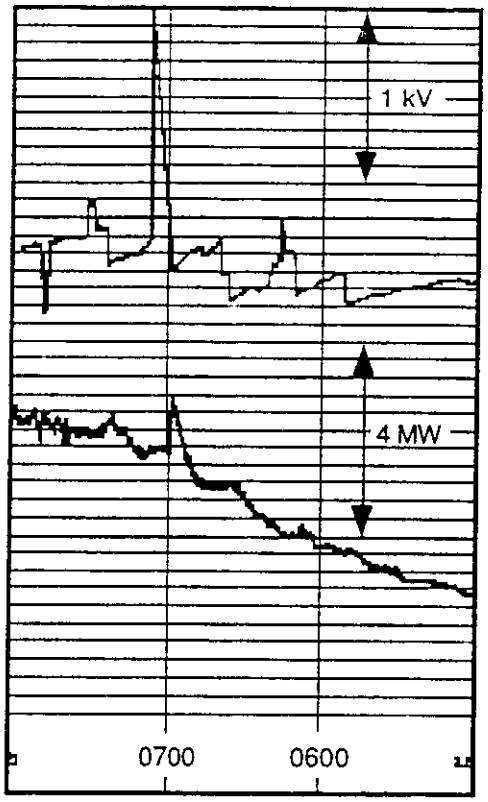

Fig. 3-7. Recording from a Danish 10-kV substation. Peak in MW load created by peak in voltage due to failure of automatic tap changer. (There is a displacement between the pens.)

contribute to the stabilizing effect at the beginning of the development of a voltage collapse. Such loads therefore tend to make the collapse faster.

Asynchronous motors can also give a special problem. A voltage collapse is often preceded by a network fault. During this fault the motors are decelerated and after the fault the simultaneous acceleration of all motors will increase the reactive load significantly. Besides leading to low voltages, this may even make it impossible to reaccelerate the motors. As a side-effect, if the motors are the auxiliaries of a thermal power plant, the unit may be lost, which will further stress the system. The common use of shunt capacitor compensation for the motor reactive power demand tends to make the power system "brittle" as regards voltage stability (capacitor reactive power output decreases as voltage squared).

3.2.7 HVDC links

HVDC links using mercury or thyristor valves for ac/dc conversion may present unfavorable characteristics for transient voltage stability. HVDC converters normally consume reactive power equal to 50–60% of the active power transmitted. The reactive power is often largely supplied locally by harmonic filters (capacitive at fundamental frequency) and by shunt capacitor banks. As with motor loads, the shunt compensation tends to make the system brittle (or weak) at the ac/dc interconnection, i.e., the effective ac system impedance seen

by the dc terminal is higher and the ratio of ac short circuit capacity to dc power is lower.

The type of HVDC converter control can substantially affect the dynamic performance by modifying the reactive power absorbed by the converter. In many HVDC schemes, inverters are controlled with constant extinction angle. This gives minimum cost, but with a weak ac system the resulting ac voltage fluctuations due to changes of the dc power are particularly large. With this control mode, a drop in the ac system voltage, e.g., caused by an increase in the dc power, leads to increased reactive power demand of the inverter, which results in further sagging of voltage.

Modern controls with constant dc voltage, constant reactive power/current, or constant ac voltage are used for inverters located in load areas where voltage stability may be a concern. Controls to reduce dc power/current during low voltage are also used to reduce converter reactive power demand. Reduction of dc power, however, could be detrimental from a rotor angle stability viewpoint.

3.3 Dynamic Behavior

Besides natural load changes there are two components with relatively slow dynamics which are decisive in the development of a voltage collapse. These are the generator current limiters and the automatic tap changing.

3.3.1 Generator current limiters

The generators always have some overload capabilities because their limits are set by the thermal conditions. It is therefore the combination of the size of the overload and its duration which determine when a limiter should be activated. Several different types of rotor and armature current limiters exist and are described in Chapter 6.

In case of a slowly developing voltage collapse, the generator currents are pushed slowly upwards. This means that some time can elapse between the initial event and the moment where the steady-state limit is exceeded. Therefore, the first overloads occurring can be small, which means that there will be an additional time delay of up to a couple of minutes before the first limiters react. However, when this happens the overload problems are rapidly accumulated on the generators where the limiters have not yet reacted, and in a short time the limiters on all generators in the critical area can be active. This phenomenon can give a critical acceleration of a voltage collapse, but there will be a time delay between the start of the voltage collapse and this phenomenon.

Field current limiting greatly increases the potential for armature current overload and limiting. As evident from Figure 3-2, voltage collapse becomes likely.

3.3.2 Automatic transformer tap changers

As the connection between the dynamics of automatic transformer tap changers and the voltage collapse can be difficult to realize, a simple example will be shown in detail with the simple network of Figure 3.8. In this very small network, the transformer is equipped with automatic tap changing trying to maintain the voltage at the load.

In the initial state the transfer impedance is X and the transformer ratio $n = 1$. The transfer impedance is then suddenly changed from X to $2X$. After this, the

transformer ratio is changed gradually until the voltage at the load and thereby the power, P, have reached their original values.

Figure 3-8 also shows the U–Q diagram for the system. Curves are shown for the need of reactive power input at the network side of the transformer for fixed P and for fixed n (resistive load), both before and after the doubling of the transfer impedance. (Fixed n corresponds to a fixed load resistance seen from the network side of the transformer). The numerical values have been chosen to give neat and illustrative curves.

If the capacitor is fixed, the system will stay at the curve for this capacitor in the U–Q diagram.

The initial point A is determined by the curve for the capacitor and the curve for the shown load impedance.With the chosen parameters, the voltage U on the network side of the transformer is 1 per unit and the power P to the load is 0.25 per unit.

When the transfer impedance is doubled, the system jumps to point B with P = 0.22 per unit. and U = 0.94 per unit. B is determined by the curve for the capacitor and the curve for the load impedance with the new transfer impedance.

As the power and therefore the voltage at the load is less than initial values, the automatic tap changer will gradually increase n. When this is done, the voltage at the load will increase, but at the same time the voltage U at the network side of the transformer will decrease. According to the tap changes, the system will move along the capacitor curve towards lower voltages. When n has been increased to 1.1, the point C is reached. At C, U has fallen to 0.9 per unit and P has grown to 0.24 per unit. Load power and thereby load voltage is still less than their initial values, and tap changes continue.

At point D, U has fallen to 0.85 per unit. and P has grown to its initial value 0.25 per unit, which means that the load voltage is also back to the initial value of 1 per unit. No further tap changes will then take place and the system will stay in D where n = 1.2.

An event like this can end in three ways. Firstly, a new stable point can be reached as in the previous example.

Secondly, the tap changer can reach its limit. No further changes will then take place, but the load voltage will not reach its initial value.

Thirdly, the voltage can collapse. This happens if no stable point is reached.

The figure also shows an event where the fixed capacitor has been replaced by a Static Var Compensator (SVC) giving the same initial point A as before. The gain of the SVC is 0.16 per unit/per unit, which is fairly small.

The event develops like the former, only now the system will follow the SVC curve. When the transfer impedance is changed, the system will jump to F. Then, according to tap changes, the system will move to G, where it will settle because the load power and the load voltage have reached their initial values. With the SVC, n is only increased to 1.1 and U only falls to 0.93 per unit. (The two stationary points G and D are both located on the curve with P = 0.25 per unit after the network change).

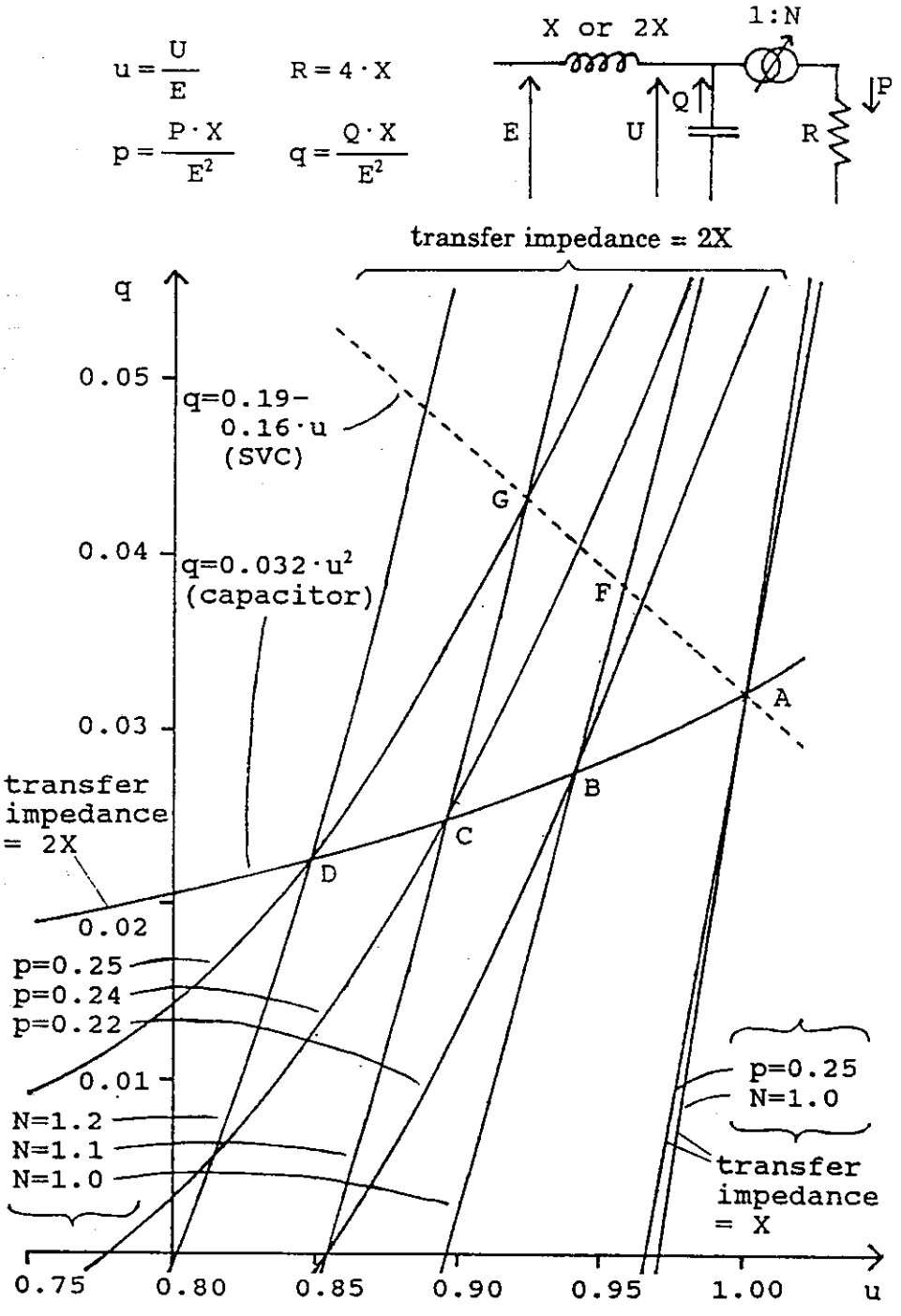

Fig. 3-8. *U–Q* curves for constant R or constant P, and a transfer reactance of X or $2X$.

If the limit is reached for the regulation of an SVC, the U–Q curve for it continues as a normal capacitor curve for lower voltages.

The speed with which a voltage collapse develops can depend strongly on the type of automatic tap changing being used. If a constant time delay of typically one minute is used between each step, the voltage collapse may be rather slow leaving several minutes for the activation of countermeasures. On the other hand, if inverse time tap controlling is used, meaning that the time delay between each step becomes very small if the difference between the desired and the actual voltage is large, then a voltage collapse can develop in less than a minute.

3.4 Critical Events or Disturbances

Even small events can initiate a voltage collapse. Normally, but not always as will be shown in Section 3.5, a voltage collapse involves systems with heavily loaded lines. When transport of reactive power from neighboring areas is very difficult, every event which calls for reactive power support can initiate a voltage collapse. A natural load increase or the loss of a single unit might be the event which triggers the different mechanisms mentioned in Section 3.2 leading to a voltage collapse. Sometimes the situation does not even look serious just after the initiating event.

3.5 Examples of Voltage Collapse

In this section the development of some real voltage collapses are illustrated. The incidents were selected to illustrate certain phenomena. In most cases, the incidents have not been widely reported. Many other incidents are described in Appendix VIII. The incidents are:

1. Incident in South Zealand, Denmark, 2 March 1979
2. Incident in the southern part of the Nordel system, 27 December 1983. (The interconnected Nordel system consists of Finland, Sweden, Norway and East Denmark.)
3. Incident in Czechoslovakia, 5 July 1985.
4. Incident in England, 20 May 1986.

The third incident is a transient voltage collapse. The other incidents are longer-term voltage collapses.

3.5.1 Incident in South Zealand, Denmark, 2 March 1979

Figure 3-9 shows the 132-kV and the 400-kV (only a single line) network of Zealand in 1979. On 2 March 1979, only one unit of 270 MW was in operation on the southern part of the island. The initiating event was the tripping of this unit at 9:42 a.m. No reactive reserves were present in the area and the voltage continued to fall slowly due to the automatic tap changing on the low voltage transformers. After fifteen minutes the voltage fell below 0.75 per unit making the start and synchronization of a 70 MW gas turbine in the area impossible. It was then decided to shed load manually in the most southern part of the network. This restored the voltage and six minutes later the gas turbine were synchronized. After another six minutes all loads were picked up again.

The voltage at the power station with the gas turbine located in the critical area is shown on Figure 3-10. The initial voltage drop is 0.10 per unit. During the next fifteen minutes the voltage falls further 0.11 per unit and then the

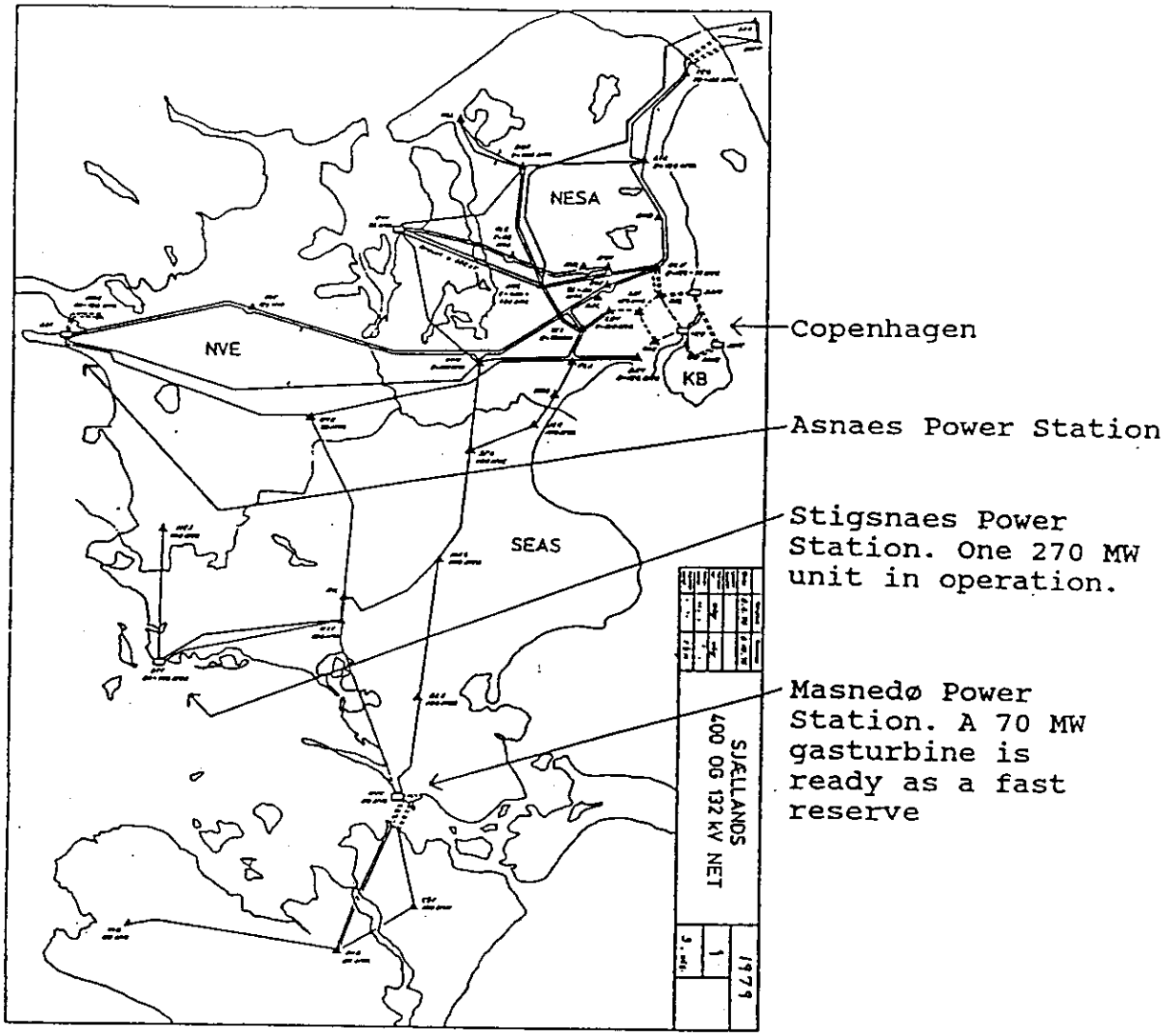

Fig. 3-9. Zealand, Denmark 400-kV (only a single line to Sweden) and 132-kV network in 1979.

voltage is restored by the manual load shedding. However, the voltage continues to be low in the area for a very long time.

Figure 3-11 shows measurements from a 125 MW unit located 100 km away from the former power station. Here the total voltage drop is only a few percent and does not indicate a severe problem. However, even the relatively small voltage drop activates a large amount of reactive power reserves on this as well as other units due to the automatic voltage regulators. This had only small influence on the voltage problems. To effectively counteract a voltage collapse reactive power reserves must be activated in the critical area where the lowest voltages occur.

The network was not heavily loaded at the time of the incident. Even after the

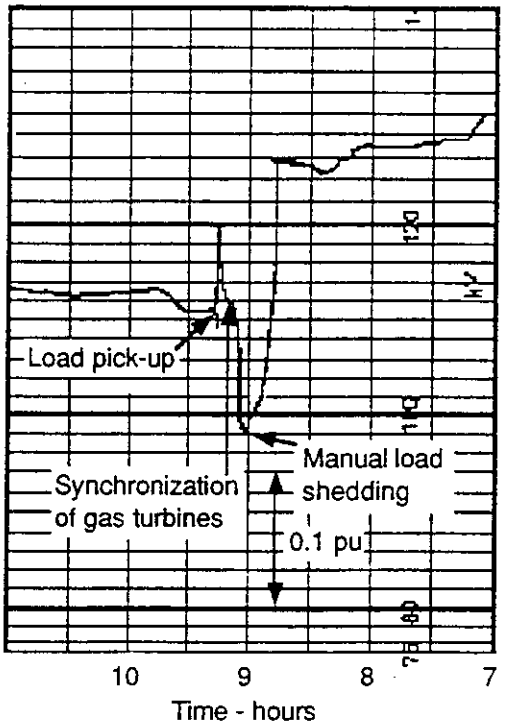

Fig. 3-10. 132-kV voltage at Masnedø power station, March 2, 1979.

initial event the active power flow into the critical area was only 20% of the short circuit duty of the feeding network.

Attempts were made afterwards to see if it was possible to predict the low voltages by simulations. Table 3-1 shows some results from these static investigations. In the power flows, the generator terminal voltages and busbar loads are maintained at the values that applied before the initial event. Compensation of voltage regulation is represented. Generally, it is assumed that all automatic changes have finished and the voltages at the consumers are restored to normal values. On the other hand, no manual interference has been made. This type of load flow is called a final load flow in contrast to the initial load flow prior to the event. From Table 3-1, it appears that the calculated voltage drops in the critical area are too small (and in reality the voltages had even not quite stopped to decrease). This indicates, that the behavior of a real network in a stressed situation with a voltage collapse in progress is very complicated, and it is doubtful whether it would have been possible to predict the development of the described event.

3.5.2 Incident in the southern part of the Nordel system, 27 December 1983

The southern part of the Nordel grid is shown on Figure 3-12 with indication of line trippings which occurred at this event.

The initial event was a busbar fault near Stockholm in Sweden. Due to unfavorable circumstances, four 400-kV lines were lost leading to a voltage drop in the Stockholm area and at the receiving ends of the remaining 400-kV lines transporting the power from the north to the large load centers.

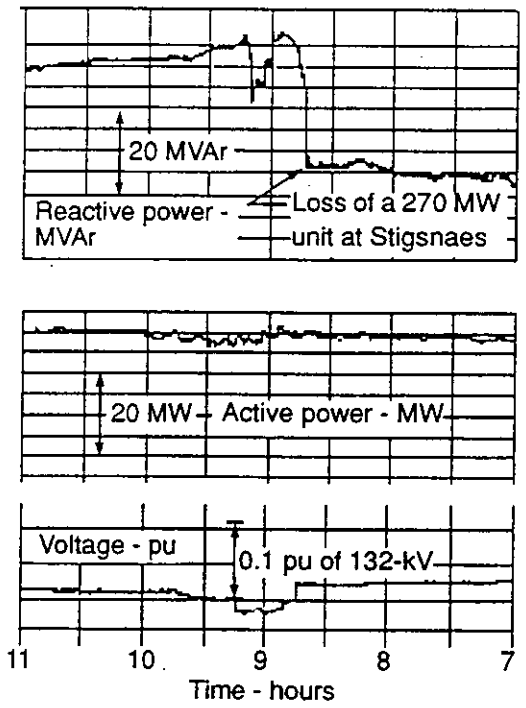

Fig. 3-11. Recording from Asnaes Power Station Unit 2 (125 MW), March 2, 1979.

Table 3-1

Voltage drops from before the loss of a 270 MW unit to fifteen minutes later in the 132-kV system in Zealand, Denmark on 2 March 1979.

Place	Measured	Computed
Amager Power Station (Copenhagen)	4.0 kV	2.1 kV
Asnaes Power Station (see Fig. 3.9)	4.5 kV	2.8 kV
Stigsnaes Power Station (see Fig. 3.9)	>25.0 kV	27.7 kV
Masnedø Power Station (see Fig. 3.9)	26.6 kV	19.8 kV
Glentegård Substation (Copenhagen)	3.5 kV	2.2 kV
Haslev Substation (Mid Zealand)	20.0 kV	15.4 kV
Teglstrupgård Substation (North Zealand)	1.8 kV	1.4 kV

As described in the text, the voltages fifteen minutes after the loss of the unit are calculated by use of final power flows.

The restoration of the consumers voltage by the automatic tap changers gave a further decrease of the voltage in the transmission system and an increase in the active power transfer from the north towards the prefault values. After

fifty-three seconds the current on the lines to the north became so large that a cascade tripping of five 400-kV lines and seven 220-kV lines occurred. One second later the interconnection between South Norway and Sweden was tripped and the southern part of the Nordel system was left isolated with an active power deficit of 50–60%. However, before the frequency had fallen more than 1 Hz the tie lines between East Denmark and Sweden were tripped by the distance relays. At the same time the last tieline from South Sweden, an HVDC link to West Denmark, was tripped. The voltage in South Sweden collapsed, while the voltage in East Denmark was restored. However, due to problems created by the event on four thermal units which were lost some minutes later, about 30% load shedding took place in East Denmark, partly automatically and partly manually.

It should be noted that in cases like this, tripping of tie lines can expose an area for a rapid change from very low voltages due to a voltage collapse to very high voltages following a load shedding in an isolated network.

Figure 3-12 also shows the voltage measured in East Denmark. The first fifty-three seconds of the voltage collapse in progress in the Stockholm area is invisible. After the splitting of the Swedish network the voltage collapses in a few seconds. This shows how difficult it can be to detect a voltage collapse in progress and thereby also to counteract it from places at some distance from the area where the initial problems develop.

The incident shows two different mechanisms of voltage collapse. The first is the slow voltage decrease created mainly by the automatic tap changers. The second is a very fast collapse due to the isolation of a part of the system with about 40% lack of active power and insufficient reactive power reserves. The heavy overload of the power stations created by the negative frequency gradient is an important factor in the resulting reactive power deficit. This second mechanism affects a large area. A large area can also be affected by loss of synchronism due to a combination of the low voltage and large active power loads on the generators.

References 1 and 10 provide additional description of this incident.

3.5.3 Incident in Czechoslovakia, 5 July 1985

The following description of the incident is from reference 14 and is an example of fast voltage collapse combined with loss of synchronism.

Voltage collapse is usually caused by the bulk power transfer from the other parts of the system following the outages of large sources or strong transmission lines. Such a case happened in a real power system, the simplified scheme of which is shown in Figure 3-13.

In the steady operational state, System 2 delivers a large amount of power to the weak System 3. The strong System 1 is approximately balanced. If the large power delivery through Link 1 is disrupted for some reason, then System 1 overtakes the role of System 2. The overloading of Link 2 with its subsequent disconnection by protection relays appeared in some cases. Time delay of the disconnection was about one second after the disruption of the power delivery from System 2. Then the long Link 3 with a large number of intermediate consumption nodes remained in operation between System 1 and the weak System

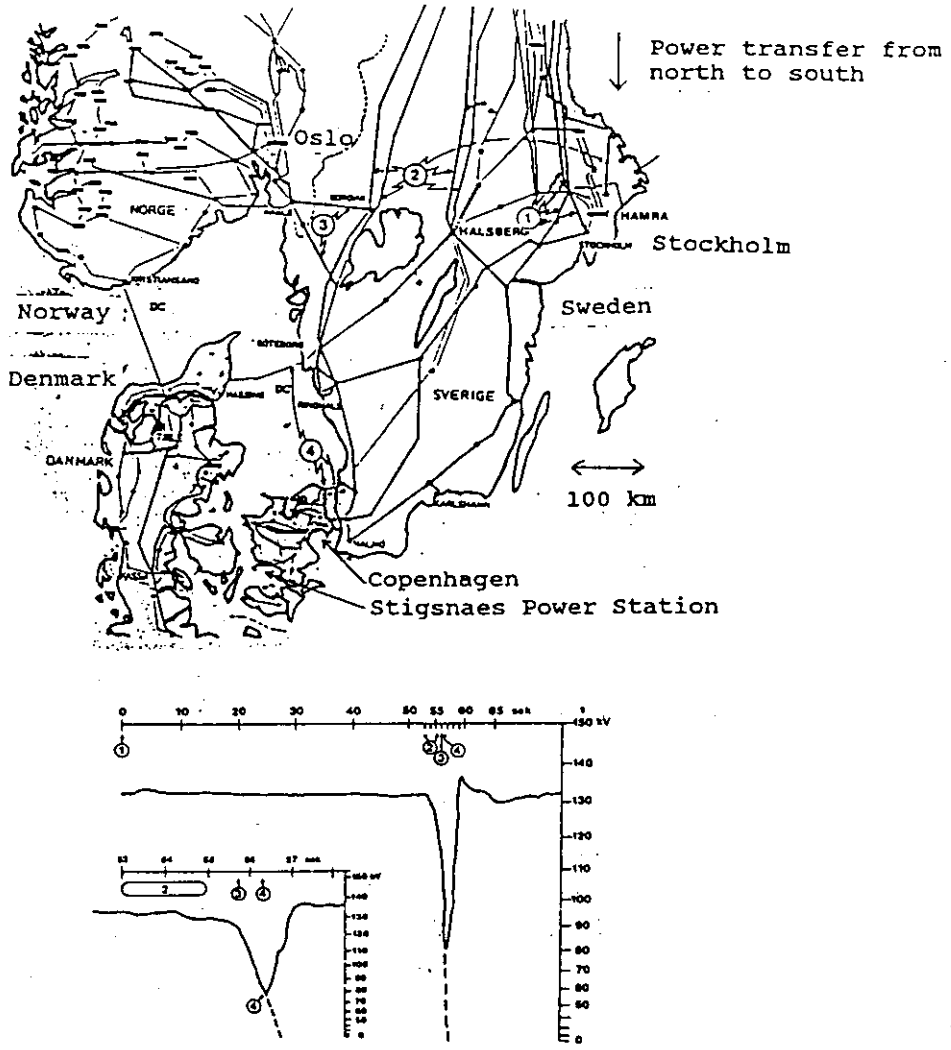

① Busbar fault at Hamra near Stockholm trips four 400-kV lines, two of which are northward.

② Five 400-kV, seven 220-kV, and all 132-kV lines at 61° northern latitude trip.

③ Two 400-kV lines between Southern Norway and Sweden trip.

④ One 400-kV and two 132-kV lines between Zealand and Sweden are tripped. About this time the Konti-Skan HVDC line trip.

Fig. 3-12. The event of December 27, 1983 at 1258 hours in the southern Nordel system. Network and measured 132-kV voltage at Stigsnaes Power Station in Zealand, Denmark.

3. Such an emergency operational state led to the voltage collapse during about two seconds and to disconnection of the last two sections of Link 3 adjacent to the node A. Behavior of voltages and currents at nodes during the disturbance was either measured or mathematically reconstructed.

tation of a group of eigenvalues and eigenvectors of the reduced system steady state Jacobian matrix. The system is considered voltage stable if all the eigenvalues of the reduced Jacobian matrix are positive, and voltage unstable if at least one eigenvalue is negative. The magnitude of each positive eigenvalue determines the weakness of the corresponding modal voltage. The smaller the magnitude of the eigenvalue, the closer the corresponding modal voltage is to being voltage unstable. If the eigenvalue is zero the system is on the verge of voltage instability.

In Appendix I, modal analysis was conducted at different time frames following the contingency. Results of modal analysis at different snapshots are shown in Table I-6. From the modal analysis results, it is concluded that the system is voltage stable before the disturbance and after the disturbance before the field currents are limited. Voltage instability occurs once the field current for machine 3 is limited. Using the time domain simulation results as benchmark, modal analysis determines correctly when system voltage instability occurs.

For the slower dynamics studied, comparison of modal analysis with time domain simulations indicates that the results obtained using the two methods generally agree. Each approach offers certain advantages depending on the task at hand. Tools based on the static approach, such as modal analysis, are very useful for assessing system voltage stability for a wide range of system conditions or contingencies. Modal analysis, coupled with other static techniques, can provide good indication of proximity to, and mechanism of, voltage instability, with much lower computational burden than dynamic simulation. Static approaches are therefore ideally suited for the bulk of planning work. However, for detailed investigation of particular incidents, postmortem analysis, or for coordination of controls and protective systems, time domain simulation is generally the tool of choice. Although time domain simulations do not provide direct measures of stability, they can show clearly the sequence of events which may lead to voltage instability.

8.3 Concluding Remarks

Appropriate device modelling is necessary for accurate assessment of system voltage stability. Certain key devices may have significant impacts on system voltage stability, and their effect must be considered in performing system voltage stability studies. These include:

- Loads (static loads, induction motors, constant energy loads, undervoltage load shedding).
- LTCs.
- Generator field current (overexcitation) and armature current limiters.
- AVR (primary and secondary voltage regulation including line drop compensation).
- HVDC control characteristics.

Conventional simulation tools for transient angle stability studies may not adequately model all these devices to properly capture their actions and interactions. Also simulation tools must be capable of simulating system behavior over time periods of sufficient length to consider the effect of these devices on

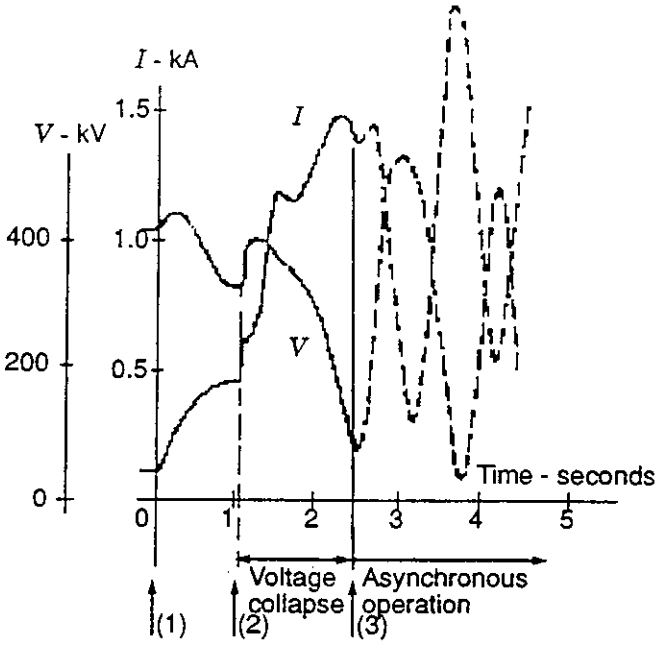

Fig. 3-14. Voltage at node A and current flow from Link 3 to node A during disturbance: (1) disturbance occurrence, (2) Link 2 disconnection, (3) minimum voltage.

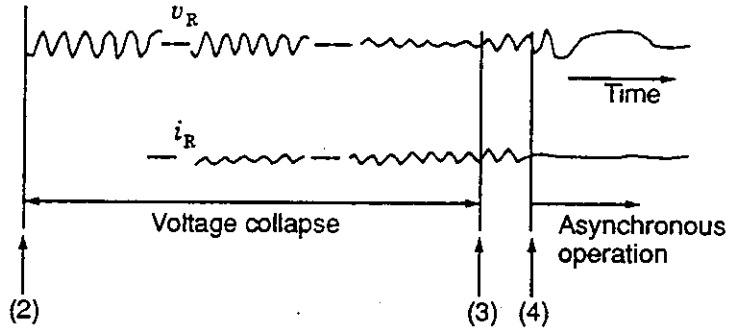

Fig. 3-15. Voltage and current of phase R measured during disturbance according to Figures 3-13 and 3-14: (2) Link 2 disconnection, (3) minimum voltage, (4) disconnection of the last two sections of Link 3.

gations showed that the Southern half of the system was approximately one minute away from unstable voltage conditions, and consequential severe disruption when the remedial actions began to take effect.

The post-fault system voltage behavior is to some extent unusual in that, while the network was required to operate close to the limits of its thermal and voltage capability, no frequency control or oscillation problems were experienced, and no significant amounts of demand were disconnected. This resulted in the power system operating at the extremes of its steady-state voltage capabilities, the underlying behavior not being obscured by other effects such as oscillations

or underfrequency load shedding.

System voltage performance was examined using both recorded data and computer simulation. The studies were confined to examination of steady-state voltage performance using an ac power flow program. The observed system behavior did not indicate requirements for a detailed examination of generator stability or fast voltage transient performance. A range of studies was carried out simulating in turn voltage reductions, gas turbine injection, and a sample Midlands–South circuit reclosure. A further aspect investigated was the supergrid and low voltage tap changing characteristics and their interaction.

Following the circuit trippings at around 1606 hours, the supergrid system entered a period of progressive voltage decline continuing over a period of approximately five minutes without indication of reaching a natural steady-state conditions. An extensive part of the 400-kV system in the southeast was affected with 15,000 km^2 falling below 90% nominal and 35,000 km^2 falling below 95% nominal (Figure 3-16). As shown on Figure 3-17, the voltage decline was halted at approximately 1611 hours by gas turbines coming onto the system in the south and then was rapidly reversed by increased output from the gas turbines, 400-kV circuit restorations and LV voltage reductions. Although implemented without delay, the voltage reductions did not begin to have an effect until approximately 1614 hours when the system had been largely secured.

System simulations were carried out to investigate separately the effectiveness of: (a) Low Voltage (LV) system voltage reductions, and (b) reclosure of one Midland–South circuit.

Each measure, if achievable within five minutes, would have been sufficient to secure the system against voltage instability in the absence of gas turbine support. Achieving effective LV system voltage reductions within five minutes would not have been possible, however, with the procedures which existed at the time. During the five minute period prior to remedial actions taking effect, the voltage supplied to the consumers did not follow the trend exhibited by the supergrid system. As far as can be ascertained from the available chart recordings, automatic tap changer activity was continually attempting to restore consumer voltages to target levels, with periods of falling voltage interspersed with correction by tapping. Consumer voltage excursions in this period are estimated to have been in the order of 2% to 4% below target.

It was judged that the behavior of LV automatic tap changers, combined with consumer load response characteristics, was the dominant influence on the performance of the supergrid voltages. LV tapping was still in progress nearly five minutes after the supergrid trippings, and this response time is considerably longer than might normally have been expected. It is speculated that there was an interaction between groups of system tap changers with differing time delays, coupled with a weak supergrid system, which effectively extended the overall system response. On this occasion the extended response time was sufficient for operator instructed remedial action to take effect.

Simulation confirmed that the supergrid system configuration and generation infeeds in the post-fault condition did not have sufficient capability to support full, pre-fault consumer demand. Network integrity was maintained during the

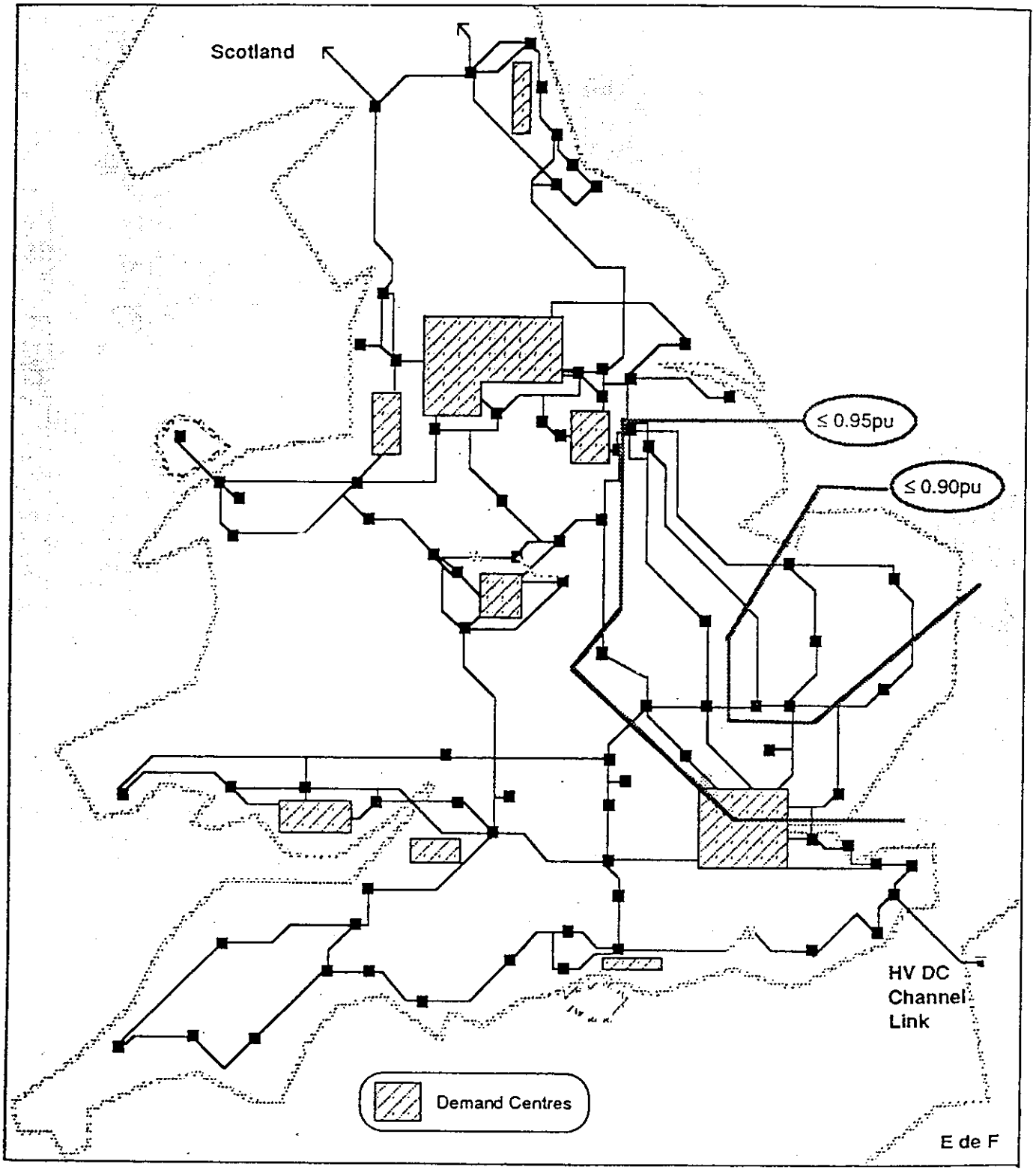

Fig. 3-16. Voltage contours at 1610 hours on 20 May 1986.

critical period by the demand relief provided by the voltage response characteristics of the consumer loads.

Automatic tap changer control of supergrid transformers was not widespread at the time of this incident, but conventional power system practice would result in relatively short time delays being provided at this level for correct coordination with lower voltage automatic tap changers.

For normal conditions, including circuit trippings which the system is planned to withstand, the short time delay, e.g. thirty seconds, would be advantageous. However, under the extreme conditions encountered during this incident with system depletion beyond planning levels, widespread automatic supergrid tapping after a short time delay would almost certainly have resulted in cancellation of demand relief and consequent system failure before gas turbine support could have been made available.

Although the supergrid trippings were beyond contingencies covered by planning and operational criteria, the studies did reveal system weak points. The East Anglia area falls into this category with particular reference to the adequacy of reactive support.

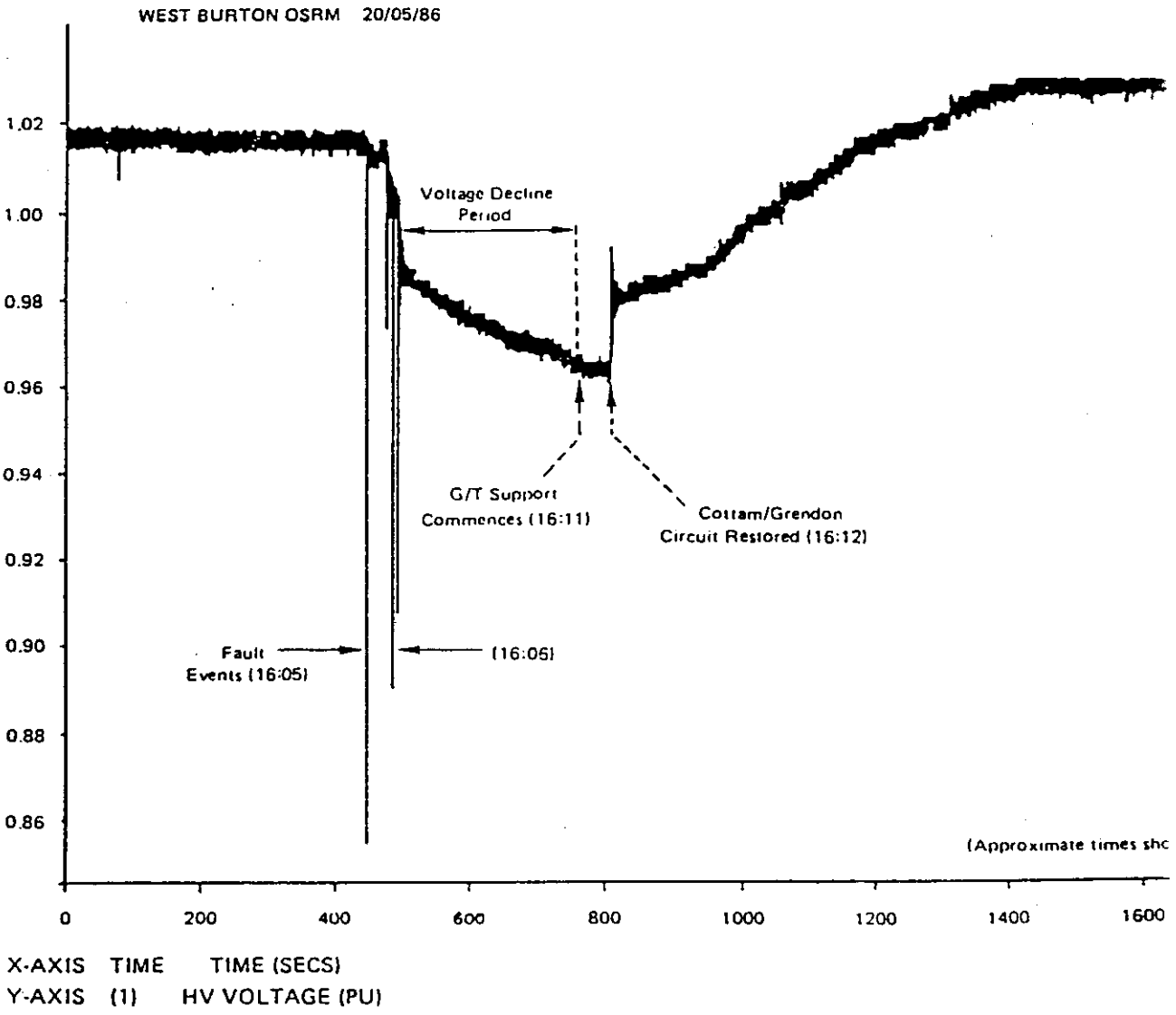

Fig. 3-17. High speed recording of West Burton 400-kV voltage.

Chapter 4

Load Characteristics and Modelling

Voltage stability depends greatly on load characteristics. In this chapter we survey load characteristics and modelling techniques.

4.1 Steady-State Real and Reactive Power Consumption as a Function of Voltage and Frequency

In power flow simulation the load as a function of voltage often needs to be modelled. Usually frequency is at rated value and no provision is made for off-nominal frequency. In dynamic simulation, static load models are frequently used and the loads are both voltage and frequency sensitive. Particularly in developed networks, frequency deviation is usually small compared with voltage deviations. We will concentrate on voltage effects on loads.

4.1.1 Characteristics of various loads

Steady-state voltage/power characteristics are the relations between power (real and reactive), torque or current, and the voltage determined at such slow variations of the operating conditions that each point may be considered as corresponding to a steady state: $P = f(V)$, $Q = g(V)$. The dynamic characteristic is the same relation, but defined for such fast variations of the operating conditions that their rate of change has to be taken into account.

A general distinction between the power consumed by a particular load at nominal conditions and under other conditions is given by:

$$P = P_0 f(V, \omega, t) \text{ and}$$

$$Q = Q_0 g(V, \omega, t)$$

where, by the definition proposed in Section 2.2.4:

P_0 is the active component of the *nominal* load

Q_0 is the reactive component of the *nominal* load

P is the active component of the *consumed* load

Q is the reactive component of the *consumed* load

This requires that the load voltage/frequency sensitivity functions, $f(V, \omega, t)$ and $g(V, \omega, t)$, are unity at nominal steady-state conditions.

Load nodes rather than individual loads are usually considered. Load nodes are groups of loads connected to a high voltage network through transforma-

tion. The characteristics of these composite or equivalent loads are needed. Two methods are available to determine composite loads. The first is to analyze the characteristics of the consumer individual elements or components (motors, lighting, heating, etc.), and then, on the basis of structure, determine overall characteristics.

The second method is measuring the characteristics at the node of the actual system. The effect on real and reactive power of voltage changes is measured. In order to understand the nature of problem, let us analyze the characteristics of the system shown in Figure 4-1. The load as seen from the 110-kV side must be determined.

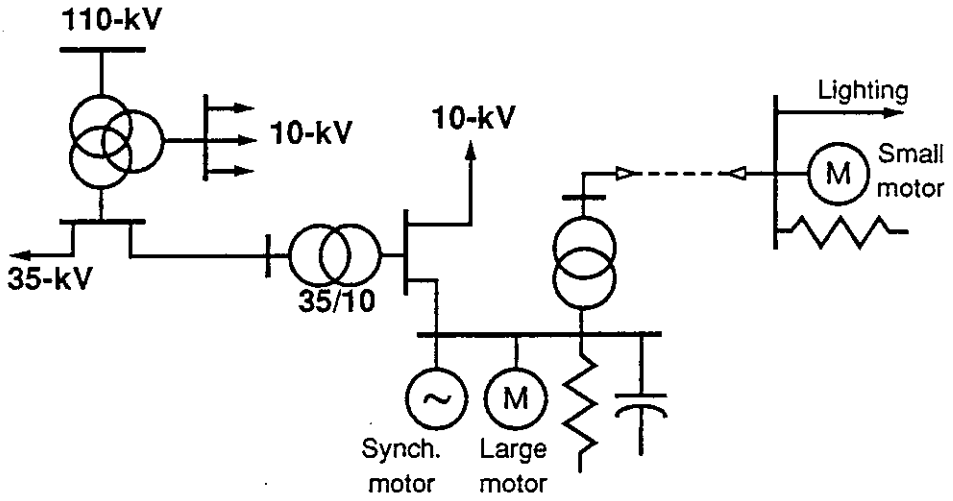

Fig. 4-1. Schematic of load node.

Lighting load. The real power consumed by a lighting load containing incandescent lamps is independent of frequency and varies with voltage approximately as $V^{1.6}$. Such a load consumes no reactive power. The real load consumed by discharge (fluorescent) lamps varies approximately as the first power of voltage. The reactive power consumption of fluorescent lamps depends on the type of ballast. Also, discharge lamps will extinguish if the voltage drops below some value, typically about 70%. The dynamic characteristics of a lighting load can be taken as identical to the steady-state characteristics.

Motor load. The steady state and dynamic characteristics of induction and synchronous motors differ greatly. In order to determine the shape of steady-state characteristics of induction motors we start with the simplified equivalent circuit of the motor shown in Figure 4-2. This diagram is simplified and obtained by assuming that the resistance of the stator and the magnetizing losses are negligible.

The real power, P, consumed by the motor, and consequently, its electromagnetic torque are determined by the mechanical power (braking torque) required for the driven mechanism, and by the drive characteristics $T_{mech} = f(\omega)$.

The driven mechanism can have three basic types of torque characteristics, $T_{mech} = f(\omega)$, as shown in Figure 4-3.

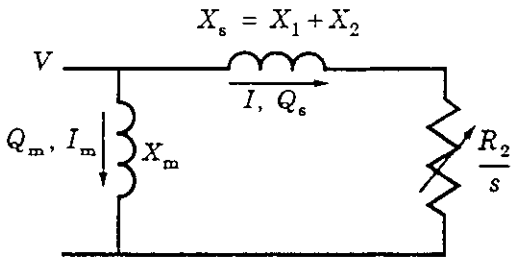

Fig. 4-2. Simplified equivalent circuit of an induction motor; s is motor slip.

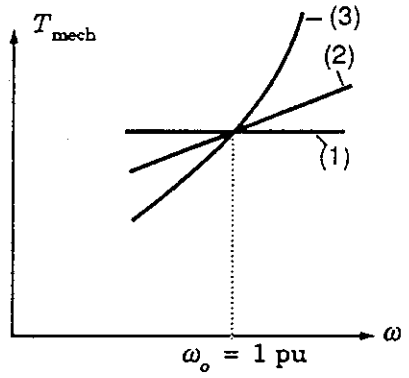

Fig. 4-3. Mechanical torque characteristics: (1) T_{mech} = constant, $P \propto \omega$ (compressors, cranes, mills), (2) $T_{mech} \propto \omega$, $P \propto \omega^2$ (textile industry), (3) $T_{mech} \propto \omega^2$, $P \propto \omega^3$ (centrifugal pumps, fans).

For simplicity we further assume that T_{mech} is independent of speed. Neglecting losses in the motor and considering steady-state conditions, we may approximately assume that:

$$T_{mech} = \frac{I^2 R_2}{\omega_o s} = \text{constant}$$

Hence, with $\omega_o = 1$ we have:

$$s = \frac{I^2 R_2}{T_{mech}} \quad \text{or} \quad s \propto I^2$$

The reactive power consumed by the motor according to the equivalent circuit consists of two components: the magnetizing component, Q_m, and the component Q_s depending on stator and rotor leakage.

$Q = Q_m + Q_s$, where

$Q_s = I^2 X_s$ and $Q_m = V^2/X_m = I_m V$

If we take into account the decrease of X_m caused by saturation, then the relation between Q_m and V departs appreciably from the square law (Figure 4-4).

The real power defined as a function of voltage, V, and slip, s, is readily obtained

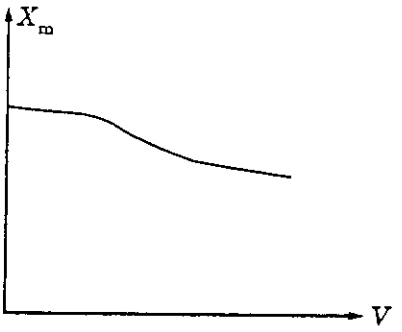

Fig. 4-4. Saturation characteristic.

from the equivalent circuit, Figure 4-2.

$$P = I^2\frac{R_2}{s} = \frac{V^2R_2}{[(R_2/s)^2+X_s^2]s} = \frac{V^2R_2s}{R_2^2+(X_ss)^2}$$

Figure 4-5 shows the plots of this function and the relation between voltage, V, and slip, s [51].

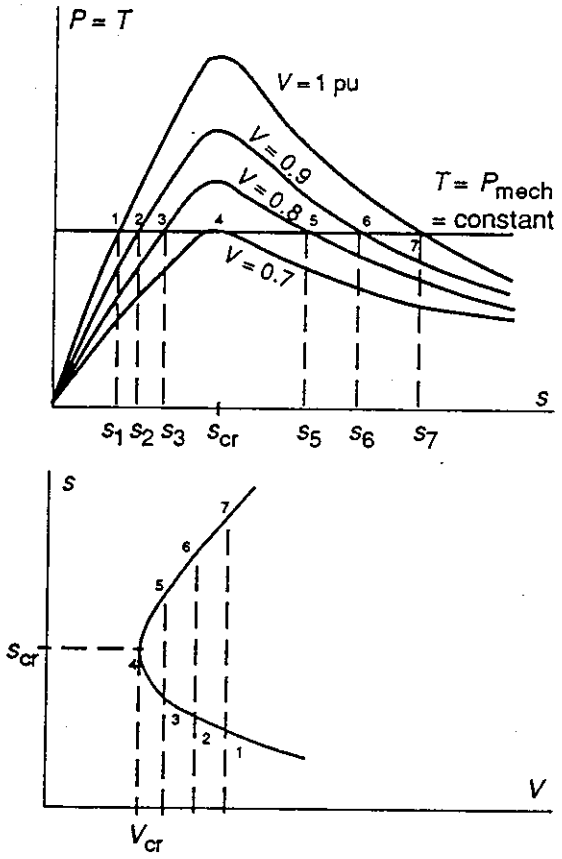

Fig. 4-5. Power -slip characteristics of motor for different applied voltages and corresponding slip as a function of voltage.

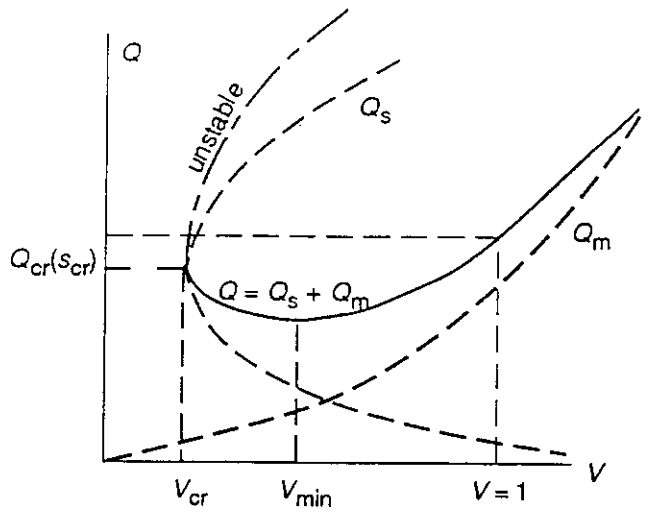

Fig. 4-6. Induction motor reactive power as a function of voltage.

Since, in this case, $Q_s = I^2 X_s$ and $I^2 \propto s$ for T_{mech} = constant, the function $Q_s = f(V)$ has the same form as the function $s = f(V)$. See Figure 4-6 [51]. The curves $Q = f(V)$ show that each motor has a certain critical condition at the voltage V_{cr} and the slip s_{cr}. At the critical condition the maximum torque developed by the motor is equal to the mechanical torque.

With the operating voltage lower than the critical one, the electrical torque will be less than the required mechanical torque. This leads to motor stalling and possible voltage collapse. At the point V_{cr} it is too late to take any measures against motor stalling. At voltage V_{min} we are entering the critical zone where consumption of reactive power starts to increase for further voltage drop. At the voltage V_{min}, $dQ/dV = 0$ which can be a practical criterion denoting danger to motor operation. It can be determined by experiment and analytically.

4.1.2 Analytical modelling of steady-state characteristics

Polynomial models. Steady-state characteristics of equivalent consumption nodes are frequently approximated by the polynomials:

$$P = a_0 + a_1 V + a_2 V^2$$

$$Q = b_0 + b_1 V + b_2 V^2$$

where P, Q, and V are expressed in per unit in relation to nominal values. By these polynomials a variety of load characteristics can be modelled. In accordance with previous section, the minimum voltage V_{min} (Figure 4-6) is easily obtained:

$$\frac{dQ}{dV} = 0, V_{min} = -\frac{b_1}{2b_2}$$

In practical examples, V_{min} for complex load nodes is within the range 0.7 to 0.0 per unit depending on consumption structure (amount of induction motor load). As an illustration, we state a few examples from the literature (where P_0 and $Q_0 = 1$).

For complex consumption [37]:

$$P = 0.83 - 0.3V + 0.47V^2$$

$$Q = 6.7 - 15.3V + 9.6V^2$$

For air conditioning load [38]:

$$P = 2.97 - 4V + 2.02V^2$$

$$Q = 12.9 - 26.8V + 14.9V^2$$

For induction motor [38]:

$$P = 0.72 + 0.11V + 0.17V^{-1}$$
$$Q = 2.08 + 1.63V - 7.6V^2 + 4.89V^3$$

Exponential models. In other cases, steady-state characteristics are modelled by:

$$P = aV^p \text{ and } Q = bV^q$$

where p and q are exponents which are close to coefficients which represent the slope characteristics: $P = f(V)$ and $Q = g(V)$ at $V = 1$ per unit and

$$K_p = \frac{dP}{dV} \approx \frac{\Delta P}{\Delta V} \qquad K_q = \frac{dQ}{dV} \approx \frac{\Delta Q}{\Delta V}$$

Here K_p and K_q are the regulation coefficients which are sometimes called self-regulation coefficients of the load node because (assuming positive coefficients) when voltage decreases, the load consumption decreases.

In steady-state analysis of the system we are often satisfied with a linearized load model:

$$P = P_o(1 + K_p \Delta V) \text{ and } Q = Q_o(1 + K_q \Delta V)$$

where the values of K_p and K_q are average values based on the structure of the consumers or estimation of load composition.

In the analysis of eventual voltage collapse, polynomial models are preferred.

Representation of loads by exponential models with exponent values less than 1.0 (or by an equivalent polynomial model) in a dynamic simulation is questionable [64].

4.1.3 Tests of steady-state characteristics on a real system

Steady-state power/voltage characteristics of one consumption node as shown in Figure 4-1 can be exactly determined only by measurement at the site. Results from tests at two 110/35-kV substations in the former Yugoslavia (Sarajevo and Gorazde) are presented here.

Real and reactive power were measured at the low side of 110/35 and 110/10-kV transformers, and measured at each voltage step of under load tap changing transformer. The voltage range was ±10% or as much as allowed by the dispatchers.

Results are summarized in Table 4-1. We see that residential loads are much

more voltage sensitive than industrial loads which have predominant motor component.

Voltage sensitivity was also higher in the afternoon when some of the motors were off-line. This shows that it is not practical to attempt high precision for load characteristics.

Table 4-1

Node	Time	Load	K_p	K_q	$P(V)$	$Q(V)$
Sarajevo 1	0900	40/60% ind./res.	0.52	3.94	$0.99V^{0.53}$	$1.04V^{3.75}$
Sarajevo 1	1500		1.15	3.70	$1.00V^{1.15}$	$1.00V^{3.68}$
Sarajevo 2	0800	50/50% ind./res.	1.56	4.72	$0.76V^{2.05}$	$1.01V^{4.66}$
Sarajevo 2	1400		1.19	4.11	$0.72V^{1.64}$	$0.96V^{4.29}$
Gorazde 1	1400	90/10% ind./res.	0.43	1.64	$1.01V^{0.43}$	$1.0V^{1.64}$
Gorazde 2	1500	20/80% ind./res.	1.18	4.06	$0.96V^{1.23}$	$0.98V^{4.15}$

4.2 Dynamic Loads

Dynamic loads are primarily motors. For transient voltage stability, induction motor performance generally dominates.

4.2.1 Comparison of static and dynamic characteristics

The dynamic characteristics of bus load as shown on Figure 4-7 represents the dependance of active and reactive power on voltage taking into account time, t, as a new parameter which is not taken into account for the steady state characteristics.

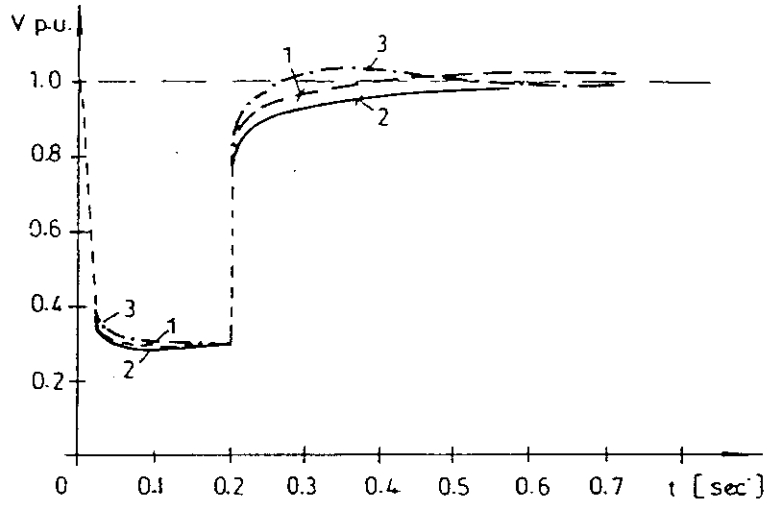

Fig. 4-7. Voltage behavior at load bus for three phase short circuit. Curve 1, simplified calculation. Curve 2, real system. Curve 3, dynamic model.

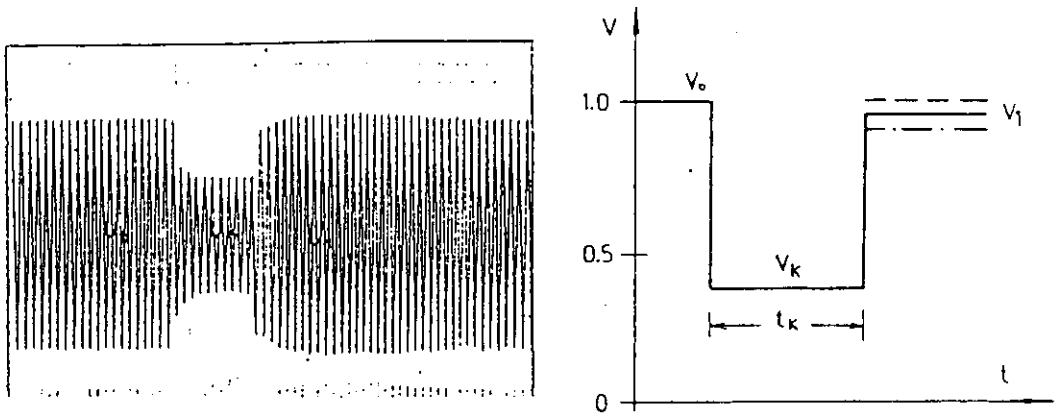

(a) voltage oscillogram (b) simplified calculation diagram

Fig. 4-8. Voltage for three phase fault.

Dynamic characteristics are approximately equal to steady state characteristics for loads such as heating, lighting, capacitor banks, and shunt reactors. Dynamic characteristics, however, differ considerably from steady state characteristics for rotating machines. Motor dynamics are dictated by rotational masses and accumulated kinetic energy. Dynamic characteristics of load busses are therefore determined by rotating machines, principally asynchronous (induction) motors. The percentage of motor load may be very high for industrial consumers.

4.2.2 Dynamic characteristics of induction motors

A transient three phase short circuit is typically used for analysis and definition of motor dynamic characteristics. During the short circuit, the voltage at the load bus drops from V_0 to some value V_k and then increases to a value close to nominal after fault clearing. See Figure 4-8. During the fault period, motors decelerate as a function of voltage and mechanical load type (fan, pump, compressor, etc.).

At the moment of voltage reestablishment, motors draw higher current from the network (Figure 4-9) and reaccelerate. If the voltage reduction is relatively severe, and the fault clearing time is longer than some critical time, the motor will stall.

If the motor stalls and if the motor is not disconnected by protection or contactor devices, the motor takes high reactive power from the system and contributes to a voltage collapse at the load bus. The dynamic characteristics of the load bus and physics of the process during system disturbances are very suitable for studying on a dynamic model. The effect of varying motor parameters, motor loading, network loading, etc. can be investigated.

4.2.3 Calculation of induction motor behavior

The essential question is whether induction motors reaccelerate or stall following fault clearing. This can be analyzed analytically [52] to provide insight into results from computer simulation.

Referring to the torque-speed curve of Figure 4-10, we have the following parameters:

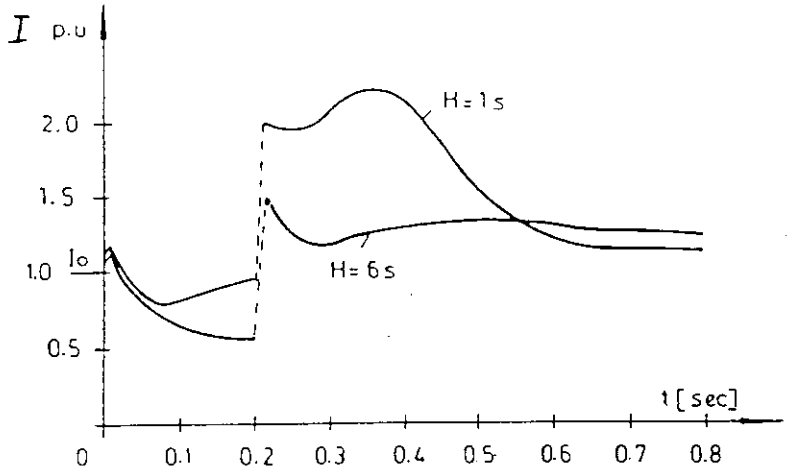

Fig. 4-9. Plots of motor current for equivalent induction motor (under 100 kW) for two values of inertia constant.

V_0	nominal voltage
V_k	voltage during short circuit
T	motor torque
T_k	motor maximum torque
T_L	load torque
s	slip
ω	speed
T_a	motor mechanical starting time = $2H$

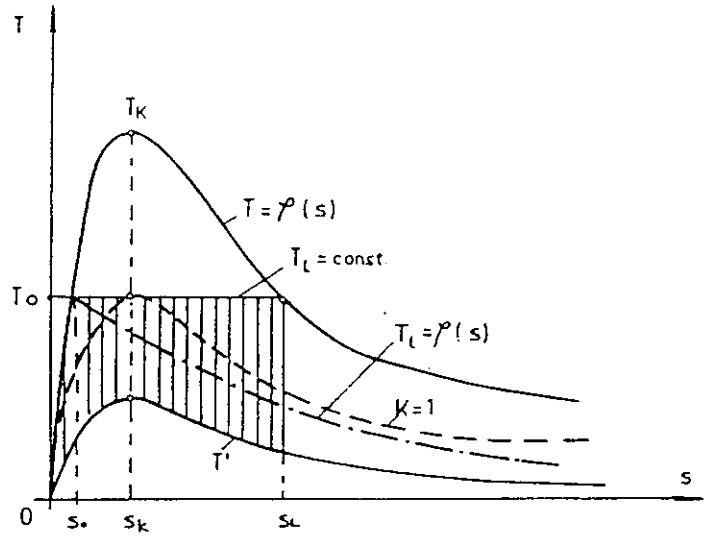

Fig. 4-10. Torque-speed curve of induction motor.

For the most unfavorable case of constant mechanical load, the differential equation for mechanical motion of the equivalent induction motor is:

$$\Delta T = \frac{T_0 - T'}{T_0} = T_a \frac{ds}{dt}$$

where ΔT is the differential between torque produced by the motor and the load torque. Solving the equation for t we have:

$$t = T_a \int_{s_0}^{s} (1 - \frac{T'}{T_0})^{-1} ds$$

Taking into account the known torque equation for induction motors [52], we have:

$$\frac{T'}{T_0} = \frac{2K}{\frac{s}{s_k} + \frac{s_k}{s}} \text{ where } K = \frac{T_k}{T_0} (\frac{V}{V_0})^2$$

Substituting and solving the integral we have:

$$t = s_k T_a \tau \text{ where}$$

$$t = \left[\frac{s}{s_k} K \ln \{ \frac{s}{s_k} \left(\frac{s}{s_k} + \frac{s_k}{s} - 2K \right) \} + \frac{2K^2}{\sqrt{1-K^2}} \tan^{-1} \frac{\frac{s}{s_k} - K}{\sqrt{1-K^2}} \right]_{s_0}^{s}$$

Boundaries of integration of s_0 and s_L are shown on Figure 4-10. Knowing the ratio

$$2\frac{T_k}{T_0} = \frac{s}{s_k} + \frac{s_k}{s}$$

we have:

$$(\frac{s}{s_k})_{0,L} = \frac{T_k}{T_0} \pm \sqrt{\left(\frac{T_k}{T_0}\right)^2 - 1}$$

Using typical values for smaller motors $\frac{T_k}{T_0} = 2$ and $s_k = 10\%$, we obtain:

$s_0 = 2.7\%$ and $s_L = 37.3\%$.

The motor slip can increase to 37% during the fault period. If the values of s_0 and s_L are used in the equation for τ, we see that the relative time of motor speed reduction τ depends only on relative loading of the motor, T_k/T_0, and the fault voltage, V/V_0.

Restricting the speed decrease to the slip, s_k, at maximum torque, the limit of integration is s_k rather than s_L. Restricting the speed decrease insures proper performance of driven loads and allows for the effect of high motor reacceleration current on bus voltage. Figure 4-11 shows a series of curves for dependence of the highest permitted relative duration of voltage reduction, τ, on the value of fault voltage, V/V_0, at different values of T_k/T_0.

Example: For a three phase short circuit, the voltage reduction is 50%. Let

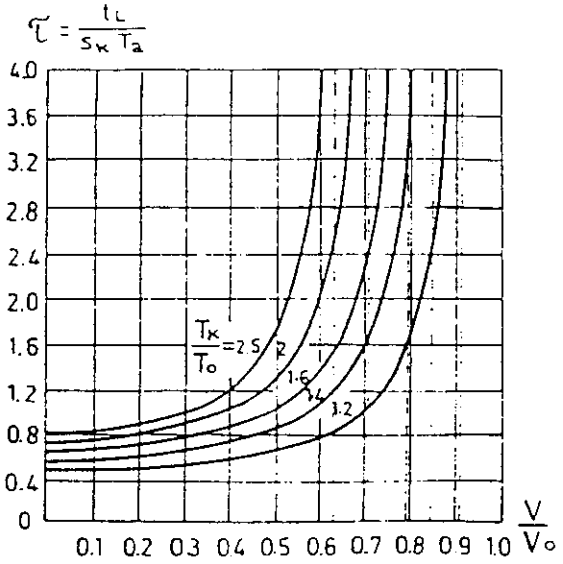

Fig. 4-11. Curves to determine fault clearing time for induction motor stability.

T_k = 2 per unit, s_k = 10%, and T_a = 2 seconds. From Figure 4-11, the value for $\tau = t_k/(s_k T_a)$ = 1.3. The critical time for voltage reduction, t_k is then 0.26 seconds.

4.2.4 Dynamic models of induction motors

When transient voltage collapse is a concern, motors dynamics should be modelled. The simplest approach is to use the steady state equivalent circuit (Figure 4-12) for the electrical effects, and the following equation for rotational motion:

$$\frac{d\omega_m}{dt} = \frac{1}{2H}(T_e - T_m)$$

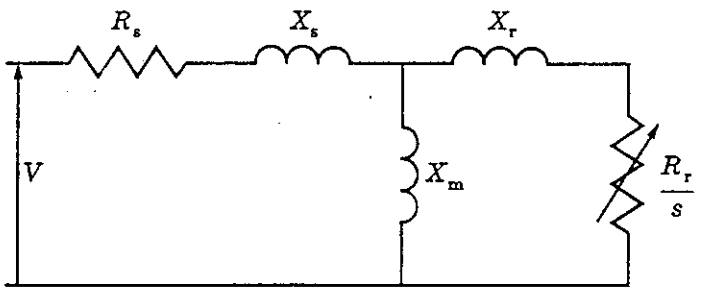

Fig. 4-12. Induction motor steady-state equivalent circuit. Double squirrel cage and deep bars may be represented by a second rotor circuit.

In voltage stability studies (and in other studies [53]) it is, however, generally desirable to represent the rotor flux dynamics—particularly for large motors close to the disturbance location. This is consistent with modern computer capabilities. For large-scale simulation with equivalent motors, a third order

model (single rotor circuit per axis) is generally adequate. If desired, a more detailed fifth order model (two rotor circuits per axis) may be used. Saturation effects may also be represented. Reference 53 and 54 provide equations for dynamic models.

Data for induction motor models and aggregated motor models are available from many sources (c.f. references 53, 45, and 55).

4.2.5 Synchronous motors

Compared to induction motors, there are far fewer synchronous motors. Although most synchronous motors have large power ratings, they nevertheless normally represent a small part of the total motor load. During stable operation their speed is essentially constant, regardless of the bus voltage. Because of the time required for flux decay and because of regulation of the motor excitation, the bus voltage is supported thereby reducing the problem of voltage collapse. An approximate equation for the support (increase in bus voltage) is:

$$\Delta V = \frac{X_k}{X'' + X_k}(V_n - V_e)$$

where V_n is the motor node voltage before the fault, V_e is the motor node voltage during the fault, X_k is the reactance of the supply system, and X'' is the subtransient reactance. With longer fault times the subtransient reactance is replaced with transient reactance.

Modelling is more complicated than induction motors and is similar to modelling of synchronous generators with excitation control. The mechanical load characteristic as a function of speed should be represented similar to induction motor models.

4.3 Constant Energy Control of Loads, Thermostats

Those loads that have control equipment to keep the power or energy constant may often be modelled as constant MVA loads in voltage collapse studies. The speed of the control determines which characteristics should be used in the transient region up to 10 seconds.

To "thermostat" control we may include all kinds of control that switch a load on and off regularly. The cycle time is normally in the time span from minutes to hours. The controlled parameter is often temperature or pressure. The following loads are often controlled by "thermostats":

- Heating
- Refrigerators
- Air Conditioners
- Compressors and pumps

The thermostat control does not affect the transient voltage characteristic of the load. The static characteristic is however changed, since the aggregated load will be connected for longer time periods if the consumed power is decreased by a voltage drop. This load is therefore a kind of "constant energy control of load" seen over a long time span. The static characteristic for the aggregated load of electric heating is constant MVA for small voltage deviations. When the voltage is so low that the electric heating is connected all the time in order to supply the heat demand, the static characteristic changes to

constant impedance. The ratio between the demand and the installed capacity determines the point when the characteristic switches over from constant MVA.

The time constant for the aggregated thermostat controlled load is normally longer than the time it takes for the on-load tap changers to restore the voltage at distribution level. It is therefore not always necessary to take into account "thermostat" characteristics, unless significant numbers of on-load tap changers will reach regulation limits following a disturbance. For long term simulation scenarios which cause sustained voltage depression on the bulk transmission system of more than about 10%, modelling of thermostatically-controlled loads may be required.

4.4 Load Tap-Changer and Distribution Voltage Regulator Operation

Several transformers are interposed in series between the main system and the load. Manually controlled and automatic voltage controlled transformer tap-changers and voltage regulators operate to restore scheduled voltages to low voltage subsystems and shunt connected reactive plant over the period of tens of seconds to minutes following either a depression or increase in main system or higher level voltage. Tap-changer operation hence affects the system dynamic response to sustained voltage disturbances arising from system contingencies.

When simulating the response of a power system to a voltage disturbance, it's normal to represent the load at a high voltage level. The dynamic behavior of this load then stems from two sources. The first is the dynamics of the consumers. These dynamics will sum up as a voltage-dependent load at the consumer voltage level together with the voltage-dependent shunt reactive load, and will be transformed up to the voltage level at which the load is to be represented. The second is the dynamics of the system control, principally the automatic tap-changer control of the transformers. Tap-changer operating time is typically from 4 to 7 seconds per tap change, excluding intentional controlled time delays, which may represent voltage increments of about 1 to 1.5%. Section 5.4 provides additional details on tap changing characteristics.

Transformer on-load tap-changers acting to restore predisturbance voltages to loads tend to cause the loads to exhibit a constant MVA characteristic. Following a voltage depression the load voltage dependence will usually result in a reduced loading seen at the high voltage supply points. Similarly the reactive generation or load due to shunt connected reactive plant will be reduced. Over the period of tens of seconds to minutes, as the transformer taps are adjusted, the load at the supply point will progressively increase to its predisturbance level. Similarly the adjustment of taps restores normal voltage to low voltage shunt reactive plant.

The time coordination of the tap-changers at the various voltage levels determines the speed of transition of the load to a constant power characteristic. If low level transformer tap-changers operate before higher level tap-changers the load will overshoot predisturbance levels once the high level tap-changers operate. It is normal to provide higher speed tap-changing response at the highest voltage level with progressively longer delays at lower voltage levels. It is also common to avoid any time delay on high level tap-changers for large

voltage disturbances to ensure that these tap-changers will nearly complete their necessary tap movement, correcting the voltage change at the low voltage bus, before lower level tap-changers make their first tap change. Where the bulk of the system shunt reactive plant is located at low voltage buses of main grid substations it is particularly important to rapidly restore voltage to these devices.

The appropriate model for transformers with on-load tap-changers is similar to that used in power flow analysis. Modelling for voltage stability analysis requires attention to the following points:

- Identification of which tap-changers automatically control bus voltage;
- Consideration of the time co-ordination of tap-changers at various levels to determine the extent of any temporary overshoot of load during tap-changer operation;
- Distribution of load and reactive plant at various voltage levels;
- Tap-changer limits;
- Representation of the effect of voltage control on the reactive power losses and generation of the elements in low voltage subsystems;
- Representation of the tap-changer control scheme, allowing for conventional automatic voltage regulators or the more complex logic possible with programmable logic controllers.

4.5 Subtransmission and Distribution System Characteristics

Voltage stability analysis requires representation of lower voltage subsystem networks. Voltage deviations below normal values in high voltage systems, prior to completion of tap changer operation, will increase the reactive power losses in subsystems due to the relationship between voltage and current through the series impedances to the load. The reactive load and generation due to shunt compensation in connected subsystems will also be altered.

Consideration must also be given to the impact of capacitor controls and line drop compensation in subsystems.

Voltage controlled subsystem capacitors and reactors will be switched according to their voltage control settings. Shunt capacitors may be switched into service after the initial voltage reduction in higher level systems. It is possible that as transformer tap-changers operate to restore voltage, the capacitors could be switched out of service.

Line drop compensation essentially adjusts the scheduled voltage to be controlled by on-load tap-changing transformers or voltage regulators. Hence its impact is over the time scale determined by the coordination of the timing of tap-changer control. The load seen by line drop compensation will vary according to the voltage behavior of the load.

4.6 Aggregation of Loads

Aggregating loads consists of choosing a simplified load model which can accurately reproduce the behavior of a group of loads for the time span of interest. In order to keep the load models relatively simple, it will be necessary to define the time span of interest and different load models will be suitable for different

time spans. In general loads can be put into the following categories:

- Induction motor
- Synchronous motor
- Loads controlled by semi-conductors, e.g., thyristor drives, aluminium smelters
- Heating
- Discharge lighting

The first three have a transient response to a voltage dip, while the last two do not and can be represented by the same model independently of the time span of the disturbance (except for thermostatically-controlled heating load). Besides the characteristics of the loads, the low voltage network containing the above load elements can have automatic on load tap changers which have the effect of changing the load characteristic as seen from the high voltage bus.

Two ways of aggregating loads are possible. The first is to do a survey of the customer load, form a complex load model with the details of the survey and the relevant parts of the network. It is then necessary to choose a simple load model which has the same characteristics as the detailed model. The other method is to do measurements and choose a load model which has the required characteristics. Intuition needs to be applied when deriving a load model, since the composition of the load is continually changing and this can happen without the magnitude of the load on the bus changing substantially.

Furthermore, if it is decided that a "factor of ignorance" will be built into the load model, the load model should be chosen to have more onerous characteristics.

4.6.1 Aggregating loads for voltage collapses occurring in the transient region, up to 10 seconds

In this time span the transients of the motor and thyristor drives will play a part. A measurement approach in this time span was reported by Shackshaft et al. [15]. This paper describes a method of determining the aggregate load at a substation where the load is supplied from one or more transformers. Another approach to determining aggregate load was reported in reference 16.

The reduction approach requires detailed model of motors, thyristor drives and the network. In some instances the torque-speed characteristic of the mechanical load on the shaft of the motor would be important.

4.6.2 Aggregating loads in the time span 10–30 seconds

In this region it is assumed that the transients are not important. It is also assumed that the on-load transformer tap changers do not react in this time period (this assumption may not be true if inverse time characteristics are used for tap changer control, see Section 5.4).

In this region the loads can be represented as a polynomial function of voltage for both the active and reactive power.

Measurements to aggregate loads in this time span are relatively simple and well known. As no load dynamics are required, the measurements are relatively crude.

The reduction approach for this time span is also relatively simple and intu-

ition in some cases would be adequate.

4.6.3 Aggregating loads in the time span 30 seconds to 1 hour

In this region it is assumed that transformer on-load tap changers and thermostatic controls can operate, overload protection can switch out overloaded apparatus, and additional load can be brought on line.

The operation of the tap changers and thermostatic controls will have the effect, while they have sufficient range, of making the load appear as constant power for both the active and reactive components.

Measurements to aggregate loads in this region are likely to be inappropriate especially if random operator intervention can be expected.

The reduction approach involving a large amount of intuition can provide a satisfactory solution. Intuition would also allow a lot of flexibility regarding the inclusion of operator intervention and overload tripping and would also allow the engineer to apply his "factor of ignorance."

Reference 40 describes the use of network reduction programs to reduce subtransmission systems for steady-state voltage stability analysis.

4.7 Undervoltage Load Shedding

Undervoltage load shedding is an attractive solution for voltage stability problems that have a low probability of occurrence. Required models consisting of a voltage relay and timer are available in most production-grade dynamic simulation programs. Inverse-time relay models may also be required. In some applications, network lines with tapped loads may need to be tripped [9,65].

Time delays of around one second are required when a large portion of the load is induction motor (e.g., air conditioning load). Time delays are less critical when much of the load is highly voltage sensitive (e.g., electric space heating).

As a contribution to Chapter 8, Appendix V describes implementation of undervoltage load shedding in the Pacific Northwest region of the U.S.A.

Chapter 5

Network Characteristics and Modelling

Transmission network modelling methods for power flow and dynamic performance simulation are well-known, but will be briefly reviewed. Characteristics specifically related to reactive power transfer and voltage control/stability will also be reviewed. Series and shunt reactive compensation methods are important for voltage stability modelling and will be described. Reference 25 expands on many of the topics in this chapter.

5.1 Transmission Line Models, Reactive Power Transmission

Transmission lines are usually modelled as pi equivalents using lumped parameters obtained by multiplying the per kilometer values of series resistance, series inductive reactance, and shunt susceptance by the line length. This is acceptable for lines up to about 150 km. Longer lines (which may be compensated) may be represented by two or three series sections, again with lumped parameter models. Voltage control is, of course, a major concern for very long lines and distributed parameter models may be required. Distributed parameter (long line) effects can be represented by correction multipliers to the lumped parameter pi models; the correction terms involve hyperbolic functions (trigonometric functions for lossless lines).

Transmission line parameters and characteristics (inductive reactance, shunt susceptance, surge impedance loading) are significantly affected by the configuration and by the number of subconductors per phase. Larger number of subconductors increase line loadability and improve voltage performance during heavy load conditions and voltage depression.

Transmission line reactive power flow capability is crucial to voltage stability. Reactive power transmission as a function of real power transfer and as a function of sending and receiving end voltages can be visualized by power circle diagrams [26]. Sending end reactive power requirements affect generator reactive power output, and high transmission line demand may cause generator current limiting. The inability to import reactive power at the receiving end may cause voltage collapse.

During heavy load, reactive power transmission requires the receiving end voltage to be lower than the sending end voltage. At some loading point, however, the transmission line consumes reactive power from both ends—even with substantial voltage gradient.

5.2 Series Compensation

Series capacitor compensation has historically been applied on very long lines for rotor angle stability benefits. Nowadays, however, several utilities are applying series compensation on relatively short lines to improve voltage stability.

Series capacitors inherently have very desirable self-regulating characteristics. Reactive power production is proportional to I^2. High production is automatically obtained when needed most.

One limitation of series compensation is voltage profile during heavy load conditions. Depending on the compensation level, current magnitude, and voltage-current phase relation (power factor), overvoltages may appear on one side of the series capacitor. This may require applying smaller amounts of compensation at several locations. In simulations, voltage at the compensation locations should be monitored.

In some applications, series capacitors are normally bypassed, but inserted following major system disturbances.

For outage of parallel lines, series capacitors may be severely overloaded. In determining capacitor bank rating, advantage is taken of the short-term (five to thirty minutes) overvoltage capability of capacitors. In voltage collapse situations, this means that the overload must be relieved (by starting gas turbines, shedding load, etc.) within the allowable overload time.

Modelling of series capacitors is straight-forward. The main complication is modelling during a short circuit. With metal oxide varistor (ZnO nonlinear resistor) overvoltage protection, the voltage waveform peaks will be clipped by nonlinear resistor conduction. References 27 and 28 provide models for fundamental frequency type simulation programs.

5.3 Static Var Systems and Breaker-Switched Shunt Capacitors/ Reactors

Previous CIGRÉ work [29] and recent IEEE work [66] describe static var compensation application and modelling. In transmission applications, the main control mode of static var compensators and systems* is voltage regulation, usually on a three phase basis. For transient voltage stability, fast acting SVCs are important for supporting the reacceleration of motors following faults [41].

For slower forms of voltage stability, the SVC reactive power output provides a "pilot" indicating voltage security (low security if SVC is near boost limit). Coordination of SVC with other voltage regulating devices is important in power flow and longer-term dynamic simulation. Coordination is through slope and setpoint values, and through slow-acting reactive power/susceptance control.

In power flow simulation of voltage stability, the static var compensator should be represented with a slope. The SVC operates as a shunt capacitor bank at its boost limit.

---

* A static var system is a combination of a static var compensator and mechanically switched capacitors and reactors under coordinated control.

In dynamic simulation, basic models are generally available. User-defined models may be needed for slower acting control of susceptance and nearby mechanically switched shunt capacitor banks and reactors. Accurate representation of SVS controllers at susceptance limits is important.

Models for voltage-controlled mechanically switched capacitors and reactors are often required. The models should have provision for both fixed time delay and volt-second integrating type of time delay (induction disc relay or electronic equivalent). Circuit breaker opening and closing times should be separately represented. Over and under voltage setting should be different to provide a hysteresis/deadband function.

5.4 Network LTC Transformers

This section relates to Section 4.4 on load characteristics as seen from the bulk power system. Automatically-controlled network LTC transformers may aid voltage stability by supporting reactive power generation of shunt capacitor banks and line/cable capacitance in the lower voltage portion of the network. Also, series real and reactive power losses in the lower voltage portions of the network are reduced. On the other hand, network LTC transformers will cause faster restoration of loads.

Models for representation of under-load tap changer (LTC) transformers in power flow simulation are well known. In post-disturbance power flow simulation, tap changing depends on the snapshot in time and on the tap changer control method. Often tap changing on network transformers are manually controlled from dispatch centers. If this is the case, taps would usually be frozen at the pre-disturbance value for simulation of a point in time one or two minutes after the disturbance.

Dynamic characteristics of tap changing equipment vary. There is always a small voltage deadband within which tap changing is not activated. Three types of timing equipment are used:

1. Constant (definite) time delay between two tap changes, typically sixty seconds, regardless of the difference between the desired and the actual voltage.

2. Inverse time characteristic with the time delay between two tap changes typically about thirty seconds when the difference between the desired and the actual voltage is small. However, when the difference between the desired and the actual voltage becomes larger, the time delay becomes smaller and will typically be as small as five seconds when the voltage difference is a few times greater than the deadband.

3. Constant or inverse initial time delay with no additional time delay between additional tap changing steps. This method, widely used in North America, is further described below.

Tap changing equipment and practices vary from country to country. A sampling of practices is described in the following paragraphs.

In North America, for bulk power delivery LTC transformers (e.g., 115/12.5-kV) and distribution voltage regulators, tap changing equipment usually has ±10% voltage range with 32 steps of 5/8% each. The voltage relay deadband is adjust-

able, but is typically set at 2 volts on a 120 volt base (±0.833%). Relay operation starts a timer with typical settings of either 30 or 60 seconds. Once the timer times out, tapping continues until the voltage is within the deadband. The only delay between taps is the mechanism delay of 4–8 seconds. Inverse-time relays are not widely used in recent installations. On large network transformers, North American practice is either to not use LTC transformers, or to control LTC transformers manually from control centers. At one utility (Bonneville Power Administration), manually controlled 500/230-kV LTC autotransformers have a tap range between 500 and 550 kV (approximately ±5% of 525 kV) in steps of either 5/8% or 1 1/8%.

In Denmark, automatic tap changers are normally used on transformers connecting subtransmission with distribution networks, e.g., 132/10-kV and 50/10-kV. Typically 14 steps of 2% each are used. Constant time between steps was previously used, but inverse time relays are now common. Therefore a fast restoration of the distribution network voltage is obtained except for the final couple of necessary tap changes. The automatic tap changes are typically blocked if the voltage drops below 70%.

In some parts of the Scandinavian network the 132-kV subtransmission network is also controlled by automatic tap changers on the 400/132-kV and 220/132-kV transformers. Typically 26 steps of 1.1% each are used. Inverse time relays have become common. Most of the transformers between the transmission and the subtransmission are, however, controlled manually by the system operators.

In Sweden, tap changers are used for all transformers between 400 and 10 kV, except for the 400/220-kV network transformers. For subtransmission transformers, constant time relays are used with a time delay of a couple of minutes between steps. In some large load centers, inverse time characteristics have been used with a minimum time of 10 seconds per step. This minimum time, however, is now being increased.

In Australia (New South Wales), main grid transformers have no intentional time delay for large voltage changes. Hence, about seven or eight tap changes can be performed in the first 60 seconds after a large disturbance.

Reference 30 provides a dynamic model for transmission and distribution system LTC transformers and voltage regulators. The model includes time delays and deadbands.

As described in Section 3.3.2, automatic tap changers are important in the development of a voltage collapse. The chances of effectively counteracting a threatening voltage collapse are closely connected with the speed at which the collapse develops. Therefore, the risk of a blackout as the result of voltage instability is greater in a system dominated by inverse time characteristics than in a system dominated by constant time characteristics. This is illustrated by Figure 3-10 in Section 3.5.1 showing a slow voltage collapse in a system which, at that time, was dominated by constant time characteristics. The voltage decreases slowly over a period of fifteen minutes, giving time for the system operators to counteract the event. As a contrast, Figure 3-12 in Section 3.5.2 shows a case from a system dominated by inverse time characteristics in the critical area where a blackout occurred in less than a minute.

Figure 5.1 shows registrations from two Danish 10-kV substations for events causing voltage drops. It takes about eight minutes for the constant time tap changer to restore the voltage after a drop of 8%, while the inverse time tap changers can restore the voltage almost instantaneously, except for the last two steps.

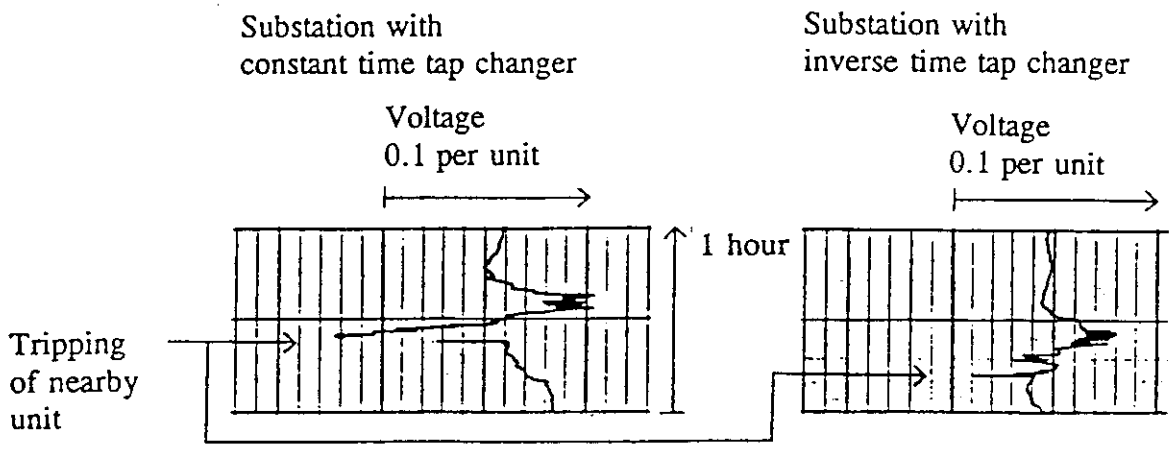

Fig. 5-1. Voltage registration from two Danish 10-kV substations. Tripping of a nearby unit creates a voltage drop. The 10-kV voltage is restored by automatic tap changers.

5.5 Protective Relaying

Of particular concern in voltage stability analysis is the operation of protective devices on overload. Several voltage collapse events have evolved due to operation of sensitively-set distance or overcurrent protective relays applied to operate only for short circuits. The 1978 voltage collapse in France was triggered by an overload relay operating twenty minutes after issuing an alarm.

These devices should be modeled. Alternatively, appropriate quantities, such as line current or apparent impedance, should be monitored in simulation programs.

5.6 HVDC

Voltage collapse is a problem when HVDC links are connected to voltage-weak power systems [31-33]. Because of wide differences in HVDC control systems, user-defined modelling capability is desirable. Detailed models are required for HVDC links connected to weak power systems. Of special interest are strategies to reduce converter reactive consumption during voltage emergencies. These controls may operate through power/current control or through voltage/extinction angle (gamma) control [42].

To improve voltage stability, some new HVDC links normally operate at higher than minimum extinction angles [34].

In power flow and longer-term dynamic simulations, care has to be taken to properly represent the different control modes of the HVDC link, the operation of the associated breaker-switched ac filters and shunt capacitors/reactors, as

well as the on-load tap changer of converter transformers. Special techniques are also available for direct assessment of voltage stability [35].

For transient simulations, proper representation of the HVDC control dynamics is crucial for voltage stability investigations. The interface of ac and dc system solutions require a certain compatibility between the models of both systems [43].

A distinction should be made between power system voltage instability and HVDC control instability [36]. Therefore, most serious investigations require detailed EMTP-type digital simulation, or analog simulation.

Chapter 6

Generation Characteristics and Modelling

Power generating equipment, including their protection and controls, can play an important part in the cause and effect scenario of voltage collapse phenomena. It is necessary to model the relevant characteristics of this equipment.

Most incidents of voltage collapse have not been associated with active power imbalance and consequent underfrequency conditions, but rather with deficiency of reactive power in portions of the system. There are cases, nevertheless, where the role of prime movers and their controls are important, particularly in isolated systems experiencing large generation/load imbalances. Although there is a need to include the dynamic aspects of the prime movers and their controls in the modelling of the voltage collapse phenomena, they will not be treated in detail in this chapter. This omission is largely justified by the fact that for long-term dynamic applications most of the actual prime mover models include the elements necessary for the larger time scale calculations needed for studying voltage collapse phenomena. In this context, an excellent reference is the work of IEEE's System Dynamic Performance Working Group on "Prime Mover and Energy Supply Models for System Dynamic Performance Studies."

The generator model suited for the simulation of voltage collapse has to represent accurately both fast and slow phenomena (from rotor oscillation to quasi steady state operation), whatever the time span considered or the speed of the collapse. Indeed, oscillatory or transient instability may happen at any moment during a slow voltage excursions. As a result, it is necessary to represent:

- The generator saturation in both axes to get a value of internal angle as accurate as possible and to take into account the evolution of control loop gain due to saturation decrease.
- The generator dampers, at least one in each axis, to get accurate information concerning oscillatory stability.

On the other hand, detailed modelling of the excitation system dynamics and automatic voltage regulator is necessary. This chapter will focus on the elements that have to be added to the actual AVR models for studying voltage collapse phenomena. They principally deal with the limiting and protection devices that protect the generator against violating capability limits during voltage collapse.

Fig. 3-3 illustrates in a three dimensional diagram the steady state capability limits of a generator in terms of active and reactive power and network voltage. The most important elements in the overexcited region are the field current limitation surface, imposed by the field winding temperature and the stator current limitation, imposed by the armature winding temperature. The effect of the armature current limitation may be influenced by the maximum developable power of the turbine and increases with higher mechanical power limitation.

In the underexcited region the limitation is imposed to avoid instability, or in some cases, to avoid armature end iron heating problems.

To protect against violating these generator capability limits, a combination of control and protective relaying is used. Modelling of these, including operator action, is important as a number of voltage collapse incidents have been associated with these slower acting elements.

6.1 Excitation Limiters and Protection

In order to protect the generator field and sometimes the excitation system from overheating, most of the automatic voltage regulator (AVR) systems are equipped with an automatic overexcitation limiter. Underexcitation limiters are also added, principally for stability reasons.

6.1.1 Standards

For overexcitation, the action of the limiter causes generator field current to stay within a reasonable steady state overload condition. For short periods of voltage decrease (e.g., during short circuits), the excitation system must reach the ceiling excitation value.

The armature and field overload capabilities are given by the ANSI standards (C50.13-1977) as listed in Tables 6-1 and 6-2, and as illustrated by Figure 6-1 [18].

Table 6-1: Armature overload capability

Time (seconds	10	30	60	120
Armature current (%)	226	154	130	116

Table 6-2: Field overload capability

Time (seconds	10	30	60	120
Field current (%)	208	146	125	112

Depending on the cooling fluid (water, hydrogen) used and the normally used inlet temperature and/or pressure, these characteristics can be displaced in the overload time plane according to the manufacturers instructions.

This time-inverse characteristic is the base for the field and armature limiting control and protection systems.

6.1.2 Overexcitation limiters (OXL) and overexcitation protection (OXP)

Although for some older units the action of limitation is realized by the operator on alarm indication, most of modern AVRs are equipped with a built-in

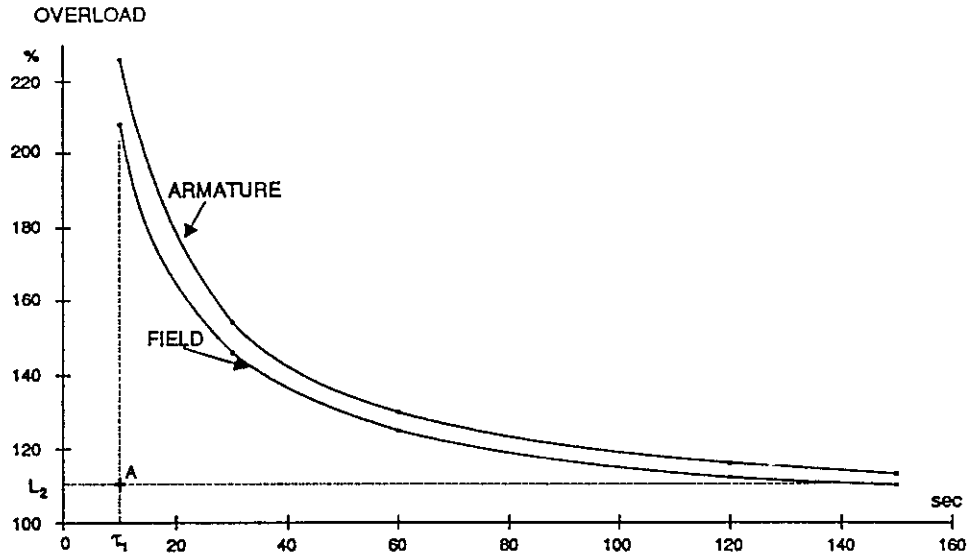

Fig. 6-1. Armature and field overload capabilities (c.f., ANSI C50.13-1977).

limiting device (OXL), combined with a protection system (OXP) independent of the AVR.

Several combinations are possible:

The simplest form of field protection is by an overexcitation limiter with fixed time delay (Case 1, Figure 6-2). Limit L2 and time delay τ_1 are defined by the asymptotic values of the field overload capability curve (Figure 6-1, point A). If the rotor current exceeds L2 for more than τ_1 seconds, the excitation current is limited to a value close to rated value. Return to normal situation is by manual reset of the OXL.

If the limiting action fails, an overexcitation protection device (OXP) trips the generator after a supplementary fixed time delay (τ_2 seconds).

This combination is used on the older electro-mechanical AVRs and some AVRs of the brushless type.

While simple in form, this scheme has the disadvantage that it will overprotect the machine, since the fixed time delay relay must be set for the maximum possible overexcitation condition that can occur. This means that for less severe overexcitation conditions, action will occur at shorter times than is required and, therefore, full advantage of the inverse-time thermal capability of the field winding characteristic cannot be obtained.

The disadvantage of the previous combination is eliminated in the Cases 2, 3, and 4 where the OXL inverse-time characteristic matches with a security space the field overload characteristic. After a time delay function of the real overload, the excitation is limited to a value close to rated value. Return to normal situation is automatic in most cases.

Different combinations may be used on the protection side.

For Case 2 (Figure 6-3), the AVR-OXL has an external backup (BOXL), with an

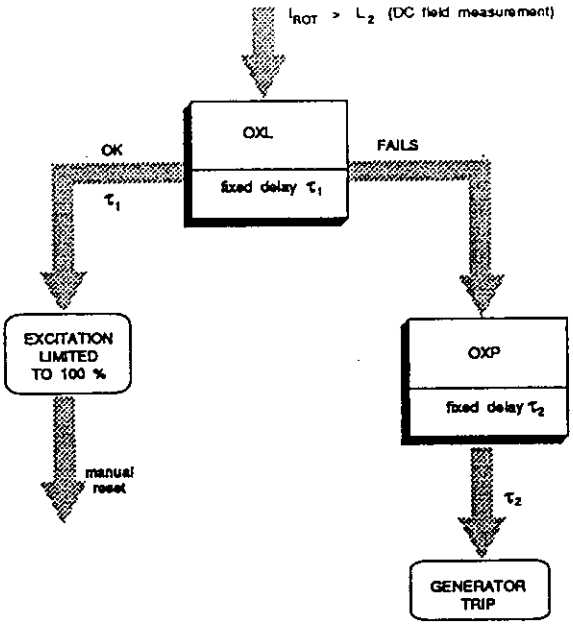

Fig. 6-2. Overexcitation limiter and protection. Case 1: Brushless and electromechanical.

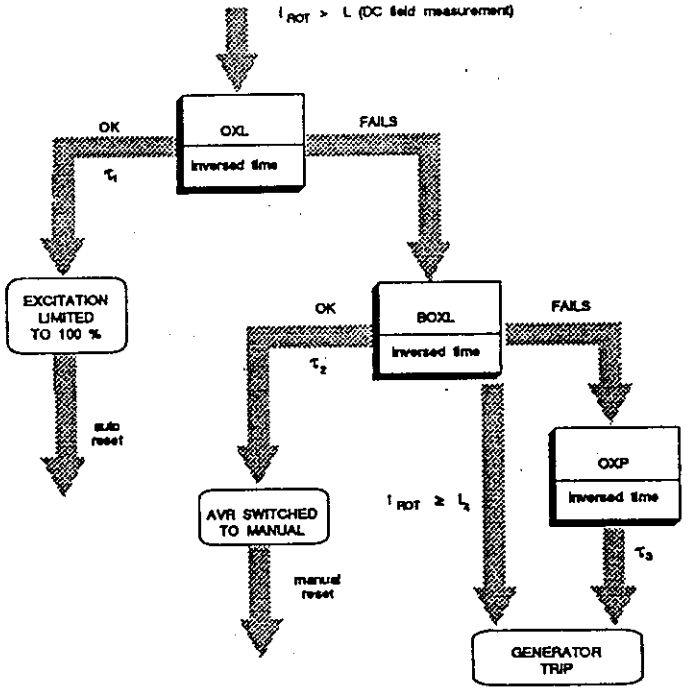

Fig. 6-3. Overexcitation limiter and protection. Case 2: Brushless.

inverse-time characteristic (curve 4 on Figure 6-4) situated between OXL (curve 3 on Figure 6-4) and the field overload characteristic (curve 1 on Figure 6-4). If the field current reaches the OXL curve (e.g., limit 1) the excitation

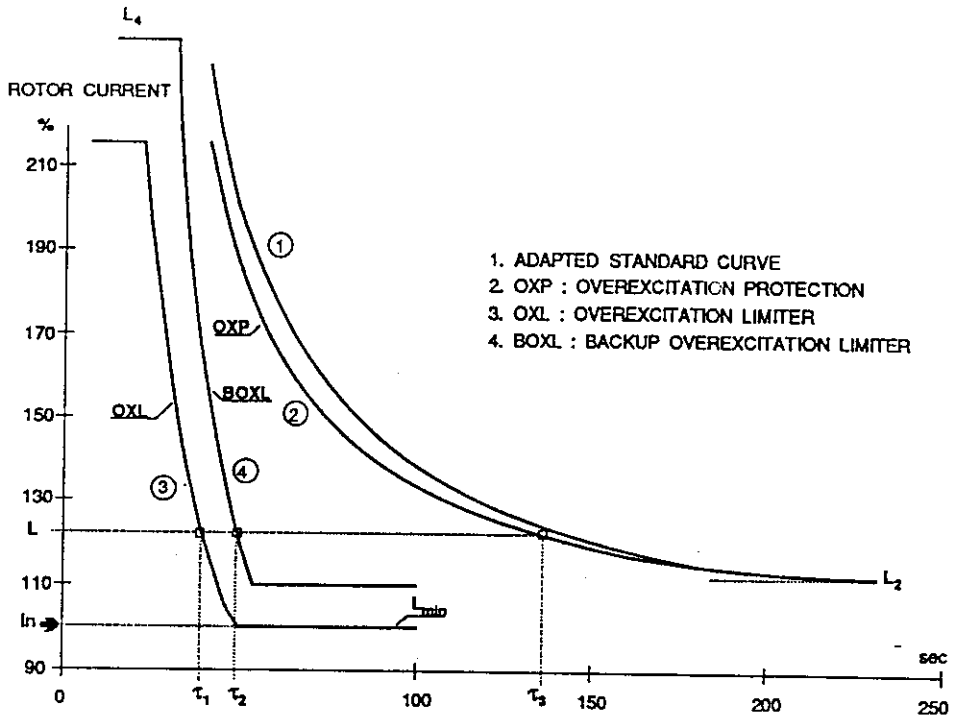

Fig. 6-4. Field current limiter and protection. Curves for 1330 MVA unit.

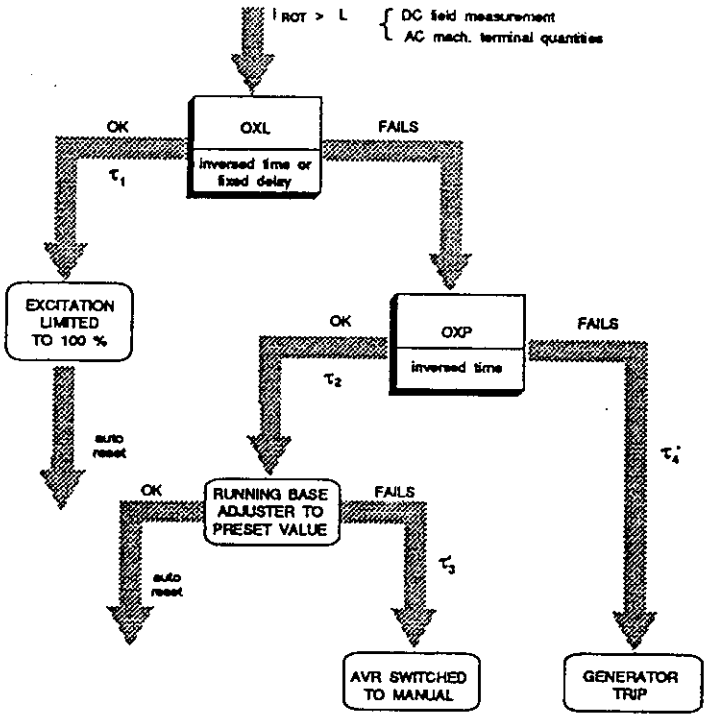

Fig. 6-5. Overexcitation limiter and protection. Case 3: Brushless.

will be limited after τ_1 seconds. If the OXL fails (internal AVR malfunction), the BOXL switches the AVR to manual after τ_2 seconds. If the overcurrent reaches L4 on the BOXL curve, BOXL trips the generator immediately. If both OXL and BOXL do not have any action on the rotor current, an inverse time protection relay (OXP) with a characteristic matching as close as possible the field overload characteristic, trips the generator after τ_3 seconds.

For Case 3 (Figure 6-5), the OXL is backed-up by an inverse-time OXP relay with the following functions:

- Normal action is running the base adjuster to a preset value (τ_2 seconds).
- If this action fails, the AVR is switched to manual after a preset fixed time (τ_3).
- If no action on rotor current after a supplementary preset time, τ_4, the generator is tripped.

For Case 4 (Figure 6-6), the OXL switches the AVR to manual after τ_1 + 5 seconds and trips the exciter field breaker after τ_1 + 10 seconds if no reduction of the rotor current is obtained by the normal OXL action. This combination is used on diode-rectified alternator excitation systems.

For modelling purposes, Figures 6-7 to 6-9 give typical examples and a functional description of OXL limiters for AVRs of different types. Figure 6-10 illustrates a typical response of the OXL of Figure 6-9 for a set point step.

6.1.3 Underexcitation limiters and protection

Since modelling of underexcitation limiters and protection devices are not relevant for voltage collapse studies, this section is limited to a simple overview of these devices.

Most of the AVRs equipped with overexcitation limiters also have built-in underexcitation limiters, in most cases to avoid stability problems (loss of synchronism). These limiters match the capability curve in the underexcited region and may be realized in different ways according to the input signals used.

Different input signals are:

- Combination of voltage and $I \sin \phi$ measurement.
- MVAr measurement.
- MVAr and MW measurement.
- Internal angle measurement.

Backing up this limiter, the generator always has a protection device tripping the unit for low excitation or loss of excitation. Two methods are used:

- Undercurrent or undervoltage relays are applied to the field current.
- A distance relay trips the generator when the operational point enters the circle characteristic. Two types of distance relays, characterized in the MW/MVAr plane are illustrated in Figure 6-11.

6.2 Stator Thermal Protection

The stator of a generator also needs protection against overheating. Two possi

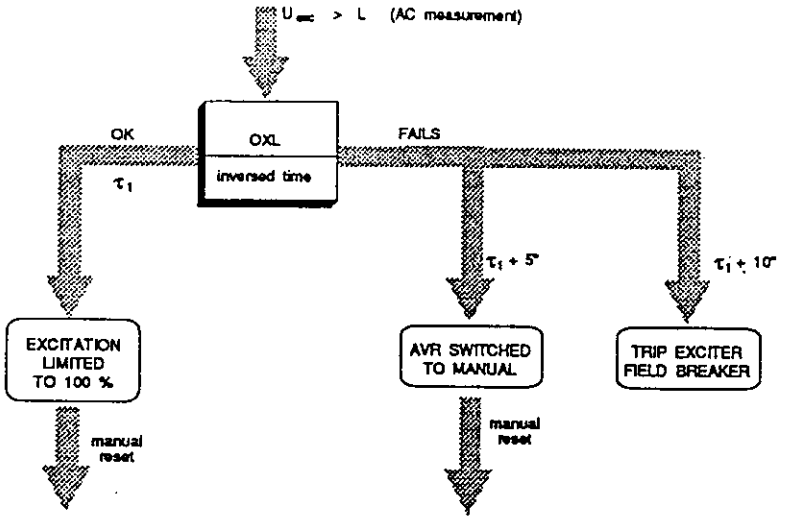

Fig. 6-6. Overexcitation limiter and protection. Case 4: Diode-rectified alternator excitation system.

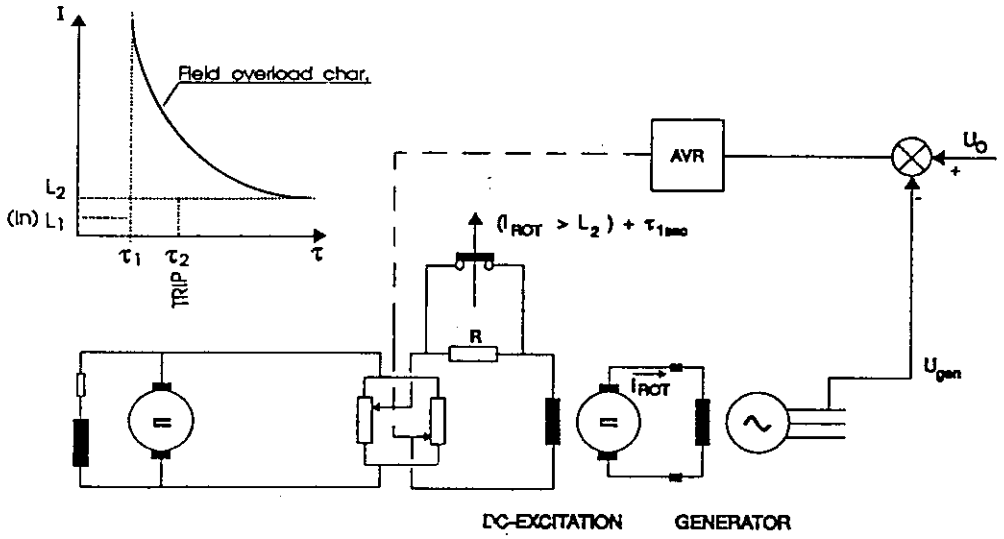

1) Normal situation (limiter out of service)

$I_{rot} < L_2$
Resistance R : out of service

2) Rotor current higher than L_2

After a fixed time τ_1(e.g. 20") ⇒ insertion of R in excitation circuit of DC-excitation machine
R is defined to limit I_{rot} to L_1 for maximum AVR output

Rem.: 1. Hand reset of limiter after return to normal situation
2. If limiter action fails : unit trip for $(I_{rot} > L_2) + \tau_2$ sec. ($\tau_2 > \tau_1$) (OXP)

Fig. 6-7. Overexcitation limiter for electromechanical AVRs (case 1).

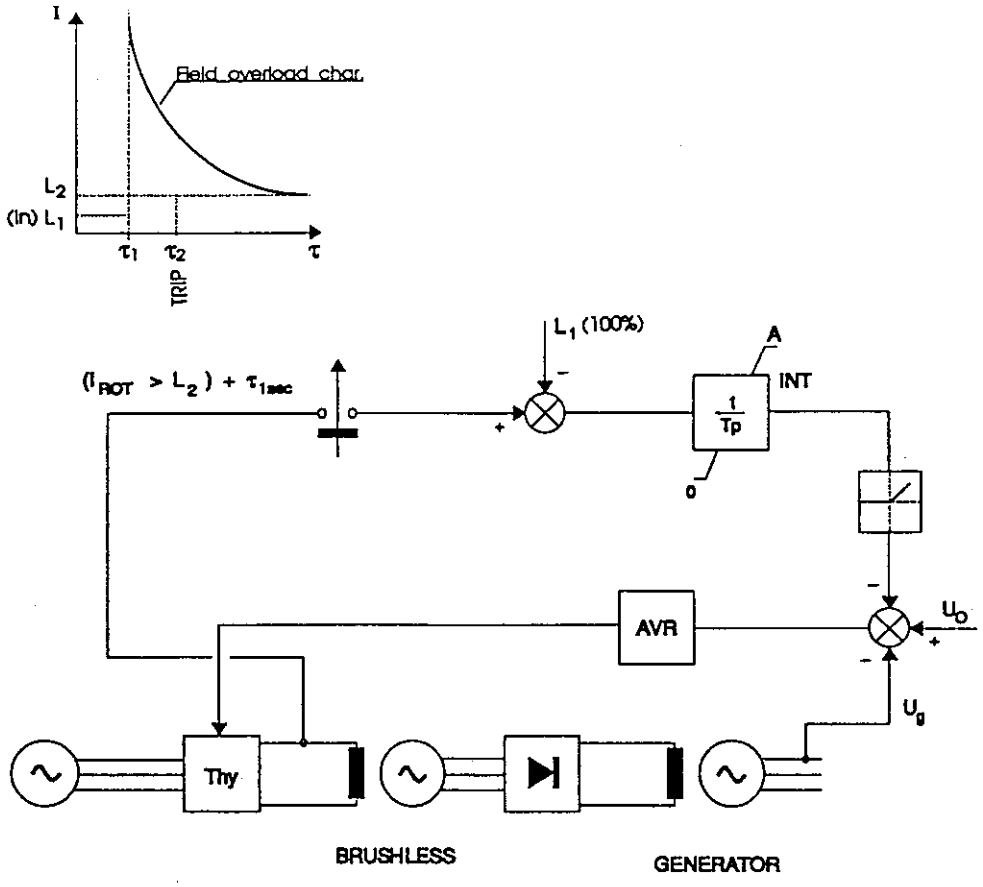

1) Normal situation (limiter out of service)

$I_{rot} < L_2$
Output Int = 0
no influence on AVR

2) Rotor current higher than L_2

After a fixed time τ_1 (e.g. 20") ⇒ limiter in service : I_{rot} limited to L_1 ($= I_n$)

3) Stabilisation value of I_{rot} during limitation

$I_{rot} = L_1$

Rem.: 1. Hand reset of limiter after return to normal situation
2. If limiter action fails : unit trip for ($I_{rot} > L_2$) + τ_2 sec. ($\tau_2 > \tau_1$)
(OXP)

Fig. 6-8. Simplified overexcitation limiter for brushless excitation systems (case 1).

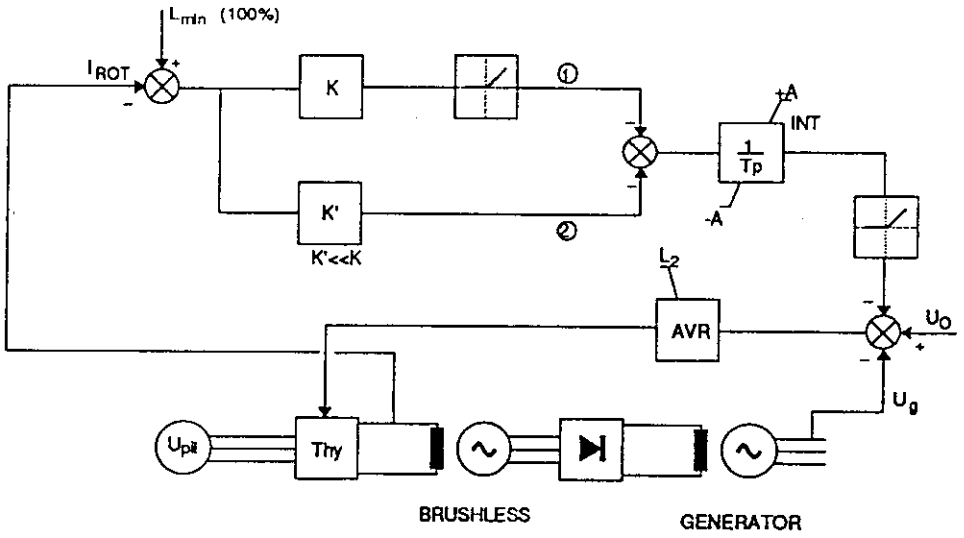

1) Normal situation (limiter out of service)

$I_{rot} < L_{min}$: outp ①: Pos ; outp ②: Pos ; K>>K'
Output Int ➡ -A
no influence on AVR

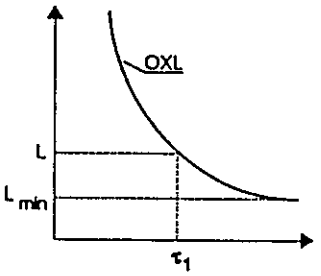

2) Rotor current higher than limit value (L_{min})

$I_{rot} > L_{min}$ (e.g. $I_{rot} = L$)
Input ① of Int ➡ 0 ; Input ②: neg
Integrator leaves minimum value (-A) and reaches 0 V
after a time $\tau_1 = \frac{A.T_1}{L.K'}$ ➡ time inverse to excitation current
Limiter starts to influence AVR

Fig. 6-9. Typical model of overexcitation limiter (case 2).

ble causes of overheating are excessive stator currents due to overload (high MW combined with high MVAr operation) and reduction or loss of the stator cooling system.

6.2.1 Standards

As for the field, there exists an armature overload capability standard, as mentioned in 6.1.1 and plotted on Figure 6-1.

6.2.2 Stator current limitation and protection

In most cases stator current limitation is realized manually by the operator responding to alarms. The operator reduces active and/or reactive load.

Overload alarm may be obtained in different ways:

- Direct measurement of armature current exceeding a fixed limit (e.g.

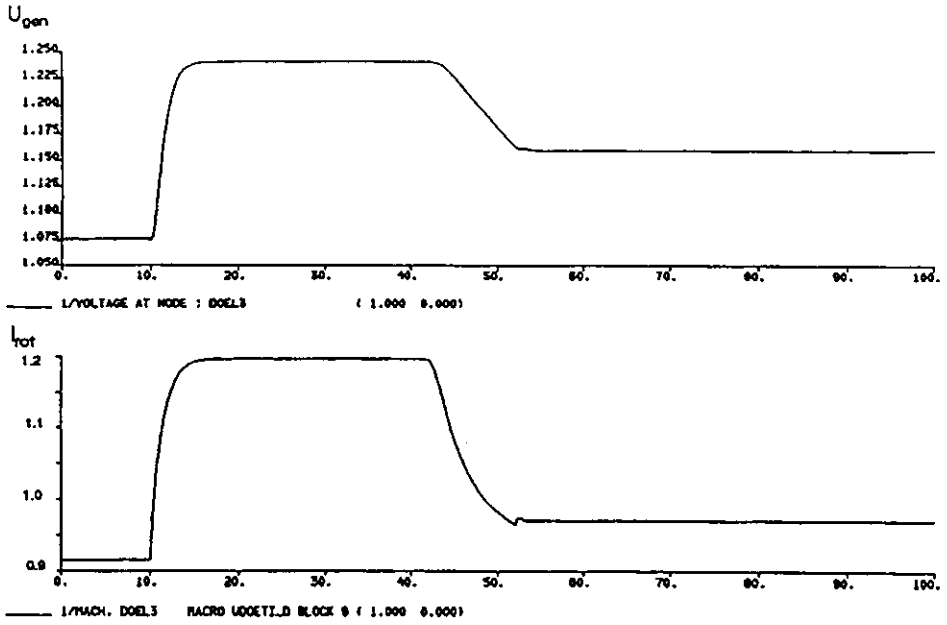

Fig. 6-10. Typical response of overexcitation limiter for a set point change.

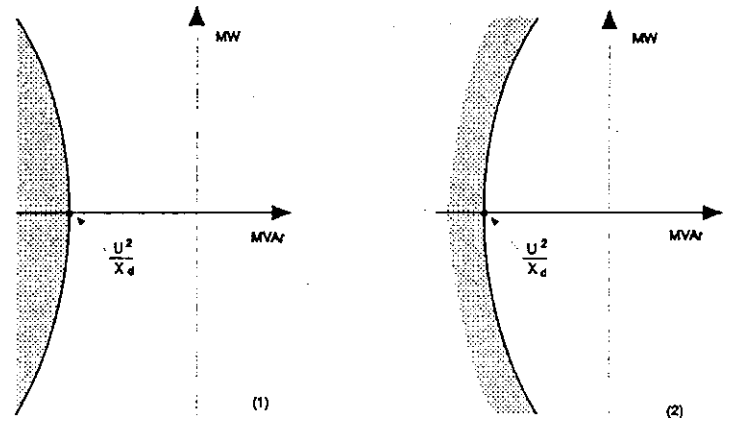

Fig. 6-11. Loss of field relays.

110% of rated current).

- Direct temperature measurement on the stator windings by resistance temperature detectors on thermocouples.

In some cases, a time-delayed stator current limiter is used (Figure 6-12). The stator current is limited by MVAr reduction through the AVR. Time delay and blocking circuits prevent intervention on short disturbances and short circuits.

If the manual or automatic limiting action fails, a trip of the generator circuit breaker (trip to house load) is realized by an inverse-time relay with settings close to the standard characteristics.

6.3 Generation Protection and System Backup Protection

Normally the generator zone is protected against short circuits by differential

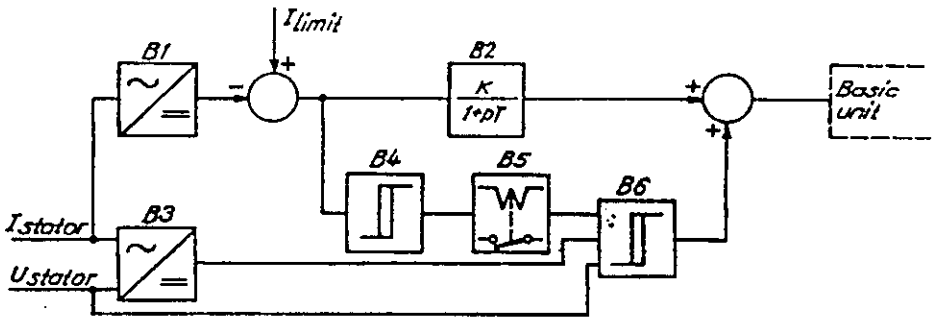

The block functions are :

B1 current measuring device

B2 proportional amplifier with adjustable gain and input filter

B3 phase-sensing rectifier

B4 flip-flop

B5 relay section

B6 flip-flop for blocking of the limiter

Fig. 6-12. Time delayed stator current limiter.

relays. In some cases, the generation zone protection is backed-up by a minimum impedance relay on the low voltage side covering 80% of the transformer impedance.

On the other hand, it is common practice [17] to provide protective relaying that will detect and operate for system faults, external to the generator zone that are not cleared due to some failure of system protective equipment. This protection, generally referred to as system backup, is designed to detect uncleared phase and ground faults on the system.

Two types of relays are commonly used for system phase fault backup: a distance type of relay, or a voltage-restrained or voltage-controlled time overcurrent relay. In order to simplify coordination, the distance backup relay is used where distance relaying is used for transmission line protection, while the overcurrent type of backup relay is used where overcurrent relaying is used for line protection.

In some cases this (distance) relay is set with a very long reach.

A condition which causes the generator voltage regulator to boost generator excitation for a sustained period may cause the system apparent impedance, as monitored at the generator terminals, to fall within the operating characteristics of the distance relay. Usually the time delay for tripping by this relay will be one second or less.

As stated in Section 6.1, modern excitation control systems include overexcitation limiting and protection devices to protect the generator field, but the time delays before they reduce excitation is several seconds. In distance relay applications for which the voltage regulator action could cause an incorrect trip, con-

sideration should be given to reducing the reach of the relay (for example to 80% of the shortest line) and/or coordinating the tripping time delay with the time delays of the protective devices in the voltage regulator.

Separating the backup protection into two relays (one on the low voltage side as stated before and one at the high voltage side) increases the selectivity of this backup protection. As a normal action, this backup protection trips the circuit breaker for transmission-side faults and trips the turbine for generation-side faults.

6.4 Performance of Auxiliaries at Low Voltage

Although undervoltage relaying for tripping auxiliaries is not commonly used at modern power plants, some auxiliary motors could trip on low terminal voltage if contactors are used. It is commonly stated that low auxiliary bus voltages (above, say, 90%) should not alone cause tripping [18].

Practical rules in this context for one country (Belgium) are:

- Auxiliaries are rated for full load production during 1 hour at 85% U_n of the generator between 48.5 and 50 Hz and during 10 minutes between 47.5 and 48.5 Hz.
- More recent units are equipped with a thermal protection, operational for $U < 85\%\ U_n$.
- No undervoltage relays active with closed generator circuit breaker (only low frequency relays at 47.5 Hz).
- With open circuit breaker (e.g., generator on auxiliaries after load rejection), a minimum voltage relay trips the auxiliary transformer for $U \leq 70\%_{\ n}$ during more than 3 seconds.

Chapter 7

Analysis Methods

Analysis methods for voltage collapse can be classified into two approaches. The first approach is based on power flow equations (steady state simulation). The second approach is based on differential equations (dynamic simulation). The latter can be further divided into transient simulation, longer-term simulation, and small-disturbance analysis.

For the purpose of analysis, it's useful to develop both static and dynamic model formulations.

7.1 Steady-State (Power Flow) Analysis

7.1.1 Enhancement of power flow calculation

Steady-state analysis methods are based on the power flow equations, where load and generator conditions are fixed at a specified value. This kind of simulation will be applied pre-disturbance and post-disturbance. Some indicators for voltage instability might be derived based on this steady state conditions.

If a system's condition is close to a critical loading, numerical troubles might be caused during conventional power flow calculations by the Newton-Raphson method. Therefore, additional special techniques should be implemented in power flow programs.

Multiple power flow solutions. As the power flow equations are quadratic simultaneous equations, multiple power flow solutions can exist. Many methods to derive the multiple solutions have been proposed. Two representative methods are as follows.

One method is to set ideal voltage support at some bus in the weak system. By reducing the voltage setting, the lower voltage solution with the same reactive power output can be obtained. The relationship between the reactive power output Q and setting voltage V is called a V–Q curve.

A second method is to change the load of a bus in the weak area into admittance with the same load consumption. By increasing the admittance, the lower voltage solution with same load can be derived.

Improvement of convergence. For deriving the solution in ill-condition, the Newton-Raphson method with modified Jacobian matrix can be applied. Considering the equation for $\mathbf{x}$,

$$\mathbf{f}(\mathbf{x}) = 0,$$

the Newton-Raphson's k^{th} iteration is

$$\mathbf{x}_{k+1} = \mathbf{x}_k + \Delta\mathbf{x}$$

where $\Delta\mathbf{x} = -\mathbf{J}^{-1}\mathbf{f}(\mathbf{x}_k)$

$\mathbf{J}$ is called Jacobian matrix of the system. If the eigenvalue λ_i of Jacobian matrix $\mathbf{J}$ becomes very small, $\|\Delta\mathbf{x}\|$ gets very large and the convergence is difficult. By modifying the $\Delta\mathbf{x}$ into $\alpha\Delta\mathbf{x}$, that is,

$$\Delta\mathbf{x} = -\alpha\mathbf{J}^{-1}\mathbf{f}(\mathbf{x}_k),$$

the magnitude of $\|\Delta\mathbf{x}\|$ is decreased and the convergence property is improved.

In the case when the node load order is over the maximum transmissible power (P_{max}), the calculation used by the conventional Newton-Raphson method does not converge, while in the ill-conditioned cases mentioned above, calculation also does not converge even though there is a solution. In order to distinguish these two cases, one method is to solve the equation in the complex domain. In this method, the imaginary solution is obtained in case of no solution while the calculation does not converge for the ill-conditioned case.

7.1.2 Static models

AGC. Active power generation is specified before voltage static analysis. But load dispatching scenario should be scheduled for snap-shot simulation.

AVR. In static simulation, the generator buses normally are set to be PV type, assuming that AVRs and governors are well behaved. In voltage stability analysis, however, the capability of the generator should be represented properly because it affects the stability of the system, especially for severe conditions.

Of particular concern is the field current limit which, if exceeded for a sufficient length of time, will cause a switch to constant field voltage control and result in decreased terminal voltage. This limit should be represented explicitly and not simply by the conventional reactive power limit (PQ bus type).

Field current limiting increases the likelihood of armature current limiting (automatic or manual), or even generator tripping. Armature current limiting is much more important than field current limiting for the reactive capability of the generator. Armature current limiting should be modelled; alternatively, armature current should be monitored.

Load characteristics. In the power system, there exist many kinds of load characteristics. They have a crucial effect on voltage stability. Voltage sensitivities of the load are normally classified into the constant power, constant current, or constant impedance type in steady-state simulation to analyze the voltage stability. Exponent load models such as:

$$P = P_0 V^{n1},\ Q = Q_0 V^{n2}$$

can also be used.

7.1.3 Transmission system characteristics (*P-V, V-Q* curves)

P-V and *V-Q* curves can be derived from steady-state simulation to illustrate some fundamental properties of AC transmission.

The *P-V* curve shows the relationship between the load of one bus or a group of buses, and the voltage of a representative bus with the assumption that load characteristics are constant. From the *P-V* curve, a maximum transmissible power of the system can be identified. Power factor has a strong influence on the maximum transmissible power and load voltages. Various reactive power

sources (for example, SVC) should be included properly in P-V curve analysis to identify the stability around the maximum transmittable power.

V–Q curve shows the relationship between the voltage and inductive load at a bus, assuming that the nominal power of the load is constant. From the V–Q curve, the system characteristic is obtained at the maximum inductive load.

It is important to select a proper load bus which should represent system characteristics for the analysis.

7.1.4 Indices for voltage collapse

Some indices for voltage collapse can be introduced to evaluate certain conditions of a system. One example is power transfer margin of the system which is the difference between maximum transmissible power and the load at the operating point. It is given for a bus, area, or for the entire system. Based mainly on steady state models, various indices have been proposed, and some of them are in practical use. Relatively well-known indices for voltage collapse, grouped by similar concepts, are the following:

1. Based on sensitivity of reactive power and voltage. (For example, dV/dQ.)
2. Based on power transfer or voltage margin (for example, P-V curve).
3. Based on sensitivity of reactive power generation to load. (For example, VCPI: Voltage Collapse Proximity Indicator defined as the sum of generated reactive power increase divided by real or reactive load increase [58].)
4. Based on the proximity of a pair of multiple solution. (For example, VIPI: Voltage Instability Proximity Indicator).
5. Based on the Jacobian matrix in the linearized steady state power flow equation.

Usually, indicators 1 and 2 are basically defined for each bus, while indices 3–5 are defined for the whole system.

The companion report *Indices for Prediction of Voltage Collapse Including Dynamic Phenomena* by Task Force 38-02-11 provides in-depth comparisons.

An example of an index based on the Jacobian matrix is presented in Appendix I.

7.2 Transient Voltage Stability Simulation

Although classical voltage instability evolves over several minutes, the possibility of transient voltage instability also exists because of the characteristics of fast response system components such as induction motors and HVDC.

The phenomena is usually analyzed by transient stability programs including dynamic models of induction machines.

Transient stability programs offer several possibilities to dynamically model motors, which may be used at transmission as well as distribution levels. One model is simplified and neglects the rotor transients, another takes the rotor transients into account with the rotor fluxes calculated assuming double rotor winding cage. Simulation and experience show that these behaviors have to be taken into account in order to understand correctly transient voltage stability.

7.3 Small-Disturbance Voltage Stability Analysis

The aim of small-disturbance voltage stability analysis is to determine whether a suggested operating point of a power system will be voltage stable in the sense described in the definition 2.2.1. To achieve this goal, the original nonlinear differential and algebraic equations which describe the dynamics of the system have to be linearized around the specified operating point and manipulated to take the standard state space form:

$$[\dot{x}] = [A][x] + [B][z]$$

where $[x]$ is the vector of state variables, $[z]$ is the vector of input variables, [A] is the system matrix, also called the "system dynamic state Jacobian" [59], and [B] is the input matrix.

The eigenvalues of the system matrix determine the dynamic response of the system for small disturbances around the operating point. The corresponding right and left eigenvectors define the shape of the corresponding modes of response. A measure of small disturbance voltage stability is the distance of the eigenvalues corresponding to voltage response modes from the right hand side of the complex plane. The dynamics that play a significant role in voltage stability problems and that can be modelled for small disturbance studies include those of load tap changers [60]. Loads can be modelled explicitly as induction motors, or as a time varying admittance [5]. Generator dynamics can also be included in small disturbance stability studies, provided that the multimachine linearized model includes the voltage dependence of system loads. Multimachine models using the constant impedance load assumption will not predict voltage instability. Second to fourth order generator models [61–63] have been proposed for voltage stability analysis. The dynamics of the excitation systems and automatic voltage regulators are included in these models. The linearized models, however, do not account for excitation limiters. The analysis of small-disturbance voltage stability when a generator reaches its excitation limit can be carried out by modelling this machine as having constant excitation.

7.4 Longer-term Simulation

Voltage instability often occurs because of system dynamics of the order of tens of seconds to minutes. Dynamics include increase of load, recovery of load after disturbances, and power coordination following a loss of generation. Longer-term dynamic simulation is used for these occasions.

Several approaches have been developed for longer-term simulation. Approaches range from simulation of only slow dynamics [19] to unified solution of fast and slow dynamics. Techniques have been used to suppress fast dynamics at appropriate times during the simulation, resulting in computer time savings [20]. The most general method involves unified solution of fast and slow dynamics using an automatically determined variable integration time step [21–23,46–52].

7.4.1 Computer simulation methods

To simulate long-term dynamics, it's important to choose a numerical integration method which achieves reasonable computational time with good precision. There are several methods such as the Euler method, the trapezoidal

method, the Runge-Kutta method, the Gear method. They are classified into basically two methods to calculate a $i+1$ step value x_{i+1} One is the explicit method where only past step values are used, and the other is the implicit method where calculation is recursive using $i+1$ step value.

$$x_{i+1} = f(x_{i+1}, x_i, x_{i-1}, \ldots) \qquad \text{implicit method}$$

$$x_{i+1} = f(x_i, x_{i-1}, \ldots) \qquad \text{explicit method}$$

Implicit methods are more stable numerically for large time step Δt. Since this feature is essential for long-term simulation, implicit methods are superior to explicit methods. It is also noted that each implicit method has various characteristics for numerical damping, e.g., the backward Euler method tends to damp add artificial damping.

One program uses Gear's method with variable time steps [21–23,49–52]. This method adapts and varies the size of time step Δt to the speed of dynamic behavior. For example, if the system settles down after an initial disturbance, a larger Δt will be used to avoid long computation. The size of time step Δt is automatically varied according to numerical error check.

Another program uses a modified trapezoidal method with automatic time step adjustment [46–48]. This program also includes a complementary numerical technique involving quasi-static algebraic modelling for systems experiencing slow variations. For this approach, only the slowly varying dynamics, such as transformer tap motion, thermostatic effects on loads, and protective device timers are explicitly tracked. Other faster dynamics are assumed to be instantaneous. This approach allows for simpler component models with less input data and faster compute times for some types of voltage collapse phenomena. Automatic switching between this mode and solution of all of the differential equations with implicit integration provides for additional flexibility.

The simulation methods must adapt to the many nonlinearities and discontinuities associated with long-term dynamics. Discontinuities include frequent transformer tap changing, generator current limiting, and undervoltage load shedding. Under conditions of voltage collapse, operation of protective devices can substantially alter the topology of the simulated system. The solution method must be able to accurately and stably calculate the dynamics through these changes, including possible system islanding.

7.4.2 Models for longer-term dynamics

The following models may be needed in longer-term dynamic simulation to supplement transient stability program models. Particularly for controls, user-defined modelling is desirable.

1. Load tap changing transformers.
2. Switching of shunt capacitor banks and shunt reactors by various control methods.
3. Static var systems including slow reactive power control and control of mechanical switched capacitor banks and reactors.
4. Generator field current limiting (overexcitation limiters) and armature current limiting or monitoring.

5. Generator centralized or local secondary voltage control.
6. Prime mover and energy supply systems.
7. Centralized automatic generation and system frequency control.
8. Start-up and shut-down of generating units including gas turbines.
9. Static voltage and frequency sensitive loads.
10. Dynamic motor representation including disconnection at low voltage.
11. Discharge lighting extinction and restart as function of voltage.
12. Constant energy, thermostatically-controlled loads.
13. Load ramping and other load changes by bus or area; ability to exclude industrial load from changes.
14. Undervoltage and underfrequency load shedding; load restoration.
15. Transformer saturation.
16. Protective relays tending to operate on overload.
17. Overfluxing (volts/hertz) protection.
18. HVDC links including converter control modes, slow (master) pole and bipole controls, converter transformer tap controls, and mechanically switched ac filters and shunt capacitors/reactors.

7.4.3 Desired features of longer-term dynamics simulation programs

In addition to comprehensive modelling, other desirable features of state-of-the-art longer-term simulation programs include:

1. Eigenvalue computation at points along time trajectory.
2. Ability to represent arbitrarily large networks. For example networks of up to 15,000 busses are sometimes represented in the eastern North American interconnection (the asynchronously-connected Quebec network is included).
3. Network reduction facilities. Since voltage stability is basically a local problem, equivalents are sometimes adequate for remote parts of the network.
4. Ability to interface with programs such as EPRI's LOADSYN [44,45] which provide load component data. For example, thermostatically-controlled load from LOADSYN should interface with simulation program load model controls.
5. Capability to interactively initiate operator-directed actions.
6. Automatic integration step size control. The integration scheme should be both numerically stable and accurate for a wide range of possible system disturbances.
7. Interface to widely-used power flow programs and dynamic data sets.
8. User-defined models without severe penalties in computer time compared to hard-coded models. Highly specific microprocessor-based

controls modelling is sometimes required.

9. Flexible output analysis for printing and plotting of system variables (including internal device variables), and combinations of system variables. Special analysis options including voltage magnitude analysis, relay margin analysis and spectral analysis. It should be possible to analyze output variables without prior declaration.

7.4.4 Available production grade programs

As for programs which are able to simulate longer-term dynamics with some or most of the above models and features, we can mention EUROSTAG [21–23,49–52], ETMSP (EPRI/Ontario Hydro), PTI PSS/E [24], and EXSTAB (General Electric/Tokyo Electric Power Company) [46–48].

In addition to the references, descriptions and comparisons of longer-term dynamics programs are included in the Task Force 38-02-08 report on long-term dynamics.

Chapter 8

Sensitivities of Voltage Stability to System Characteristics

8.1 General

Modelling power systems for the analysis of voltage stability requires a clear understanding of how system characteristics influence dynamic performance. We are not particularly interested in events which can initiate voltage instability, such as the loss of line or generator, but rather we are interested in determining how the system responds to such events, the devices which react, the sequence in which they react, and the parameters which may influence the course of events. Experience shows that apparently minor events may trigger a complex sequence of actions, involving a number of control or protective devices, which may lead to voltage instability. Although there are many system parameters which can subtly influence stability, a few key factors have been identified which may have significant impact.

Induction motor performance may prove critical in determining voltage stability, primarily due to the increased reactive power demand from these devices at reduced voltage. Sustained undervoltage may cause motor stalling accompanied by high reactive draw, or motor tripping by protective relaying. Motor tripping can prove critical to voltage stability as was demonstrated in the South Florida blackout in May 17, 1985 [1], in which plant auxiliaries were lost during low voltages, leading to unit tripping and contributing to subsequent voltage instability.

Load characteristics and action of load tap-changers (LTC) are well known as key factors influencing system voltage stability. Loads which are very stiff (such as constant MVA) will not be influenced by voltage reductions and can in themselves pose problems when system voltage is weak. On the other hand, soft loads (such as constant impedance), will decrease as voltage is reduced. Though this helps a weak system, LTCs will eventually react to restore load voltage and often bring on voltage instability. For example, the December 27, 1983 Swedish blackout was a result of a large disturbance in which the systems were unable to meet active and/or reactive power demands. The voltage dependency of natural loads, and the restoring of loads through LTC actions were key factors in the voltage collapse.

Generator excitation characteristics have been contributing factors in a number of voltage instability incidents. In both the January 12, 1987 French incident, and the December 28, 1982 Florida incident [1], generators were tripped on excitation protection leading to reduced system voltages and/or overloading

of remaining units. Even if units are not tripped, a reduction in reactive capability due to the action of field current limiters can prove devastating on a weakened system.

Most incidents of voltage instability involve a combination of the above factors, and it is often difficult to isolate any one action as responsible for the instability. The influence of these factors can be best demonstrated using simulations which serve to isolate the individual effects of certain system characteristics. In this chapter, test systems are used with time domain simulations to illustrate the potential impact and sensitivities of various system characteristics. In addition, the use of static analysis as a complementary approach to dynamic analysis is presented.

8.2 Simulation Results

Voltage stability simulation results of different test systems are presented in Appendix I–VII. Materials from some of the contributors have been edited to fit the volume of the report. Originals can be obtained upon request.

The main objectives of the studies are:

- Voltage stability analysis of small and large test systems.
- Dynamic simulation using different programs (EUROSTAG, ETMSP, etc.).
- Sensitivity of voltage stability to load characteristics.
- Sensitivity of voltage stability to generator excitation characteristics.
- Sensitivity of voltage stability to generator line drop compensation and secondary voltage regulation.
- Sensitivity of voltage stability to undervoltage load shedding.
- Sensitivity of voltage stability to weak systems.
- Sensitivity of voltage stability to HVDC control.
- Comparison of static and dynamic voltage stability analysis results.

In Appendix I, two test systems are considered. System A is a small system consisting of 10 buses, 14 branches and 3 generators. System B, based on an actual system used in planning studies, is a large system with 622 buses, 1083 branches and 129 generators. The program used for time domain simulation is the Extended Transient/Midterm Stability Program (ETMSP) developed by Ontario Hydro.

In Appendix II, the small test system as shown in Figure II-1 is studied. Sensitivities to generator automatic voltage regulators (including overexcitation limiting), secondary voltage regulation, and LTC transformers are demonstrated.

Appendix III considers the voltage stability of a practical system. The simulation program used is the EUROSTAG package, jointly developed by Electricité de France and Tractebel.

Appendix IV considers the transient voltage stability of a practical system comprising 240 buses, 267 lines, and 30 equivalent generators. The effect of load

representation (constant impedance versus constant power) on the simulation of voltage collapse is studied.

Appendix V considers the voltage stability of a very large (5000 bus) system using the ETMSP program. Following a major disturbance, load restoration is simulated by a combination of many induction motor equivalents, LTC transformer regulated loads, and thermostatically-controlled loads. Sensitivities to undervoltage load shedding and generator line drop compensation are demonstrated.

Appendix VI considers transient voltage stability in weak systems. In weak systems, voltage instability and collapse will occur within a few seconds.

Appendix VII considers transient voltage stability associated with HVDC links. The dominant effect of HVDC control characteristics is demonstrated.

8.2.1 Sensitivity to load characteristics

Load characteristics are very important in the study of system voltage stability. Following a major disturbance, voltages at load buses will decrease. If load is not modelled as constant MVA, load power will generally decrease before LTCs operate, because of the voltage dependency of natural load characteristics. It is unlikely, unless voltages have declined to the point at which induction motors stall, that voltage instability will occur until LTCs begin to operate to restore load bus voltages.

Effect of LTC operation. Once LTCs start to operate, voltages at load buses will gradually be brought up toward their pre-disturbance values, and hence the load power will increase. As load power increases, field currents of some generators will exceed their limits, and field current limiters will start to bring the field currents to within their limits. The limiting of generator field currents causes the generator terminal voltages to be reduced, thereby reducing load bus voltages. If the effect of increasing load bus voltage through LTC operation is greater than the effect of decreasing load bus voltage by field current limiter action, the net effect will be an increase in load bus voltage, and hence the system remains voltage stable. If on the other hand, the effect of field current limiter is greater than that of LTC operation, the net effect is a decrease in load bus voltage, and the system is voltage unstable.

In Appendix I, cases with and without LTC operations are studied. We see from Figure I-2 that the system is voltage stable without LTC operations. With LTC operations, the system becomes voltage unstable as shown in Figure I-3.

In Appendix II, we demonstrate that the timely blocking of LTC actions can stop the development of voltage instability process.

In Appendix III, a case is simulated in which tripping of a unit when LTCs are present leads to more units being tripped due to the actions of under voltage protection. This in turn leads to voltage collapse.

In Appendix IV, the effect of constant power load versus mixed constant power, constant admittance load representation is studied. It is shown that if constant power load representation is used, the system exhibits voltage instability, as shown by the response of the system for a relatively minor disturbance. In the 50% constant power, 50% constant admittance load representation case, the

system does not exhibit voltage problems, while in the 90% constant power, 10% constant admittance case, the voltage oscillates before reaching its steady state value.

Effect of induction motors. The amount of reactive power drawn by an induction motor increases drastically as motor terminal voltage decreases. This increase in reactive demand may significantly impact system voltage stability. Also, an induction motor starts to decelerate as its terminal voltage decreases. Once voltage becomes very low, voltage instability due to induction motor stalling may follow in a very short period of time.

Two cases are considered in Appendix I. The first case (Case C) has one of the two loads modelled as 100% constant MVA load, and the second case (Case D) has the same load modelled as 50% constant MVA load and 50% induction motor load. It is seen (Figure I-4) that, with induction motor load included, voltage instability occurs slightly earlier following the contingency. The sharp increase of motor reactive power as voltage decreases is also shown (Figure I-5).

Effect of undervoltage load shedding. Appendix V shows an example of voltage stability improvement using an undervoltage load shedding program that is implemented in the Pacific Northwest region of the U.S.A.

8.2.2 Sensitivity to generator excitation characteristics

Generators generally represent the most important sources of reactive power and voltage support to a system. AVR action attempts to maintain the generator terminal voltage at its pre-set reference value by continuously adjusting the field voltage and consequently the field current. However, an AVR is able to control generator terminal voltage only if the field current is within its steady state continuous limit. Once the field current becomes higher than its continuous limit, field current limiter action starts to reduce the field current to within its limit. The time it takes for the field current limiter to reduce the field current to within its limit depends on the setting of each field current limiter and how much the field current goes beyond its limit. Typical continuous field current limit is 5% above the field current at rated machine terminal voltage, with rated MVA output at rated power factor. Each machine may have a different field current limiting device. Typically, if the field current is at a level just above the continuous limit, the limiter will bring the field current back to within limits in about 30 seconds.

If no field current limits are imposed, an AVR regulates the machine terminal voltage towards its pre-set reference value, with a slight reduction due to the droop characteristic of the AVR control loop. The reduction in machine terminal voltage due to AVR droop characteristic, as machine output increases, depends on the equivalent gain factor of the overall AVR control loop. As an alternative, line drop compensation may be used to regulate the high voltage bus, or to compensate for a portion of the generator step up transformer impedance. As demonstrated in Appendix I and Appendix V, this technique can improve voltage stability.

In Appendix I, the following cases with different generator excitation characteristics are considered:

1. Field currents of different machines limited (Case C, E & F, Figure I-3, Figure I-6–I-10)

2. Effect of AVR line drop compensation (Figure I-11–I-13).

3. Effect of AVR droop characteristics.

Voltage stability of the large system, with and without generator field current limits, is also studied. The results are shown in Figure I-14 and Figure I-15. The system is voltage stable without generator field current limits imposed, and voltage unstable with generator field current limits included.

Appendix II considers two cases, the first (Test PT) with no generator field current limit and the second (Test PLT) with generator field current limits. Simulation results show that without generator over-excitation limit the system is voltage stable for reasonable load perturbations (Figure II-5 and Figure II-8). With generator overexcitation limits included, the system becomes voltage unstable as a result of 50% increase in load admittance (Figure II-11 and Figure II-12).

In Appendix III, voltage instability due to shortage of reactive power is simulated for a large realistic system. Results of preventing voltage instability using curative measures are also shown (Figure III-4).

In Appendix V, voltage stability improvement, in the form of reduced undervoltage load shedding, results from generator line drop compensation.

8.2.3 Sensitivity to secondary voltage regulation

Sensitivity of system voltage to secondary voltage control is studied in Appendix II (Test PLST). The block diagram of secondary voltage regulation is shown in Figure II- 3. Results of dynamic voltage stability analysis including the effect of secondary voltage regulation are shown in Figure II-13–Figure II-19.

This system voltage regulation is obtained by an hierarchical control structure consisting of an automatic Reactive Power Regulator for each of the controlled power plants, which controls the plant reactive power through the set points of the local unit AVRs. This Reactive Power Regulator actuates the request coming from the higher level Regional Pilot-Node Voltage Regulator which controls, in closed loop, the main bus voltage in the region by the local controlled power plants.

Secondary voltage regulation helps improve overall system voltage stability if no overexcitation limits are imposed on generators. With overexcitation limits included, secondary voltage regulation has little effect on overall system voltage stability.

8.2.4 Sensitivity to HVDC control system characteristics

Appendix VI describes voltage stability considerations associated with HVDC links, including computation of the "voltage stability factor," VSF. Time simulations confirm results using the VSF, showing, in particular, the stability improvement with HVDC inverters operating in dc voltage control rather than constant extinction angle control.

8.2.5 Static modal analysis

Details of voltage stability assessment using modal analysis technique can be found in reference 2. The basic process of modal analysis involves the compu-

tation of a group of eigenvalues and eigenvectors of the reduced system steady state Jacobian matrix. The system is considered voltage stable if all the eigenvalues of the reduced Jacobian matrix are positive, and voltage unstable if at least one eigenvalue is negative. The magnitude of each positive eigenvalue determines the weakness of the corresponding modal voltage. The smaller the magnitude of the eigenvalue, the closer the corresponding modal voltage is to being voltage unstable. If the eigenvalue is zero the system is on the verge of voltage instability.

In Appendix I, modal analysis was conducted at different time frames following the contingency. Results of modal analysis at different snapshots are shown in Table I-6. From the modal analysis results, it is concluded that the system is voltage stable before the disturbance and after the disturbance before the field currents are limited. Voltage instability occurs once the field current for machine 3 is limited. Using the time domain simulation results as benchmark, modal analysis determines correctly when system voltage instability occurs.

For the slower dynamics studied, comparison of modal analysis with time domain simulations indicates that the results obtained using the two methods generally agree. Each approach offers certain advantages depending on the task at hand. Tools based on the static approach, such as modal analysis, are very useful for assessing system voltage stability for a wide range of system conditions or contingencies. Modal analysis, coupled with other static techniques, can provide good indication of proximity to, and mechanism of, voltage instability, with much lower computational burden than dynamic simulation. Static approaches are therefore ideally suited for the bulk of planning work. However, for detailed investigation of particular incidents, postmortem analysis, or for coordination of controls and protective systems, time domain simulation is generally the tool of choice. Although time domain simulations do not provide direct measures of stability, they can show clearly the sequence of events which may lead to voltage instability.

8.3 Concluding Remarks

Appropriate device modelling is necessary for accurate assessment of system voltage stability. Certain key devices may have significant impacts on system voltage stability, and their effect must be considered in performing system voltage stability studies. These include:

- Loads (static loads, induction motors, constant energy loads, undervoltage load shedding).
- LTCs.
- Generator field current (overexcitation) and armature current limiters.
- AVR (primary and secondary voltage regulation including line drop compensation).
- HVDC control characteristics.

Conventional simulation tools for transient angle stability studies may not adequately model all these devices to properly capture their actions and interactions. Also simulation tools must be capable of simulating system behavior over time periods of sufficient length to consider the effect of these devices on

system voltage stability. Therefore, transient stability simulation tools have to be enhanced for longer-term voltage stability studies.

Time domain simulations are essential for the fast dynamics associated with transient voltage stability. For longer-term voltage stability, time domain simulations are necessary for detailed dynamic analysis and studies requiring coordination of control and protection. However, time domain simulation usually takes large amounts of CPU time.

Voltage stability analysis using static approaches such as modal analysis of the reduced Jacobian matrix is computationally less intensive and provides more insight into the mechanism of instability.

A set of system conditions, or snapshots, which closely approximates a point along the time domain trajectory has to be obtained for static voltage stability assessment. System conditions at different snapshots can be obtained by solving a set of steady state algebraic equations with appropriate models for controls and limits, including those associated with LTCs and generator overexcitation limiters.

Chapter 9

Conclusions

A power system is a dynamic system, and voltage instability and collapse involve various dynamic phenomena. The definitions provided in Section 2.2, which are similar to stability definitions for other dynamic systems, reflect this fact. The dynamics are very complex, involving generation, transmission, distribution, and load elements of power systems. Both continuous and discontinuous dynamics are present. Chapter 3 describes mechanisms of voltage collapse phenomena.

From a simulation viewpoint, a key question is the appropriateness of various steady state analysis methods for fast, approximate analysis. As shown in Chapter 8, steady state methods are often valuable for analysis of longer-term voltage collapse. Near stability boundaries and for other reasons discussed in Chapter 8, however, dynamic simulation is vital.

Fortunately, sophisticated computer programs for simulation of longer-term dynamics are now available. The appendices provide many examples of dynamic simulation. As shown in the appendices, the various aspects and mechanisms of voltage instability and collapse can be demonstrated by time domain simulation. Available computer programs are described in Chapters 1 and 7. Chapter 7 describes desirable features of simulation programs.

Chapters 4–6 describe characteristics and models of the many power system components important for voltage stability simulation. Contrasted with steady state and dynamic analysis for other purposes, voltage stability analysis may require detailed representation of loads, including expanded representation of subtransmission networks and possibly equivalents for distribution network impedances. Dynamic modelling of aggregated load components may be required. Generator modelling may require detailed representation of generator current limiting controls. In power flow programs, simple switching from PV to PQ generator bus type may not be sufficiently accurate.

Future industry work is needed to improve models. Specific areas for improvements are:

1. Standardization of models and data exchange parameters for overexcitation limiters and protection.
2. Load modelling, including representation of subtransmission and distribution impedance effects.

While models and simulation techniques will continually improve, simulation— especially for longer-term events— will never closely match real system response to voltage stability threatening disturbances. For example, operator actions are difficult to predict. For a second example, modelling of

aggregated induction motors will not capture the possibility of a stall-prone motor at the end of a feeder that could start a cascading of motor stalling. For high-fidelity simulation, the amount of data required for loads and for control and protection equipment is overwhelming.

Power systems must therefore be designed with sufficient margins for uncertainties. The required margins should take into account the probability of extreme conditions threatening voltage stability as well as backup protection such as undervoltage load shedding.

References

1. IEEE Committee Report, *Voltage Stability of Power Systems: Concepts, Analytical Tools, and Industry Experience*, IEEE/PES 90TH0358-2-PWR, 1990.
2. B. Gao, G. K. Morison, and P. Kundur, "Voltage Stability Evaluation Using Modal Analysis," *IEEE Transactions on Power Systems*, Vol. 7, No. 4, pp. 1529–1542, November 1992.
3. D. J. Hill, Per-Anders Löf, and G. Andersson, "Analysis of Long-Term Voltage Stability" *Tenth System Computing Conference*, pp. 1252–1259, Graz Austria, 1990.
4. IEEE Committee Report, "Proposed Terms and Definitions for Power System Stability," *IEEE Transactions on Power Apparatus and Systems*, Vol. PAS-101, No. 7, pp. 1894–1898, July 1982.
5. M. K. Pal, "Voltage Stability Conditions Considering Load Characteristics," *IEEE Transactions on Power Systems*, Vol. 7, No. 1, pp. 243–249, February 1992.
6. Th. Van Cutsem, "Dynamic and Static Aspects of Voltage Collapse," *Proceedings: Bulk Power System Voltage Phenomena—Voltage Stability and Security*, EPRI EL-6183, pp. 6-55–6-79, January 1989.
7. B. M. Weedy, *Electric Power Systems*, Third Edition Revised, John Wiley & Sons, 1987 (earlier editions 1967, 1972, and 1979).
8. E. S. Cate, K. Hammaplardh, J. W. Manke, and D. P. Gelopulos, "Time Frame Notion and Time Response of the Models in Transient, Mid-Term and Long-Term Stability Programs," *IEEE Transactions on Power Apparatus and Systems*, Vol. PAS-103, No. 1, pp. 143–151, January 1984.
9. C. W. Taylor, "Concepts of Undervoltage Load Shedding for Voltage Stability," *IEEE Transactions on Power Delivery*, Vol. 7, No. 2, pp. 480–488, April 1992.
10. CIGRÉ TF 38-01-03, "Planning Against Voltage Collapse," *Electra*, No. 111, March 1987.
11. CIGRÉ TF 38-01-03, *Planning Against Voltage Collapse*, extensive version with all appendices, October 1986.
12. M. S. Baldwin and D. P. McFaddem, "Power System Performance as Affected by Turbine-Generator Controls During Frequency Disturbances," *IEEE Transactions on Power Apparatus and Systems*, Vol. PAS-100, No. 5, May 1981.
13. W. R. Lachs, "Reactive Power Pulses for System Voltage Control," IEEE PES Winter Meeting 1979, Paper A 79 014-2.
14. P. Modlitba, P. Pavlinec, V. Vyskocil, F. Kozák, V. Kalousek, "Analytical Method for Evaluating Power System Transfer Capability with Regard to Voltage Stability," *CIGRÉ* 1986, 38-06.
15. G. Shackshaft, O. C. Symons, and J. G. Hadwick, General-Purpose Model of Power-System Loads, *Proc. IEE*, Vol. 124, No. 8, August 1977.
16. S. A. Y. Sabir and D. C. Lee, "Dynamic Load Models Derived from Data Acquired During System Transients," *IEEE Transactions on Power Apparatus and Systems*, Vol. PAS-101, No. 9, pp. 3365–3372, September 1982.
17. IEEE Committee Report, *IEEE Guide for AC Generator Protection*, ANSI/IEEE C37.102-1987.
18. C. W. Taylor, "Generating Plant Control and Protection under Abnormally Low Network Voltages," presented at panel session on Dynamic Security Assessment from and Operational Standpoint, IEEE/PES 1991 Summer Meeting, 30 July 1991.

19. General Electric Company, *Long Term Power System Dynamics*, EPRI Final Report, Research Project 90-7, April 1974.
20. R. J. Frowd, J. C. Giri, and R. Podmore, "Transient Stability and Long-Term Dynamics Unified," *IEEE Transactions on Power Apparatus and Systems*, Vol. PAS-101, No. 10, pp. 3841–3849, October 1982.
21. M. Stubbe, A. Bihain, J. Deuse, and J. C. Baader, "STAG - A New Unified Software Program for the Study of the Dynamic Behaviour of Electrical Power Systems, *IEEE Transactions on Power Systems*, Vol. 4, No. 1, pp. 129–138, February 1989.
22. M. Stubbe, A. Bihain, J. C. Baader, and J. Deuse, "Simulation of the Dynamic Behaviour of Electrical Power Systems in the Short and Long Terms," CIGRÉ 38-03, 1988.
23. J. Deuse and M. Stubbe, "Dynamic Simulation of Voltage Phenomena," *Proceedings of International Workshop on Bulk Power System Voltage Phenomena: Voltage Stability and Security*, Deep Creek Lake, Maryland, 4–7 August 1991.
24. F. P. de Mello, J. W. Feltes, T. F. Laskowski, and L. J. Oppel, "Simulating Fast and Slow Dynamic Effects in Power Systems," *IEEE Computer Applications in Power*, Vol. 5, No. 3, pp. 33–38, July 1992.
25. T. J. E. Miller, editor, *Reactive Power Control in Electric Systems*, John Wiley & Sons, New York, 1982.
26. Westinghouse Electric Corporation, *Electrical Transmission and Distribution Reference Book*, East Pittsburgh, Pennsylvania, 1964.
27. D. L. Goldsworthy, "A Linearized Model for MOV-protected Series Capacitors," *IEEE Transactions on Power Systems*, Vol. PWRS- 2, No. 4, pp. 953–958, November 1987.
28. C. Nguyen, M. Cousel, and R. Lord, "Modelling MOV-Protected Series Capacitors for Short-Circuit Studies," *Power Technology International 1990*, pp. 97–99.
29. CIGRÉ TF 38-01-02, *Static Var Compensators*, 1986.
30. M. S. Calovic, "Modeling and Analysis of Under-Load Tap Changing Transformer Control Systems," *IEEE Transactions on Power Apparatus and Systems*, Vol. PAS-103, No. 7, pp. 1909–1915, July 1984.
31. A. Gavrilovic et al., (CIGRÉ/IEEE committee paper), "Interaction Between DC and AC Systems," *CIGRÉ Symposium on AC/DC Transmission Interactions and Comparisons*, paper 200-20, Boston, 28-30 September 1987.
32. L. A. S. Pilotto, M. Szechtman, and E. Salgado, "The Problem of Voltage Collapse in AC/DC Systems," *I Symposium of Specialists in Electric Operational Planning*, Rio de Janeiro, August 1987.
33. IEEE Committee Report, "HVDC Controls for System Dynamic Performance," *IEEE Transactions on Power Systems*, Vol. 6, No. 2, pp. 743–752, May 1991.
34. A. E. Hammad, H. Koelsch, and P. Dachler, "Active and Reactive Power Controls for the Gezhouba–Shanghai HVDC Transmission Scheme," *Fifth International Conference on AC and DC Power Transmission*, IEE Conference Publication No. 345, pp. 279–284, 17–20 September 1991.
35. A. E. Hammad and W. Kühn, "A Computation Algorithm for Assessing Voltage Stability at AC/DC Interconnections," *IEEE Transactions on Power Systems*, Vol. 1, No. 1, pp. 209–216, February 1986.
36. L. A. S. Pilotto, M. Szechtman, and A. E. Hammad, "Transient AC Voltage Related Phenomena for HVDC Schemes Connected to Weak AC Systems," *IEEE Transactions on Power Delivery*, Vol. 7, No. 3, pp. 1396–1404, July 1992.
37. K. V. Korobschuk, "Calculation of Steady State Behaviour of Large Power

System Taking Account of Voltage Load Characteristics," ISSN 0204-3599, Techn. Elektrodinamika, 1990, No. 2, USSR.

38. R. B. Adler and C. C. Mosher, "Steady State Power Characteristics for Power System Loads," IEEE paper 70CP 706-PWR.
39. M. H. Kent, W. R. Schmus, F. A. McCrackin, and L. M. Wheeler, "Dynamic Modeling of Loads in Stability Studies," *IEEE Transactions on Power Apparatus and Systems*, Vol. PAS-88, No. 5, pp. 756–763, May 1969.
40. J. D. McCully, J. F. Dorsey, J. F. Luini, R. P. Mackin, and G. H. Molina, "Subtransmission Reduction for Voltage Instability Analysis," paper 92 WM 127-7 PWRS, IEEE/PES Winter Meeting, New York, January 1992.
41. A. Hammad, M. El-Sadek, "Prevention of Transient Voltage Instabilities due to Induction Motor Loads by Static VAr Compensators," *IEEE Transactions on Power Systems*, Vol. 4, No. 3, pp. 1182–1188, August 1989.
42. A. Hammad, J. Gagon, and D. M. McCallum, "Improving the Dynamic Performance of a Complex AC/DC System by HVDC Control Modifications," *IEEE Transactions on Power Delivery*, Vol. 5, No. 4, pp. 1934–1943, October 1990.
43. J. Reeve and R. Adapa, "Evaluation of Developments in DC Models for AC/DC Transient Stability Programs," *CIGRÉ Symposium on AC/DC Transmission Interactions and Comparisons*, paper 100-04, Boston, September 1987.
44. W. W. Price, K. A. Wirgau, A. Murdoch, J. V. Mitsche, E. Vaahedi, and M. A. El-Kady, "Load Modeling for Power Flow and Transient Stability Computer Studies," *IEEE Transactions on Power Systems*, Vol. 3, No. 1, pp. 180–187, February 1988.
45. F. Nozari, M. D. Kankam, and W. W. Price, "Aggregation of Induction Motors for Transient Stability Load Modeling," *IEEE Transactions on Power Systems*, Vol. 2, No. 4, pp. 1096–1103, November 1987.
46. A. Kurita, H. Okubo, K. Oki, S. Agematsu, D. B. Klapper, N. W. Miller, W. W. Price, J. J. Sanchez-Gasca, K. A. Wirgau, and T. D. Younkins, "Multiple Time-Scale Power System Dynamic Simulation," paper 92 WM 128-9 PWRS, IEEE/PES Winter Meeting, New York, January 1992.
47. W. W. Price, D. B. Klapper, N. W. Miller, A. Kurita, and H. Okubo, "A Multi-Faceted Approach to Power System Voltage Stability Analysis," CIGRÉ-205, 1992.
48. N. W. Miller, R. D'Aquila, K. M. Jimma, M. T. Sheehan, and G. L. Comegys, "Voltage Stability of the Puget Sound System Under Abnormally Cold Weather Conditions," IEEE paper 92 SM 534-8, IEEE PES Summer Meeting, Seattle, 1992.
49. B. Meyer and M. Stubbe, "EUROSTAG, a Single Tool for Power-System Simulation," *Transmission and Distribution International*, pp. 47–52, March 1992.
50. P. Bornard, B. Meyer, J. P. Antoine, and M. Stubbe, "EUROSTAG: a Major Step in Power System Simulation," IERE meeting, Rio de Janeiro, May 1991.
51. G. Douard, A. Giard, M. Jerosolimski, and B. Meyer, "EUROSTAG: Presentation of the Program and of an Application," *Proceedings of IERE Workshop on New Issues in Power System Simulation*, pp. 30–37, Caen (France), March 30–31, 1992.
52. J. Deuse and M. Stubbe, "Dynamic Simulation of Voltage Collapse," paper 92 SM 396-2, IEEE PES Summer Meeting, Seattle, 1992.
53. V. Venikov, *Transient Processes in Electrical Power Systems*, Mir Publishers, Moscow, 1977.
54. R. Rüdenberg, *Transient Performance of Electric Power Systems*, McGraw-

Hill, New York, 1950.

55. J. M. Undrill and T. F. Laskowski, "Model Selection and Data Assembly for Power System Simulation," *IEEE Transactions on Power Apparatus and Systems*, Vol. PAS-101, No. 9, pp. 3333–3341, September 1982.
56. D. S. Brereton, D. G. Lewis, and C. C. Young, "Representation of Induction-Motor Loads During Power-System Stability Studies," *Transactions AIEE*, Vol. 76, Part III, pp. 451–461, August 1957.
57. General Electric Company, *Load Modeling for Power Flow and Transient Stability Computer Studies*, EPRI Final Report EL-5003, January 1987.
58. J. Carpentier, R. Girard, and E. Scano, "Voltage Collapse Proximity Indicators Computed from an Optimal Power Flow," *Proceedings of the 8th Power System Computing Conference*, pp. 671–678, Helsinki, 1984.
59. P. W. Sauer and M. A. Pai, "Power System Steady State Stability and the Load Flow Jacobian, *IEEE Transactions on Power Systems*, Vol. 5, No. 4, pp. 1374–1383, November 1990.
60. R. Marconato, "Some Considerations about: a) On-load Tap- hangers and Voltage Instability, b) Voltage Collapse Phenomenon," ENEL internal report, May 1991, prepared for CIGRÉ TF 38-02-11.
61. V. A. Venikov et al., "Estimation of Electrical Power System Steady-State Stability, *IEEE Transactions on Power Apparatus and Systems*, Vol. 94, pp. 1034–1040, May/June 1975.
62. C. D. Vournas and N. Krassas, "Voltage Stability as Affected by Static Load Characteristics," *IEE Proceedings*, Part C, (to appear).
63. C. Rajagopalan, B. Lesieutre, P. W. Sauer, and M. A. Pai, "Dynamic Aspects of Voltage/Power Characteristics," *IEEE Transactions on Power Systems*, Vol. 7, No. 3, pp. 990–1000, August 1992.
64. M. K. Pal, discussion of "An Investigation of Voltage Instability Problems," by N. Yorino et al., *IEEE Transactions on Power Systems*, Vol. 7, No. 2, pp. 600–611, May 1992.
65. IEEE Power System Relaying Committee Working Group K12, "System Protection and Voltage Stability," Draft 5, September 1992.
66. IEEE Special Stability Controls Working Group, "Static Var Compensator Models for Power Flow and Dynamic Performance Simulation," paper 93 WM 173-5-PWRS, IEEE/PES 1993 winter meeting.

Appendix I, Contribution to Chapter 8
Sensitivities of Voltage Stability to System Characteristics, Part 1

P. Kundur, B. Gao, G. K. Morison
Ontario Hydro, Canada

I.1 Test Systems

Two test systems are used to illustrate the basic phenomenon of voltage instability and to demonstrate static and dynamic analysis techniques.

Test system 'A', shown in Figure I-1, is a small system consisting of 10 buses, 14 branches, and 3 generators. Cases with different combination of device modelling were studied to assess the sensitivity of system voltage stability to the dynamics of different system components. This small system was selected for testing because the performance of the components can be easily tracked. Most of the important factors influencing system voltage stability are readily identified in studying this simple system.

Test system 'B', based on an actual system used in planning studies, is a large system with 622 buses, 1083 branches and 129 generators. The simulations conducted using this representation illustrate the importance of accounting for factors key to voltage stability in modelling large practical power systems.

The computer program used for time domain simulation is the Extended Transient/Midterm Stability Program (ETMSP), developed by Ontario Hydro under EPRI Project RP1208-9. The program has the modelling capability to account for the important dynamics for voltage stability analysis.

I.2 Sensitivity to Load Characteristics: System A

The voltage stability of system A following the opening of one of the branches between bus 6 and bus 7 was studied. Time domain simulations were conducted for up to 180 seconds following the contingency, with different combination of models for loads, LTC transformers, and generator field current limits.

Effect of Load Models without LTCs. To demonstrate the effect of load modelling at bus 8, Case A and Case B, as shown in Table I-1, are considered.

Table I-1, System Modelling for Case A and Case B

		Case A	Case B
Loads	Bus 8	Constant impedance	Constant MVA
	Bus 11	Constant impedance	Constant impedance
I_{fd} Limits	Machine 1	Infinite bus	Infinite bus
	Machine 2	Limited	Limited
	Machine 3	Limited	Limited
LTC	Bus 10–Bus11	Disabled	Disabled
	Others	Disabled	Disabled

Figure I-2 shows, for both Case A and Case B, the voltages at bus 11 following the contingency. It is seen that system voltage stability is maintained in both cases.

Effect of LTC Operation. To demonstrate the effect of LTC operation, we consider Case C shown in Table I-2, with dynamics of the transformer LTC between bus 10 and bus 11 included. Time delays for LTC operation are assumed to be 30 seconds for the first tap movement and 5 seconds for subsequent tap movements.

Table I-2, System Modelling for Case C

Loads	Bus 8	Constant MVA
	Bus 11	Constant impedance
I_{fd} Limits	Machine 1	Infinite bus
	Machine 2	Limited
	Machine 3	Limited
LTC	Bus 10–11	Enabled
	Others	Disabled

Figure I-3 shows the plot of voltage at bus 11 following the contingency. LTC restores the voltage at bus 11 to its pre-contingency value at about 45 seconds. At 60 seconds, voltage at bus 11 is reduced below its pre-contingency value due to generator field current limiter action, and the LTC starts to operate again. At about 65 seconds following the disturbance, voltage at bus 11 starts to decrease with the increase in the tap ratio, and voltage instability occurs. It is also seen that, at about 120 seconds following the disturbance, the system becomes transiently unstable, as indicated by the large oscillation in bus voltages. However, it is important to observe that transient instability is the result, rather than the cause, of voltage instability. The driving force of overall system instability, manifested as voltage instability first followed by transient instability, is the restoration of load power by LTC operation and limiting of generator field currents.

Effect of Induction Motors . To demonstrate the effect of induction motor load on overall system voltage stability, we consider two cases. The first case is the same as Case C above, and the second case is the Case D shown below in Table I-3, in which the load at bus 8 is modelled as 50% constant MVA and 50% induction motor.

Voltages at bus 11 following the contingency for the two cases are shown in Figure I-4. It is seen that, with induction motor load, voltage instability occurs slightly earlier following the contingency. Figure I-5 shows the time response of the motor reactive power.

I.3 Sensitivity to Generation Excitation Characteristics: System A

Field Currents of Both Machine 2 and Machine 3 Limited. Figure I-6 shows the field currents for machine 2 and machine 3 for Case C. As LTCs operate, machine 3 reaches its field current limit first, and at about 60 seconds

the field current limiter starts to reduce the field current. At about 80 seconds the field current for machine 3 is reduced to within its continuous limit. The field current limiter for machine 2 starts to actuate at about 120 seconds. At about 130 seconds, before the field current for machine 2 reaches its continuous limit, the system starts to oscillate. Voltage at bus 11 is the same as that shown in Figure I-3. It is seen that voltage instability occurs as soon as the field current of machine 3 is limited at about 60 seconds. At this time the voltage at bus 11 starts to decrease as LTCs attempt to increase the bus voltage.

Table I-3, System Modelling for Case D

Loads	Bus 8	50% constant MVA 50% motor
	Bus 11	Constant impedance
I_{fd} Limits	Machine 1	Infinite bus
	Machine 2	Limited
	Machine 3	Limited
LTC	Bus 10–11	Enabled
	Others	Disabled

Field Current of Only Machine 3 Limited. We now consider the following Case E in which the field current limit of only machine 3 is imposed (Table I-4).

Table I-4, System Modelling for Case E

Loads	Bus 8	Constant MVA
	Bus 11	Constant impedance
I_{fd} Limits	Machine 1	Infinite bus
	Machine 2	Unlimited
	Machine 3	Limited
LTC	Bus 10–11	Enabled
	Others	Disabled

Figure I-7 shows the field currents for machine 2 and machine 3. Figure I-8 shows the voltage at bus 11 for the same case. It is interesting to observe that even though voltage instability occurs as soon as the field current of machine 3 is limited, the final value of bus voltage stays at a low value of about 0.82 pu. This is referred to by some as partial voltage collapse.

Field Currents of all Machines Unlimited. In this case, all the machines have their field currents unlimited, as described in the following Case F (Table I-5).

Figure I-9 shows the unlimited field currents for machine 2 and machine 3, and

Figure I-10 shows the voltage at bus 11 for the same case. It is seen that voltage stability is maintained if all the machines have their field currents unlimited.

Table I-5, System Modelling for Case F

Loads	Bus 8	Constant MVA
	Bus 11	Constant impedance
I_{fd} Limits	Machine 1	Infinite bus
	Machine 2	Unlimited
	Machine 3	Unlimited
LTC	Bus 10–11	Enabled
	Others	Disabled

Effect of AVR Line Drop Compensation (LDC). With AVR line drop compensation included, the regulated voltage is $V_C = \left|\dot{V}_t + \dot{I}_t (R_C + jX_C)\right|$, where $\dot{V}_t$ and $\dot{I}_t$ are the complex generator terminal voltage and current respectively. If R_C and/or X_C are non-zero, the regulated voltage is different from the generator terminal voltage.

For case C, Figure I-11 shows the voltage at bus 11 with three different values of X_C for machine 2. R_C=0 for all the three cases. The case with X_C=0 is the same as that shown in Figure I-3 where no line drop compensation is modelled.

From Figure I-11, it is seen that the AVR line drop compensation can have a large effect on overall system voltage stability. The effect of AVR line drop compensation depends on: (1) the location of the machine, and (2) the size of the compensation impedance. Figure I-12 shows the terminal voltage of machine 2 with different values of X_C. Figure I-13 shows the field current of machine 2 with different values of X_C.

The addition of AVR LDC in effect serves to distribute post contingency reactive supply from generators, in a pattern different from that obtained without LDC, by forcing units to adjust their terminal voltages in order to control the remote voltages. This could have positive or negative impacts on system voltage stability. In some cases, the LDC could redistribute reactive supply in such a way as to prevent critical machines from hitting field current limits, and thus prevent instability. This is the case as shown in Figure I-12 and I-13 for X_C = -0.09.

Effect of AVR Droop Characteristics. If no field current limits are imposed, an AVR regulates the machine terminal voltage to its pre-set reference value, with a slight reduction due to the droop characteristic of the AVR control loop. The reduction in machine terminal voltage due to AVR droop characteristic, as machine output increases, depends on the equivalent gain factor of the overall AVR control loop.

I.4 Sensitivity to Generation Excitation Characteristics: System B

Simulation of system response following the opening of a major 500-kV transmission line was conducted for system B. For buses where load LTC dynamics

are included, loads are modelled as constant impedances. All the other loads are modelled as constant MVA. Voltage at bus 1062 is plotted in Figure I-14. Two cases were considered. The first case has LTC operation but no generator field current limits. The second case has both LTC operation and generator field current limits. Similar to the results shown in Figure I-2 and Figure I-3, it is seen that, without generator field current limits, the system is voltage stable because the load bus voltage increases towards its desired value as the LTCs operate. With generator field current limits imposed, the system becomes voltage unstable. Figure I-15 shows the field currents for two machines, with and without field current limits. Similar to the results shown in Figure I-3 for system A, bus voltage starts to oscillate as the voltage goes down, indicating that the system starts to become transiently unstable. Once again transient instability is caused by voltage instability, and LTC operation and generator field current limiting are the main causes of instability.

I.5 Static Voltage Stability Study Using Modal Analysis: System A

For system A, modal analysis was conducted at different time frames following the contingency of opening one of the branches between bus 6 and bus 7. System modelling is the same as for Case C shown in Table I-2. Field currents for all the machines, except machine 1, are assumed limited. Load at bus 11 is modelled as constant impedance and load at bus 8 is modelled as constant MVA. To take into account the effect of LTC operation, a linearized continuous LTC model is included for the transformer between bus 10 and bus 11. System conditions at different time frames following the contingency were obtained by taking different snapshots along the transient trajectory.

Table I-6 shows the three smallest eigenvalues of the reduced Jacobian matrix at different snap shots following the contingency. Referring to the time plots shown in Figure I-3, it is seen that the system is voltage stable before the disturbance and after the disturbance before the field currents are limited. Voltage instability occurs once the field current for machine 3 is limited. It is concluded that the modal analysis determines correctly when system voltage instability occurs.

Table I-6, System A: Modal Analysis Results

Critical Eigenvalues	Time following the contingency			
	Before	20 sec.	80 sec.	130 secs
λ_1	19.1712	16.1957	-10.1571	-12.1703
λ_2	137.2924	128.2478	59.7989	51.9547
λ_3	436.7280	414.2229	80.2043	73.6167
Stability (Modal Analysis)	Stable	Stable	Unstable	Unstable
Stability (Simulation)	Stable	Stable	Unstable	Unstable

I.6 Data for System A

Transmission Lines (R, X & B in pu on 100 MVA Base)

	R	X	B
5-6	0.0000	0.0040	0.0000
6-7	0.0015	0.0288	1.1730
9-10	0.0010	0.0030	0.0000

Transformers (R & X in pu on 100 MVA Base)

	R	X	Ratio
1-5	0.0000	0.0020	0.8857
2-6	0.0000	0.0045	0.8857
3-7	0.0000	0.0125	0.9024
7-8	0.0000	0.0030	1.0664
7-9	0.0000	0.0026	1.0800
10-11	0.0000	0.0010	0.9600

Shunts

Bus	MVAR
7	763
8	600
9	300

Loads

Bus	P(MW)	Q(MVAR)
8	3369	1046
11	3486	0

Load Flow Generator Data

Bus	P(MW)	V(pu)
1	4219	0.9800
2	1736	0.9646
3	1155	1.0400

Machine Parameters

Machine 1 : Infinite Bus
Machine 2 : H = 2.09, MVA Base = 2200 MVA
Machine 3 : H = 2.33, MVA Base = 1400 MVA

The following stator and rotor parameters apply to both machine 2 and machine 3 :

$R_a = 0.0046$	$X_d = 2.07$	$X_q = 1.99$
$X_l = 0.155$	$X'_d = 0.28$	$X'_q = 0.49$
$X''_d = 0.215$	$X''_q = 0.215$	
$T'_{do} = 4.10$	$T'_{qo} = 0.56$	
$T''_{do} = 0.033$	$T''_{qo} = 0.062$	

Exciters

Both machine 2 and machine 3 have thyristor exciter with a gain of 400 and the sensing circuit time constant of 0.02 second.

Field Current Limiter for Machine 2

$I_{fdmax1} = 2.95$ $I_{fdmax2} = 3.95$ $I_{LIM} = 9.17$
$K_1 = 0.248$ $K_2 = 12.6$

Field Current Limiter for Machine 3

$I_{fdmax1} = 3.0$ $I_{fdmax2} = 4.0$ $I_{LIM} = 9.17$
$K_1 = 0.248$ $K_2 = 12.6$

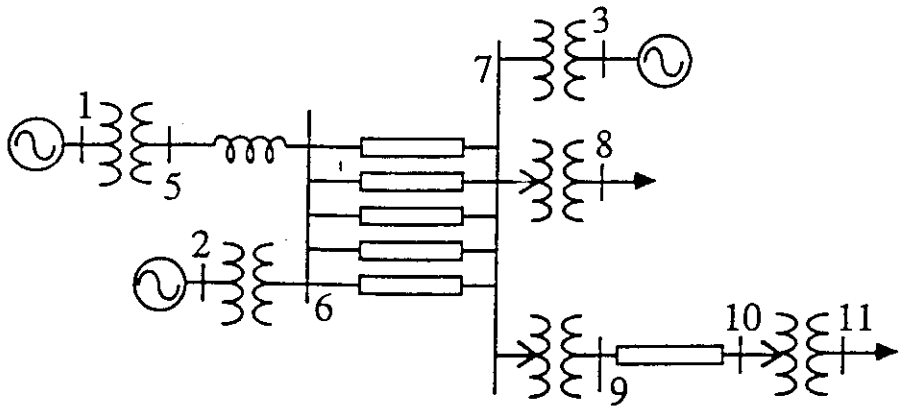

Fig. I-1. Test system A.

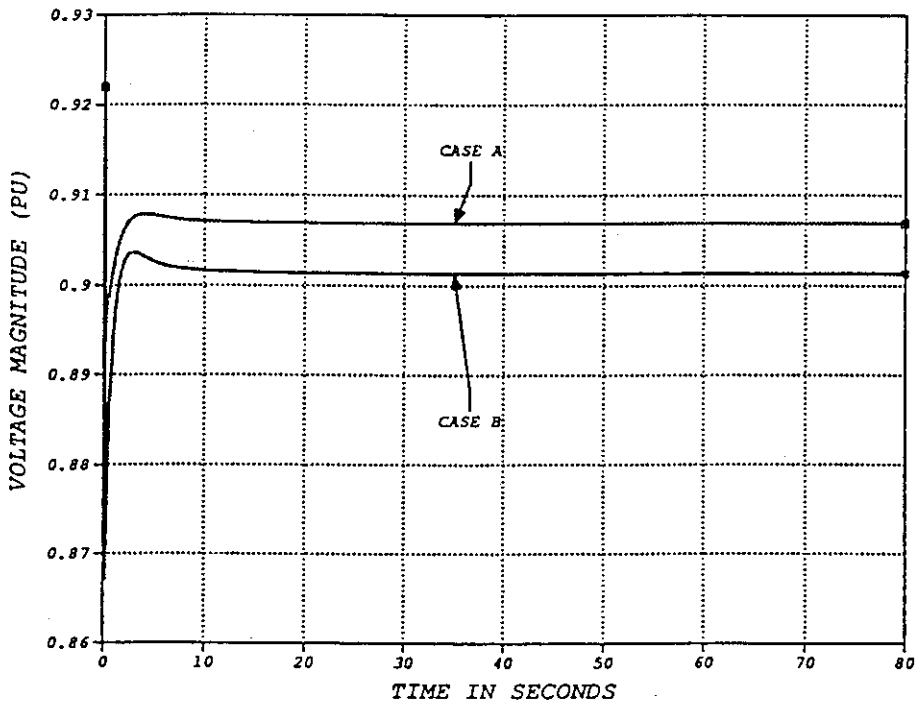

Fig. I-2. System A: Voltage at bus 11 (Case A and Case B).

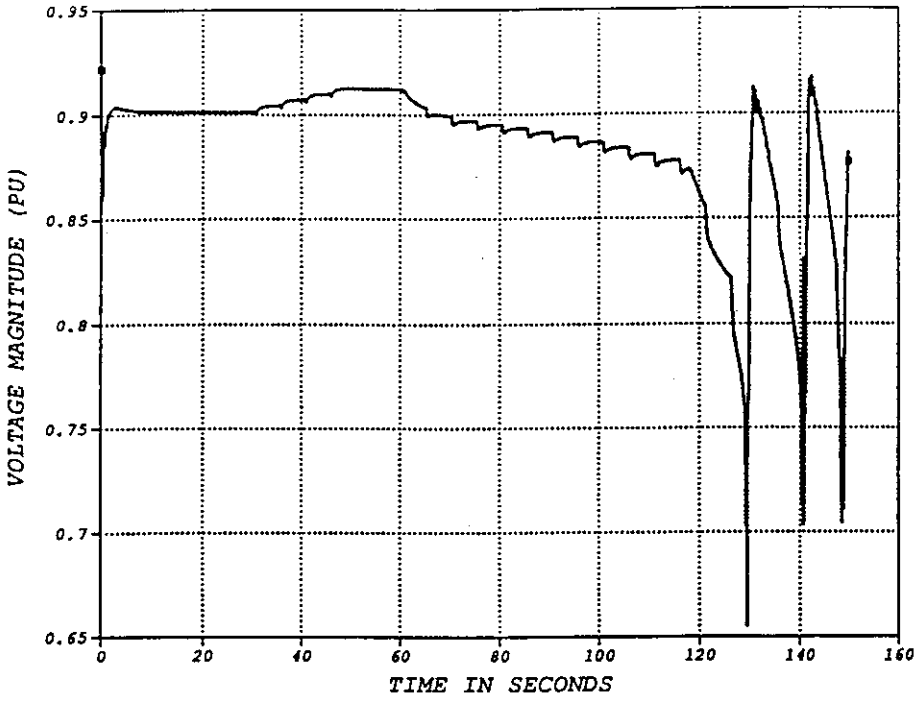

Fig. I-3. System A: Voltage at bus 11 (Case C).

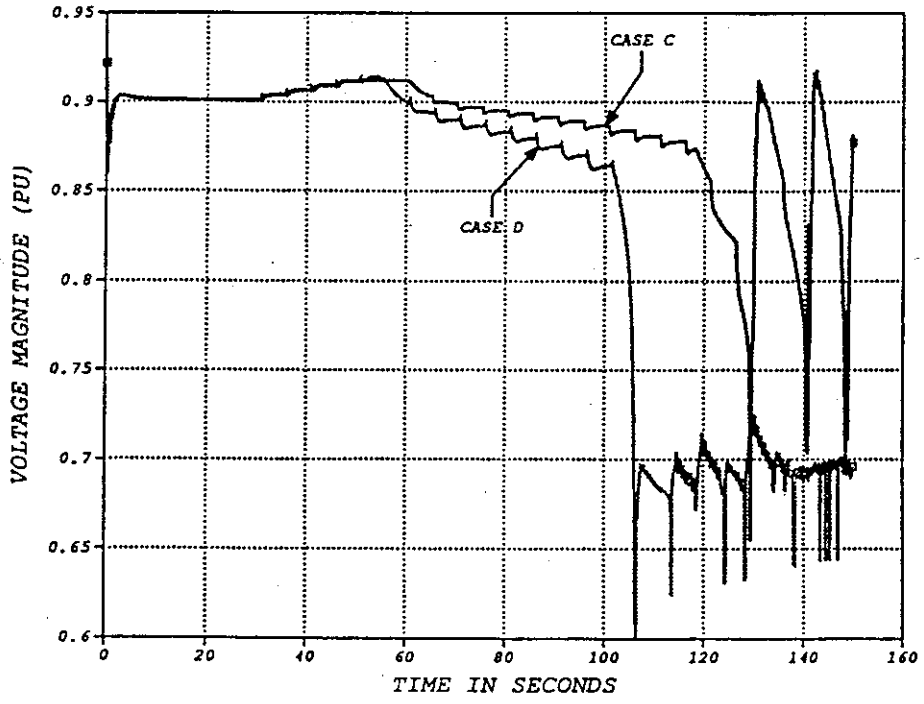

Fig. I-4. System A: Voltage at bus 11 (Case C and Case D).

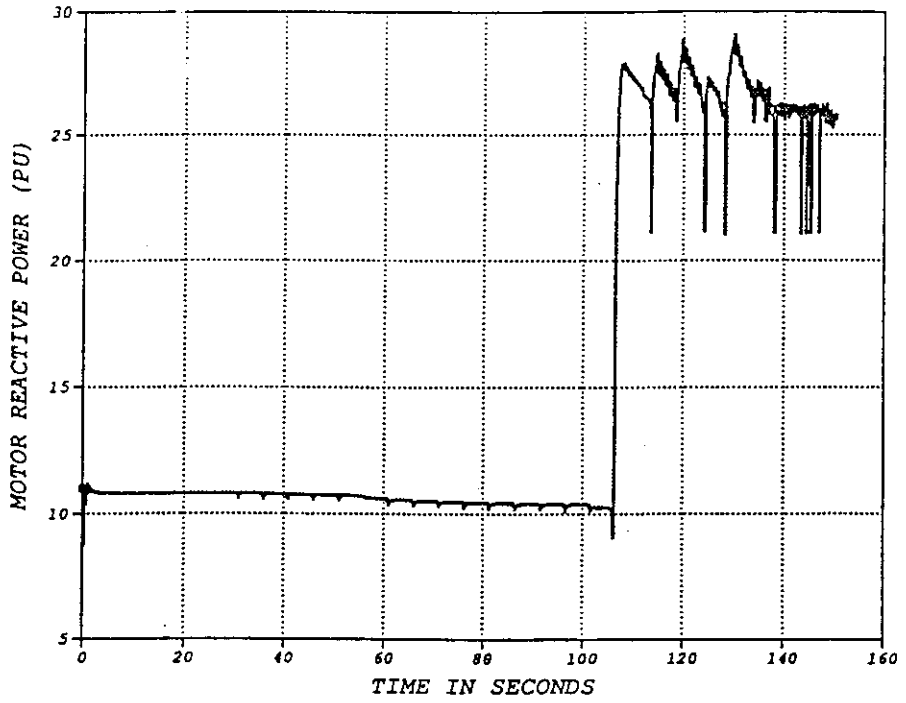

Fig. I-5. System A: Motor reactive power (Case D).

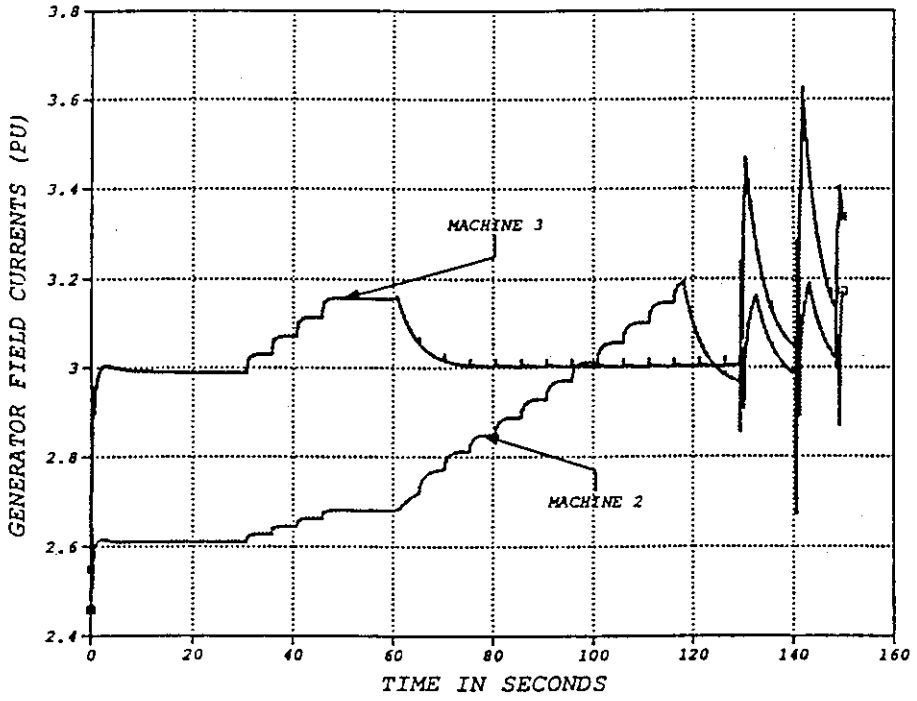

Fig. I-6. System A: Field currents for machine 2 and machine 3 (Case C).

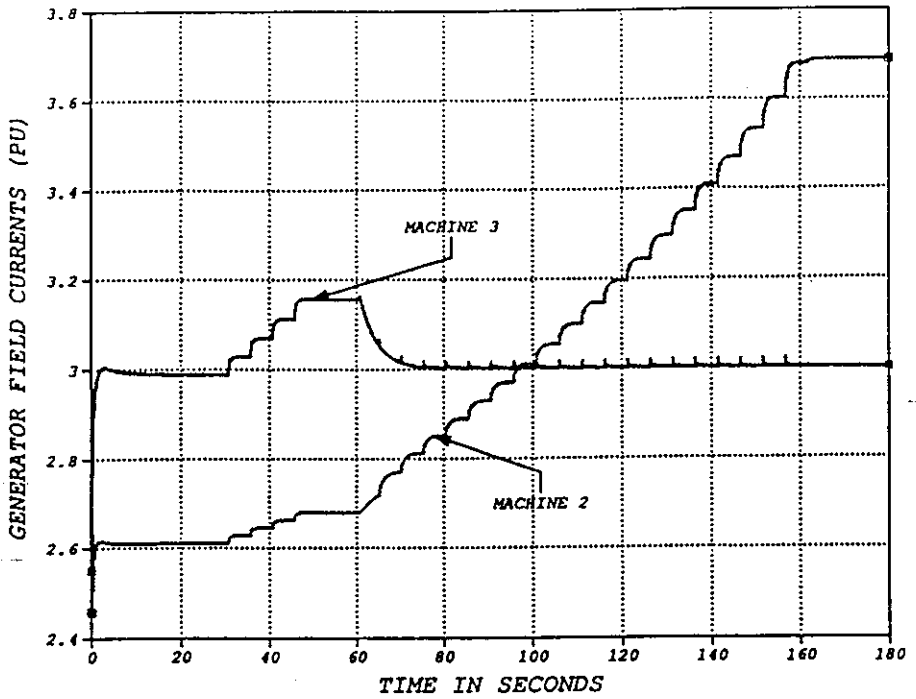

Fig. I-7. System A: Field currents for machine 2 and machine 3 (Case E).

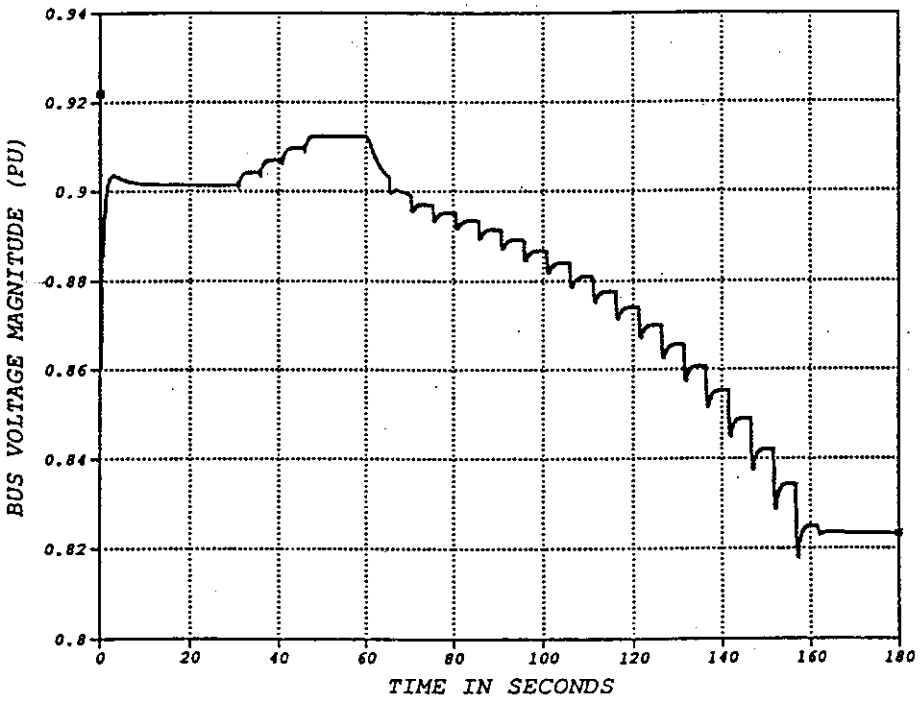

Fig. I-8. System A: Voltage at bus 11 (Case E).

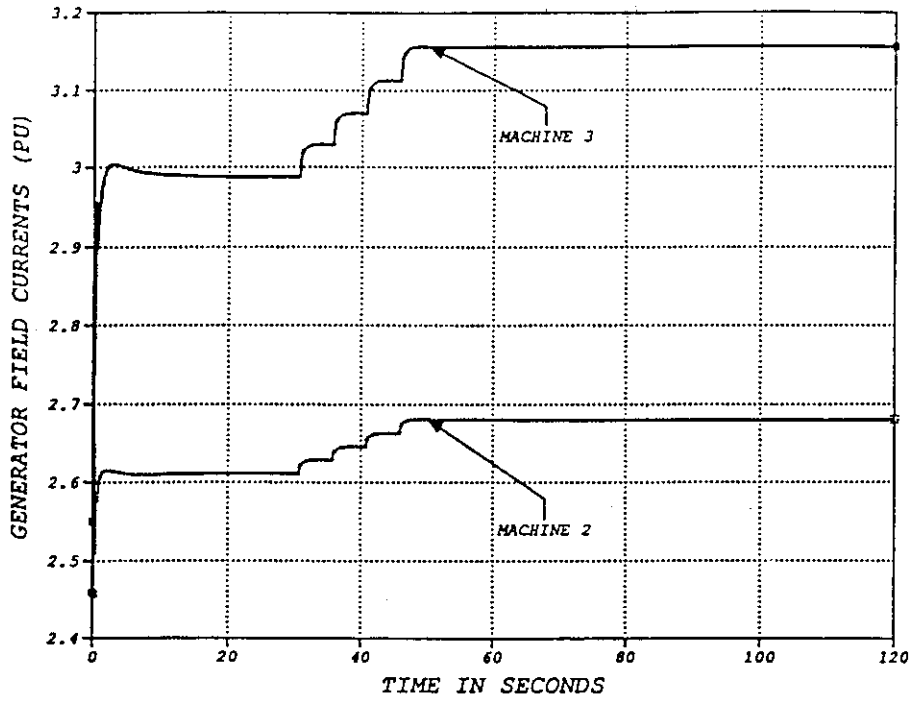

Fig. I-9. System A: Field currents for machine 2 and machine 3 (Case F).

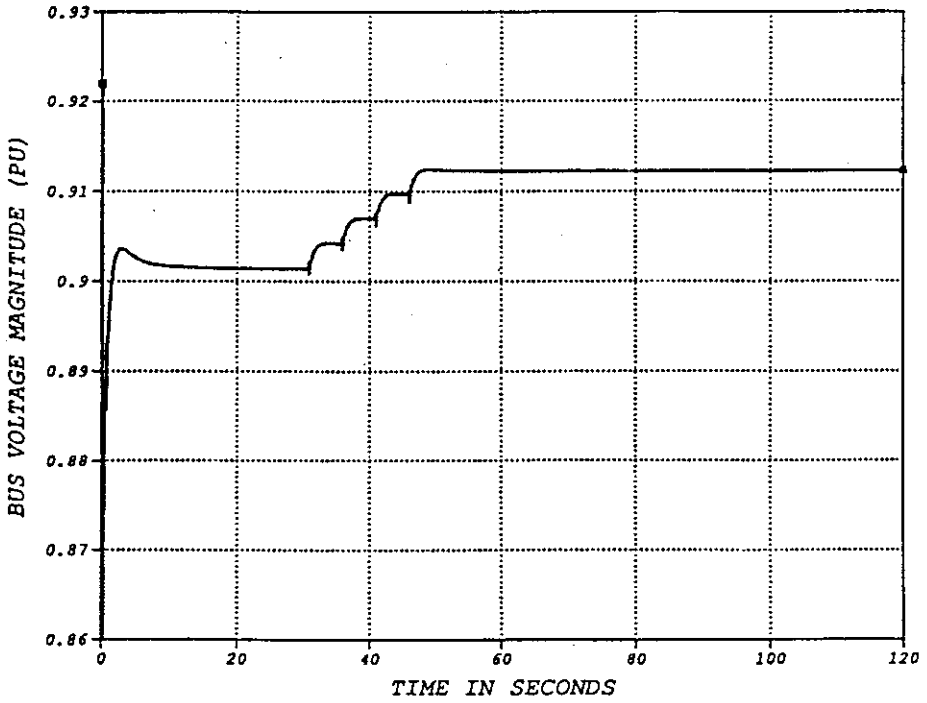

Fig. I-10. System A: Voltage at bus 11 (Case F).

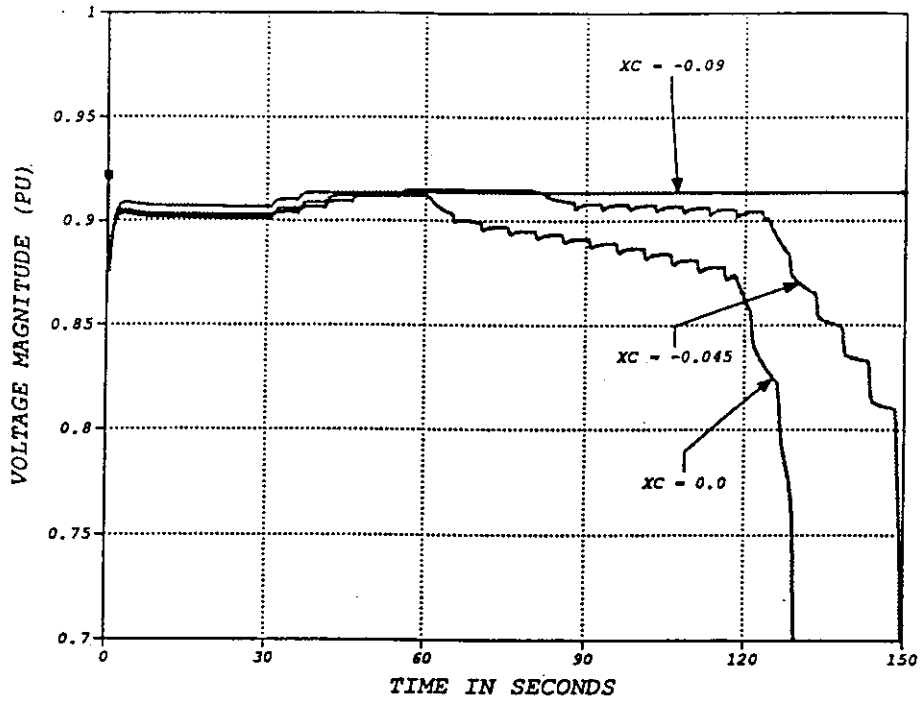

Fig. I-11. System A: Voltage at bus 11 (with different values of X_C).

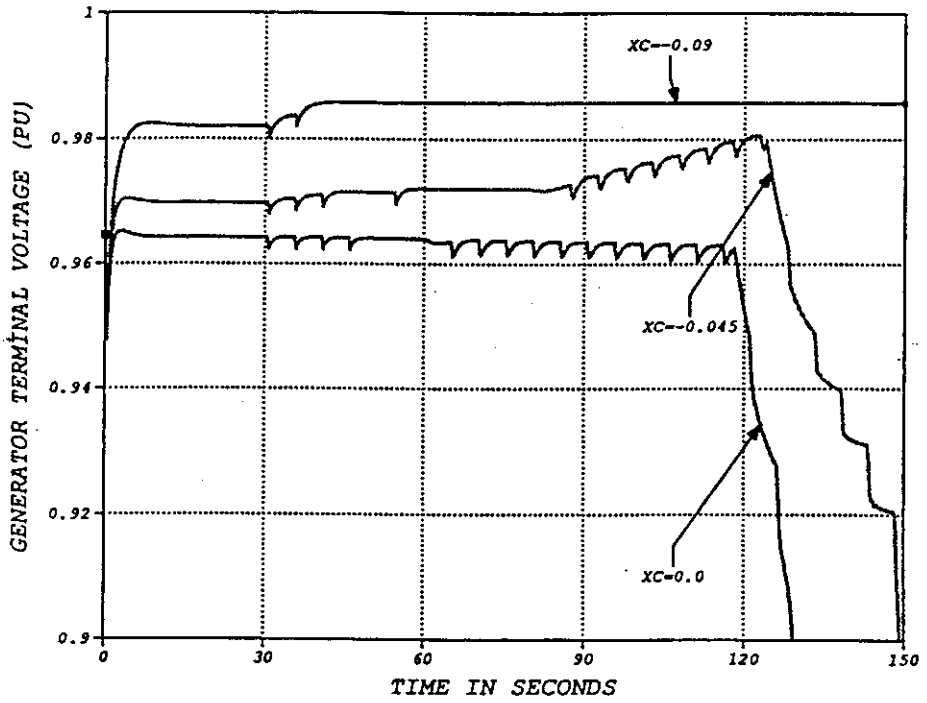

Fig. I-12. System A: Terminal voltage of machine 2 (with different values of X_C).

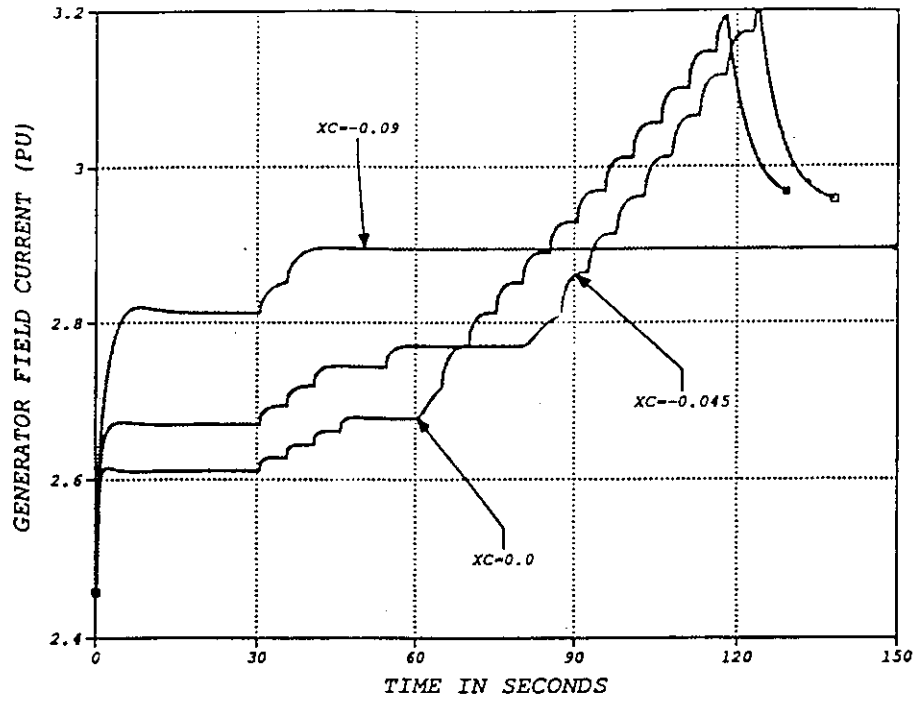

Fig. I-13. System A: Field current of machine 2 (with different values of X_C).

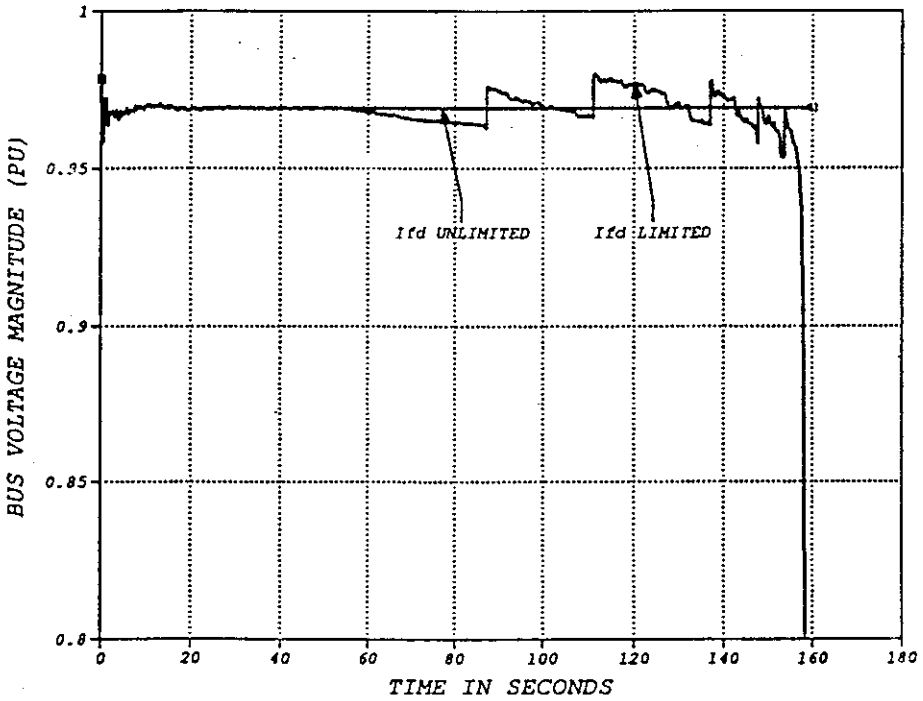

Fig. I-14. System B: Voltage at bus 1062 (with and without field current limited).

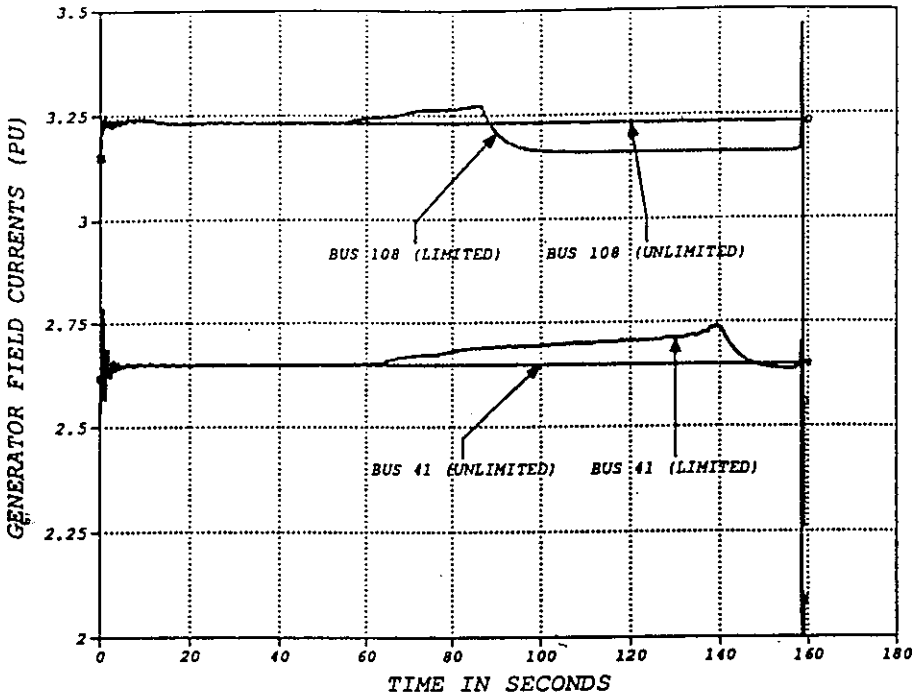

Fig. I-15. System B: machine field currents (with and without limits).

Appendix II, Contribution to Chapter 8
Analysis of Voltage Instability in a Power Network with Secondary Voltage Regulation

S. Corsi and M. Pozzi
ENEL, Italy

II.1.0 Introduction

This appendix documents analysis conducted by ENEL to demonstrate how system voltage stability is influence by:

- Primary voltage regulation,
- Secondary voltage regulation,
- Load tap changer action.

The test system used is shown on Figure II-1. The effect of primary voltage regulation is captured through the modelling of automatic voltage regulators (AVRs) on the generators. Secondary voltage regulation is represented by the modelling of a special control loop through which the generators are used to control the voltage of a *pilot* node. In this example, the pilot node is represented by $V_7 = V_3 = V_4$. Load tap chanter (LTC) action is represented using a continuous model connecting a load on bus 5 to the high voltage bus 6.

Modelling details are provided below, and results of dynamic analysis are presented.

II.1.1 Mathematical Model of the Equivalent Power System

In the test system used, each equivalent generator is represented by a detailed sixth order model. The unit transformers are simply modeled by their leakage reactances (X_{t1}, X_{t2}). The LTC transformer is represented by its primary (X_{tcp}) and secondary leakage reactance (X_{tcs}) and its transformation ratio (N_{tc}).

The equivalent load supplied by the LTC transformer is assumed linear and is modeled by an equivalent admittance (Y_u), shown as conductance (G_u) and susceptance (B_u). The interconnection lines are described by their equivalent reactances (X_{l1}, X_{l2}, X_{lc}, and X_{le}).

Referring to Figure II-1, the numerical values of the unit powers P_i and Q_i and of the reactances X_{li} and X_{li} are expressed in per unit of A_{ni} and V_{n2}/A_{ni} respectively. All the other powers and reactances are similarly referred to $(A_{n1} + A_{n2})$.

The initial conditions shown in Figure II-1 have been chosen to represent a system condition near the voltage stability limit.

II.1.2 Primary Voltage Regulation

Figure II-2 shows the block diagram of the unit primary voltage regulation, used for modelling the voltage V_1 and V_2 control system of both equivalent generators.

The unit voltage V is controlled, depending on its global setpoint $V_{ref} + V_{sec}$ through the Automatic Voltage Regulator (AVR). The AVR includes the additional stabilizing feedbacks from the active power P and the electrical speed ω with gains K_p and K_ω respectively. These feedbacks act to damp the electrome-

chanical oscillations. Also included is an overexcitation limit for restraining the field current I_f to below its maximum value I_{flim}.

II.1.3 Secondary Voltage Regulation

Figure II-3 shows the block diagram of the pilot node voltage V_s control loop. The voltage V_s corresponds to $V_3 = V_4 = V_7$ and the equivalent unit used for secondary voltage regulation is U_1.

The control structure consists of a Power Plant Reactive Power Regulator (PPPR), which controls the reactive power Q through the setpoints $V_{ref} + V_{sc}$ of the units AVRs. PRPR actuates the reactive power request Q_{ref} coming from an external and slower control loop, which regulates the pilot node voltage V_s to the desired value V_{sref} by the Pilot Node Voltage Regulator (PNVR).

II.1.4 Load Tap Changer Control Loop

The load voltage V_c is controlled, as shown in Figure II-4, through the LTC HV/LV transformation ratio N_{tc} in such a way as to keep V_c at the value fixed by the setpoints V_{cref}. The voltage V_c corresponds to the voltage V_6 of the linear load bus.

An integral-continuous control scheme has been used rather that a discrete-time scheme, because the load tap changer of the equivalent system represents the overall LTC control action in a real power system which is effectively continuous.

II.2.0 Dynamic Analysis

The dynamic analysis of voltage instability involves examination of the impacts and interactions of primary voltage regulation, secondary voltage regulation, and LTC actions. In the simulations conducted, the transient response of the system and its component control loop have been examined for different system load perturbations using various control loop settings. Three levels of control modelling were considered:

AVR and LTC action included (Case TEST PT)

AVR, LTC and I_{flim} included (Case TEST PLT)

AVR, LTC, I_{flim}, PRPR, and PNVR included (Case TEST PLST)

Table II-1 shows the various initial conditions and control settings considered for simulations using the three levels of control modelling. Key results are presented here.

II.2.1 TEST PT: System Transients with Primary Voltage Regulation and LTC Control Loop

Figure II-5–Figure II-8 show the transient responses of the system following a fast load variation with primary voltage regulation and LTC control action modelled.

For a load perturbation $\Delta Y_u = 40\%$ (See Figure II-5 and Figure II-6), the system recovers to the voltage levels fixed by the regulation loop setpoints, with a time interval and an evolution mainly determined by the LTC control loop dynamics. Following the load variation, the load voltage V_6 takes about 100s to recover to its set-point value.

With a load perturbation ΔY_u = 60% (see Figure II-7 and Figure II-8), the LTC control loop saturates for a short interval between 70-80 seconds. While the loop is unsaturated, the system is voltage unstable and will have a positive eigenvalue related to the LTC control loop. Once the LTCs reach their limits however, the system becomes stable.

If the load perturbation exceeds about 70%, the system shows non-reversible voltage degradation and voltage instability despite the LTC reaching its limit. This leads ultimately to voltage collapse and loss of machine synchronism.

II.2.2 TEST PLT: System Transients with Primary Voltage Regulation, Over-Excitation Limits and LTC Control Loop

Figure II-9–Figure II-12 show the transient behavior of the electrical system in Figure II-1 in response to a fast load variation with modelling of primary voltage regulation, unit overexcitation limits, and LTC control loop action included.

With a load variation ΔY_u = 40% (see Figure II-9 and Figure II-10), the dynamic behavior of the system is completely different from the previous one shown in Figure II-5 and Figure II-6, because the unit overexcitation limits are reached (about 50 seconds after the load variation), causing destabilization of the LTC control loop. Upon reaching the excitation limits, instability starts but the system regains stability (about 45 seconds after its appearance) when the saturation and therefore the cutting-off of the LTC control loop are reached. The voltage levels of this new steady-state condition are necessarily different from the regulation loop setpoints.

With a load perturbation of ΔY_u = 50% (see Figure II-11 and Figure II-12), over-excitation limits are reached and the system becomes unstable at about 50 seconds. The LTC control loop saturates (about 10 seconds later), but a non-reversible voltage degradation has started and voltage collapse results. Finally the units lose synchronism.

II.2.3 TEST PLST: System Transients with Primary and Secondary Voltage Regulation, OverExcitation Limits and LTC Control Loop

Figure II-13–II-17 show the transient responses of the system following a fast load variation and with primary voltage regulation, secondary voltage regulation, unit over-excitation limits, and the LTC control loops modelled.

For a load perturbation ΔY_u = 30%, (see Figure II-13–II-15), load voltage V_6 recovers, due to the LTC control loop, and the pilot node voltage V_4 recovers through the secondary voltage regulation. About 200 seconds are needed for the new steady-state conditions to be reached. With respect to the conditions of Figure II-6 and Figure II-1, these results show higher transformation ratio N_{tc} value, due to a weaker control action of the tap-changer in the presence of the secondary voltage regulation. Moreover, we note a reversal of direction in the N_{tc} transient: this is due to the recovering, at a lower response velocity, of the secondary voltage regulation with respect to the LTC control loop action.

A load perturbation ΔY_u = 50%, (See Figure II-16 and Figure II-17), causes voltage instability to occur immediately. This is followed by the LTC control loop saturation (about 65 seconds later) and then by the non-reversible voltage collapse phenomenon. Finally, about 35 seconds later, the synchronous gener-

ators lose synchronism. The transients are very similar to those shown in Figure II-11 and Figure II-12.

II.2.4 General Conclusions on Dynamic Analysis

The simulation results demonstrate the strong impact of the behavior and the dynamic interaction of the unit overexcitation limits and the LTC regulation loop on system voltage stability. More precisely, the control loop of the LTC transformation ratio N_{tc} affects both the load voltage profile V_6 (at the LV bus) and the pilot node voltage V_4 (at the HV bus). It therefore modifies the working and stability conditions of the equivalent units, as well as the exchanges with the infinite power network.

If the units overexcitation limits could be disabled for reasonable load perturbation, the system would not be exposed to any voltage instability or collapse risk. In fact, in this condition, the time evolution of the system variables are substantially determined by the dynamic characteristics of the LTC control loop, which remain stable for all the admissible N_{tc} values.

The unit overexcitation limits operation considerably modifies the controllability of the load voltage V_6 and results in, for high values of Y_u and low values of Ntc, LTC control loop instability. Such instability causes the degradation of network voltage V_4 and load voltage V_6. The degradation of bus voltages, in the most favorable case, stops when the LTC control loop saturates.

The timely LTC shut-down with the subsequent control loop cut-off can stop, in some cases, the evolution of voltage instability. However, voltage instability often becomes a non-reversible phenomenon, which may result in voltage collapse and to the subsequent loss of synchronism.

As long as unit overexcitation limits do not operate, secondary voltage regulation improves the controllability of the load voltage V_6 and reduces the variations in N_{tc}. However, if the controlling units work in over-excitation limit conditions, the secondary voltage regulation is in open loop and therefore does not affect the possible subsequent voltage degradation phenomenon. Nevertheless it has to be pointed out that, within moderate load variation, the secondary voltage regulation helps to keep the LTC control loop stable.

Moreover, with secondary voltage regulation included, the voltage degradation process develops more slowly as shown in Figure II-18 and Figure II-19. This is despite the fact that the unit overexcitation limit is reached slightly earlier, causing the LTC control loop to become unstable,

Moderate improvements of LTC control loop stability, or slowing down the voltage degradation when LTC control loop is unstable, are also achieved with secondary voltage regulation.

It is shown that system voltage instability phenomenon can sometimes be interrupted by timely blocking the tap-changers and therefore cutting-off their control loops. A check of this simple coordination criterion between the LTC control action and the unit overexcitation limit intervention (and/or saturation of the secondary voltage regulation) is shown in Figure II-20–II-21. Compare Figure II-20–II-21 with Figure II-10 and observe the interruption of the voltage instability phenomenon.

Timely blocking of the LTC and the consequent interruption of the voltage instability phenomenon avoids, in some cases, the starting of a non-reversible voltage collapse. This is shown in Figure II-22–II-23 where the LTC is shut-down after a waiting time LD which varies from 0 to 30 seconds. Comparison between Figure II-22 and Figure II-23 shows that a time delay of 30 seconds is already too long to avoid the system voltage collapse.

II.3 Final Remark

The simulation results presented for the simple system shown in Figure II-1 help to better understand the mechanism of voltage instability and voltage collapse. The results also provide good reference for detailed study of more complex multi-node systems. For voltage stability study of large systems, all the unit regulation and limitation loops are important for system voltage stability and therefore have to be considered. Furthermore, modelling of these regulations and limits are important for both steady state and dynamic analysis of voltage stability.

Appendix II references

1. V. Arcidiacono, "Automatic Voltage and Reactive Power Control in Transmission System", CIGRÉ-IFAC Survey Paper - Firenze, September 1983,
2. V. Arcidiacono, S. Corsi et al., "Regolzione Secondaria di tensione del nodo di Sorgente", AEI - Catania, September 1987.
3. V. Arcidiacono, S. Corsi et al., "New Development in the Application of ENEL Transmission System Voltage and Reactive Power Automatic Control", CIGRÉ - Paris, August–September, 1990.

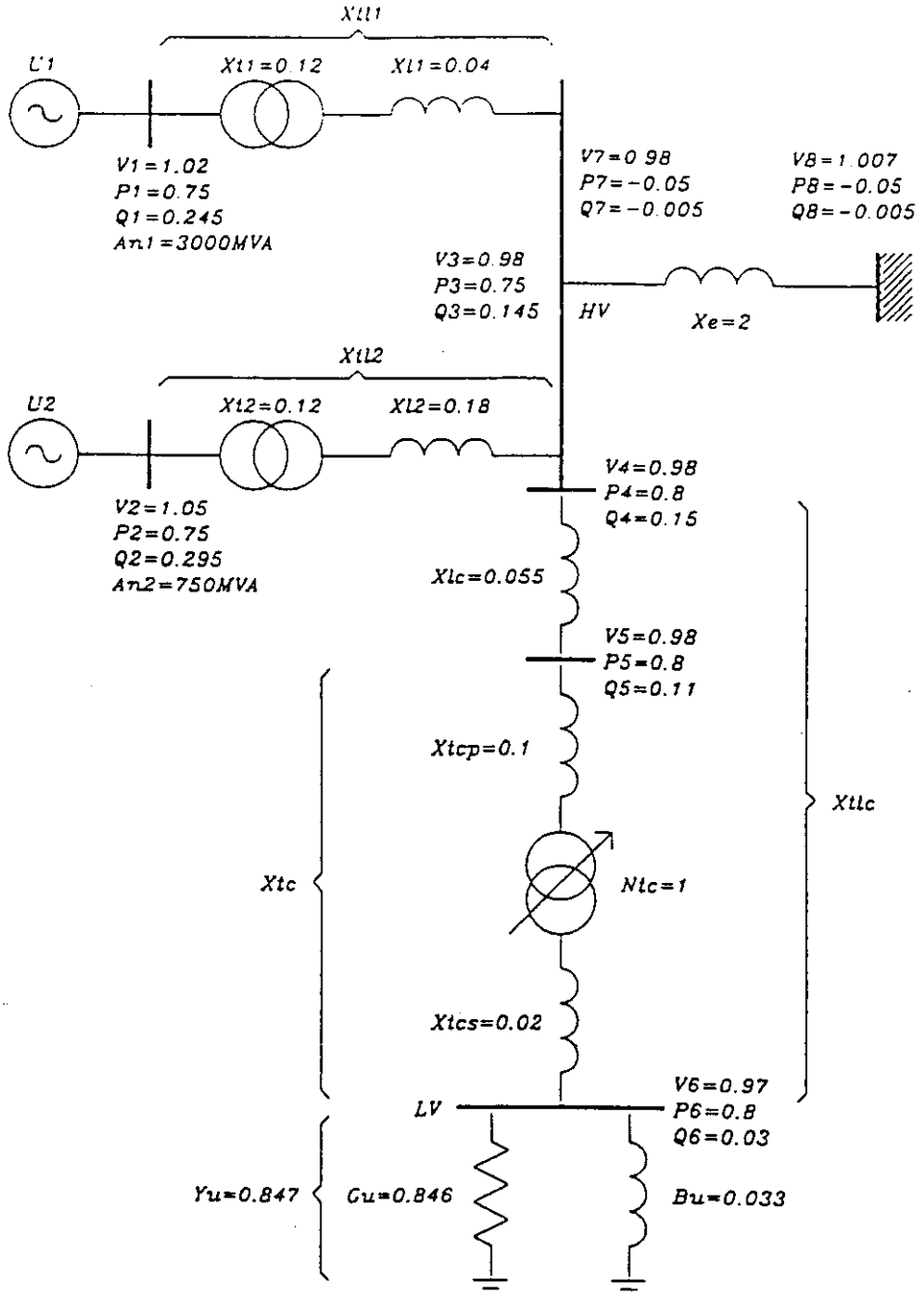

Electrical system: network and power units

Fig. II-1. Simplified power system.

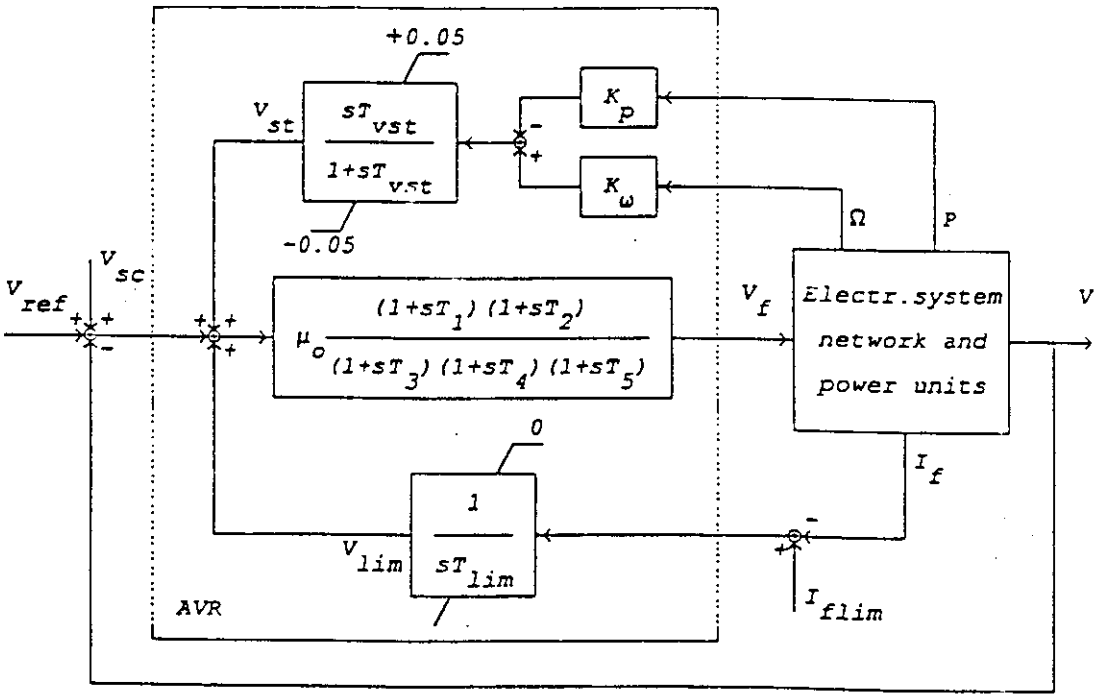

T_1 = 2 s
T_2 = 0.05 s
T_3 = 30 s
T_4 = 0.005 s
T_5 = 0.001 s

μ_o = 500 pu/pu
K_p = 0.3 pu/pu
K_ω = 5 pu/pu
T_{vst} = 3 s
T_{lim} = 10 s

Fig. II-2. Block diagram of primary voltage regulation.

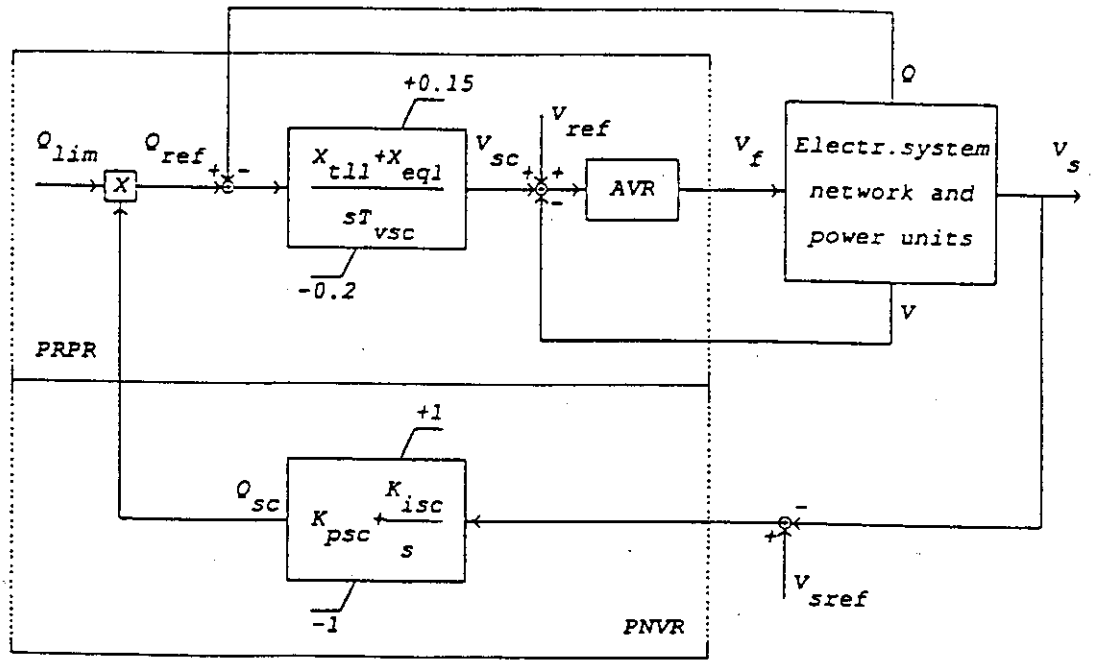

$$K_{psc} = \frac{1}{Q_{lim} X_{t1l}} \text{ pu/pu} \qquad T_{vsc} = 5 \text{ s}$$

$$K_{isc} = \frac{1+K_{psc} Q_{lim} X_{eql}}{T_{qsc} Q_{lim} X_{eql}} \text{ s}^{-1} \qquad T_{qsc} = 50 \text{ s}$$

$$X_{eql} = f(X_{t12}, X_{t1c}, Y_u, X_e)$$

Fig. II-3. Block diagram of secondary voltage regulation.

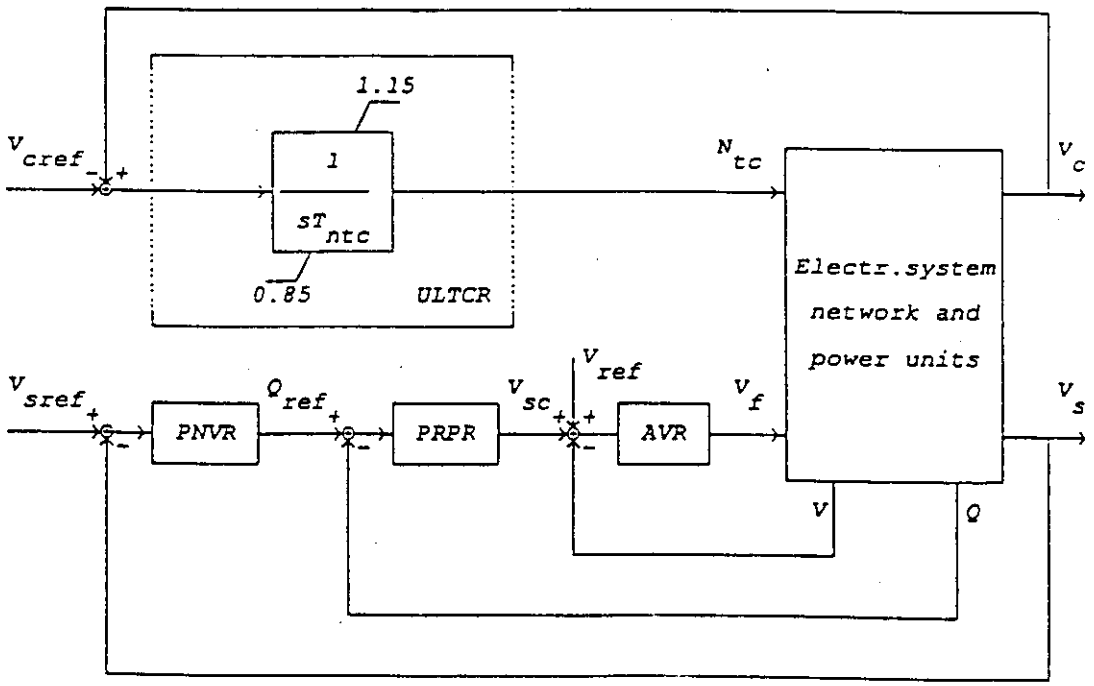

Fig. II-4. Block diagram of LTC control loop together with primary and secondary voltage control loops.

Table II-1
A Synthetic Overview of the Cases Considered for Dynamic Analysis

	TEST PT	TEST PLT	TEST PLST
ULTC	closed loop $0.85 \le N_{tc} \le 1.15$	closed loop $0.85 \le N_{tc} \le 1.15$	closed loop $0.85 \le N_{tc} \le 1.15$
Equivalent linear load	$Y_{un}=0.847pu$	$Y_{un}=0.847pu$	$Y_{un}=0.847pu$
Infinite bus interconnection	$X_{en}=2pu$	$X_{en}=2pu$	$X_{en}=2pu$
Over-excitation limits U1	unlimited	limited	limited
Over-excitation limits U2	unlimited	limited	limited
Secondary voltage regulation	open loop	open loop	closed loop
Simulation time	$t_{tot}=300s$	$t_{tot}=300s$	$t_{tot}=300s$
Variation starting	$t_1=100s$	$t_1=100s$	$t_1=100s$
Load gradient	$\Delta Y_u/\Delta t=1\%/s$	$\Delta Y_u/\Delta t=1\%/s$	$\Delta Y_u/\Delta t=1\%/s$
Fast load variation	$\Delta Y_u=40\%$	$\Delta Y_u=30\%$	$\Delta Y_u=30\%$
Figure	II-5, II-6		II-13, II,14, II-15
Fast load variation	$\Delta Y_u=50\%$	$\Delta Y_u=40\%$	$\Delta Y_u=40\%$
Figure		II-9, II-10	
Fast load variation	$\Delta Y_u=60\%$	$\Delta Y_u=50\%$	$\Delta Y_u=50\%$
Figure	II-7, II-8	II-11, II-12	II-16, II-17

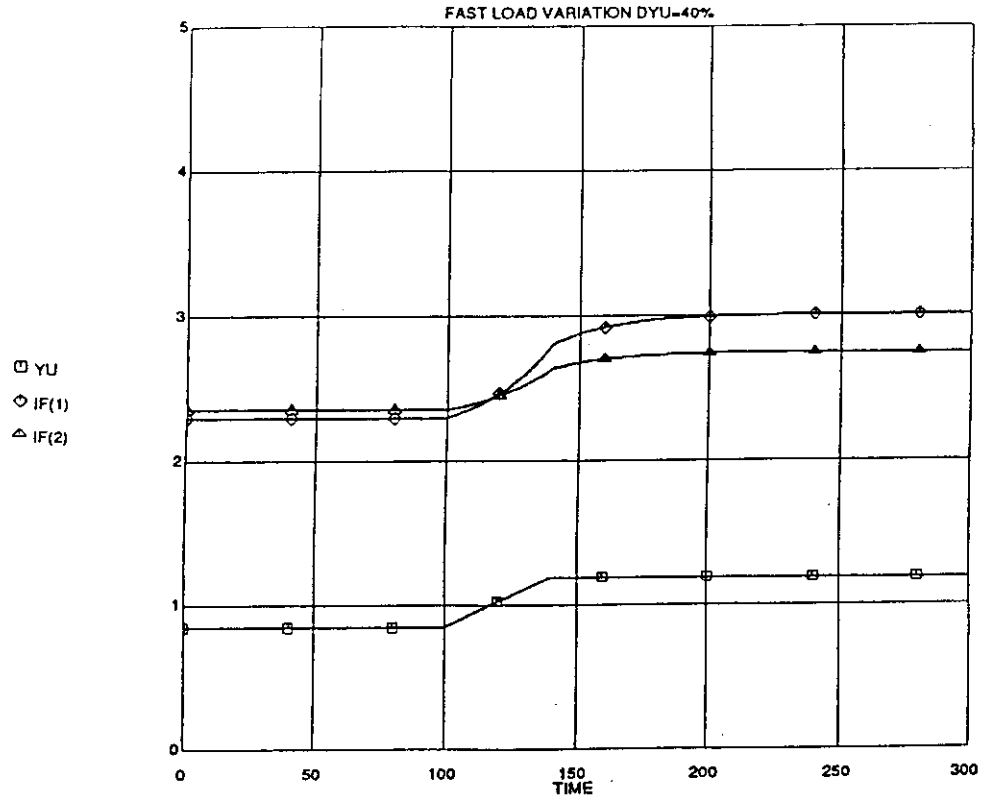

Fig. II-5. Test PT: Y_u, I_{f1}, I_{f2} transients with $\Delta Y_u = 40\%$.

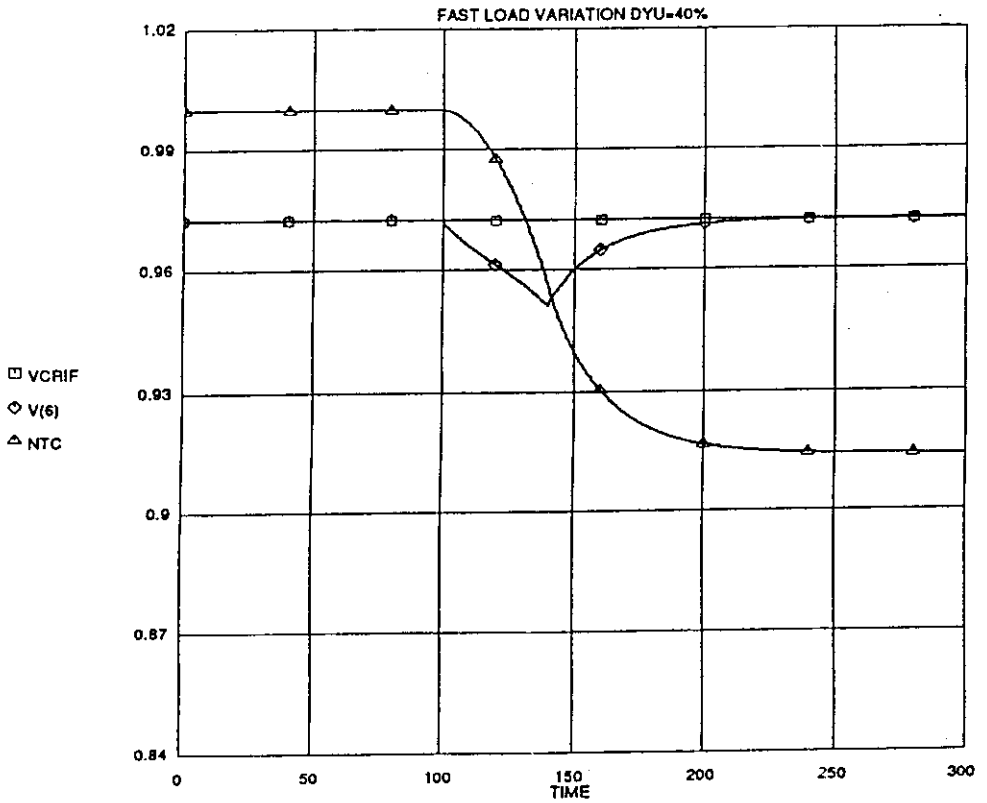

Fig. II-6. Test PT: V_{cref}, V_6, N_{tc} transient with $\Delta Y_u = 40\%$.

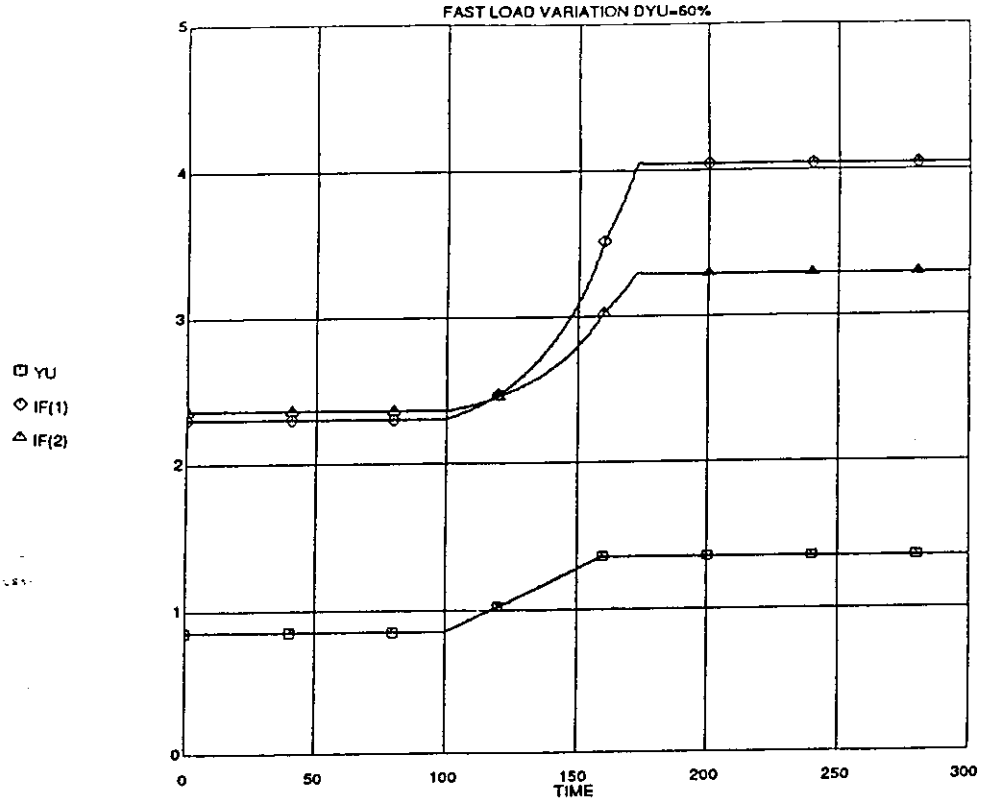

Fig. II-7. Test PT: Y_u, I_{f1}, I_{f2} transients with $\Delta Y_u = 60\%$.

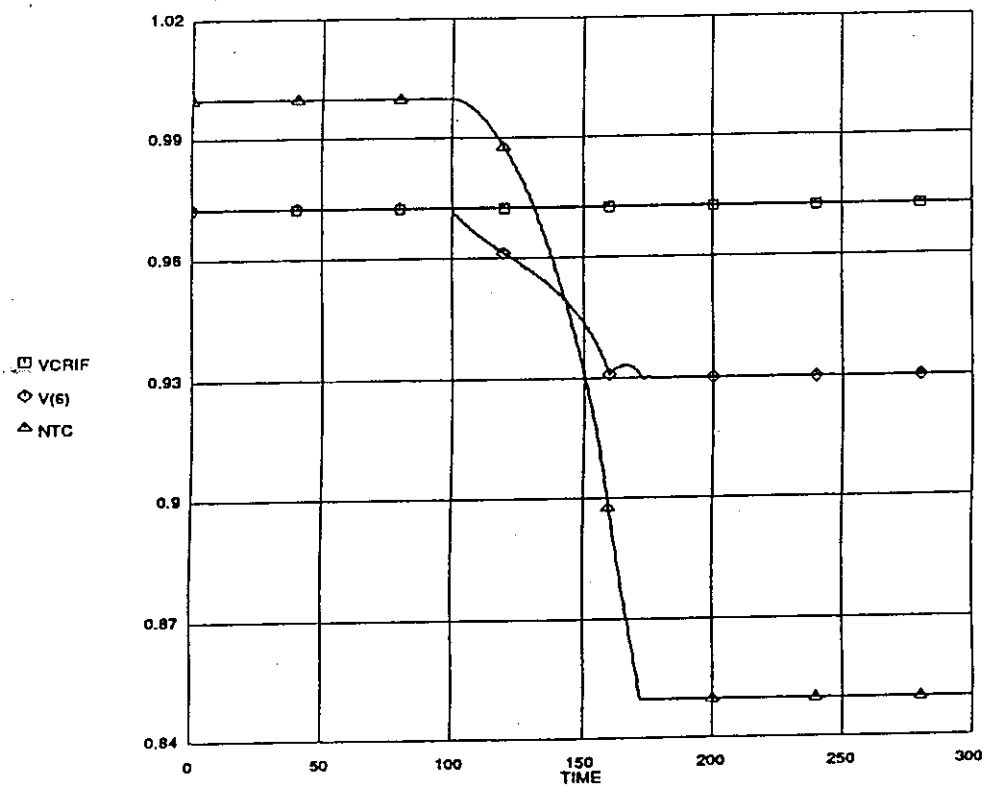

Fig. II-8. Test PT: V_{cref}, V_6, N_{tc} transients with $\Delta Y_u = 60\%$.

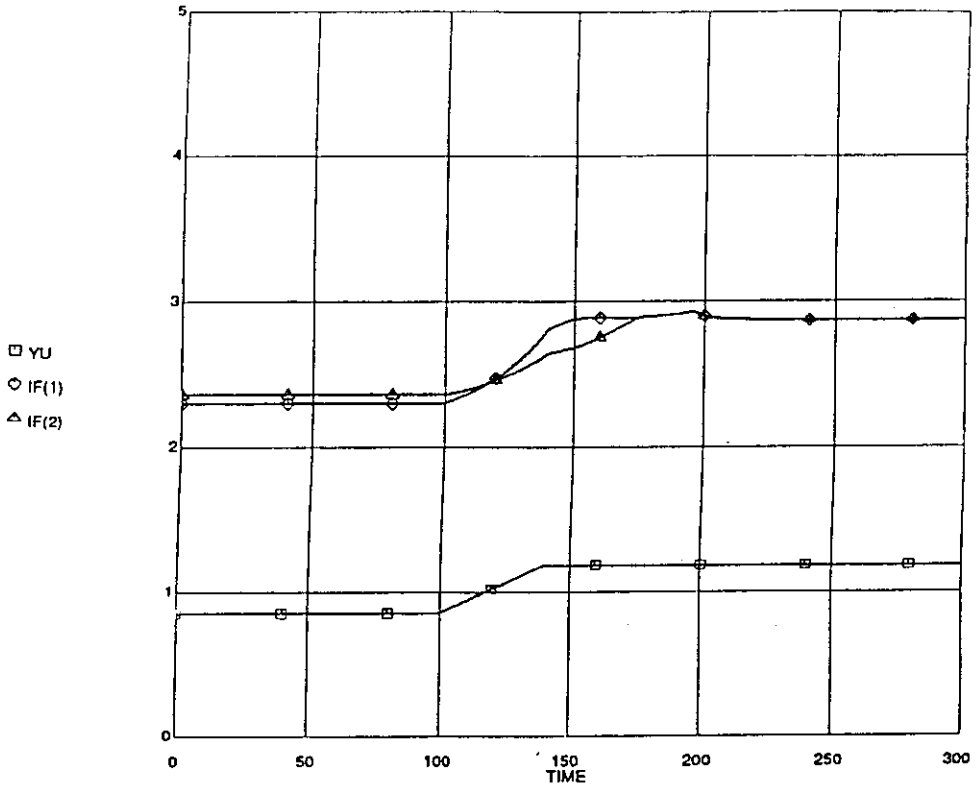

Fig. II-9. Test PLT: Y_w, I_{f1}, I_{f2} transients with $\Delta Y_u = 40\%$.

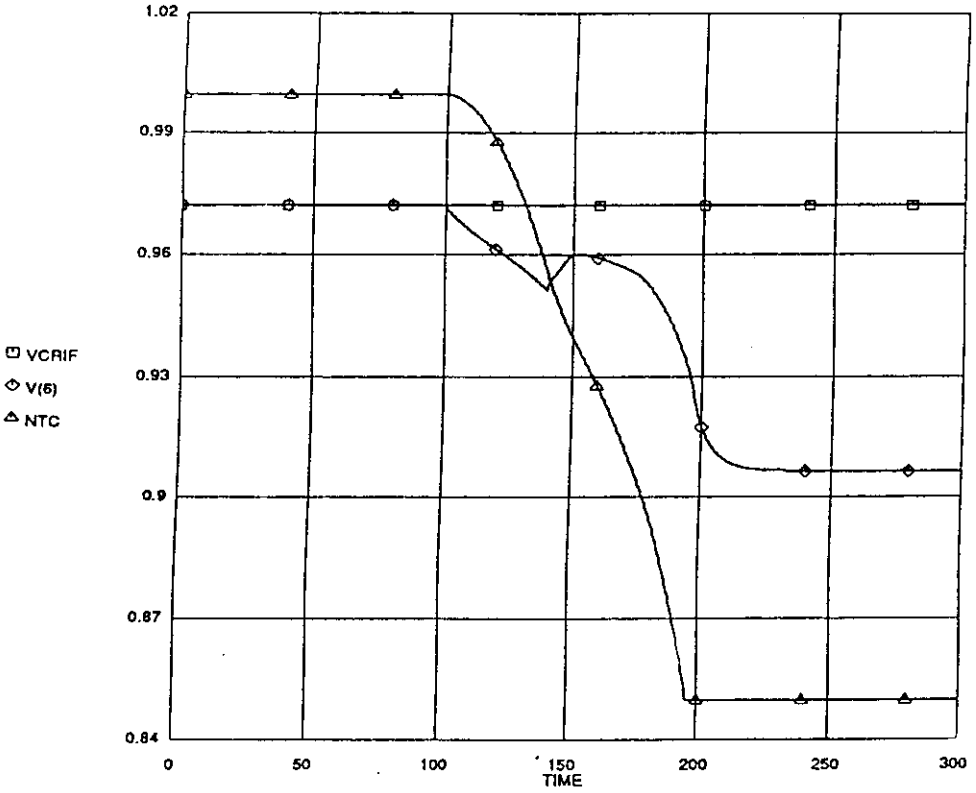

Fig. II-10. Test PLT: V_{cref}, V_6, N_{tc} transients with $\Delta Y_u = 40\%$.

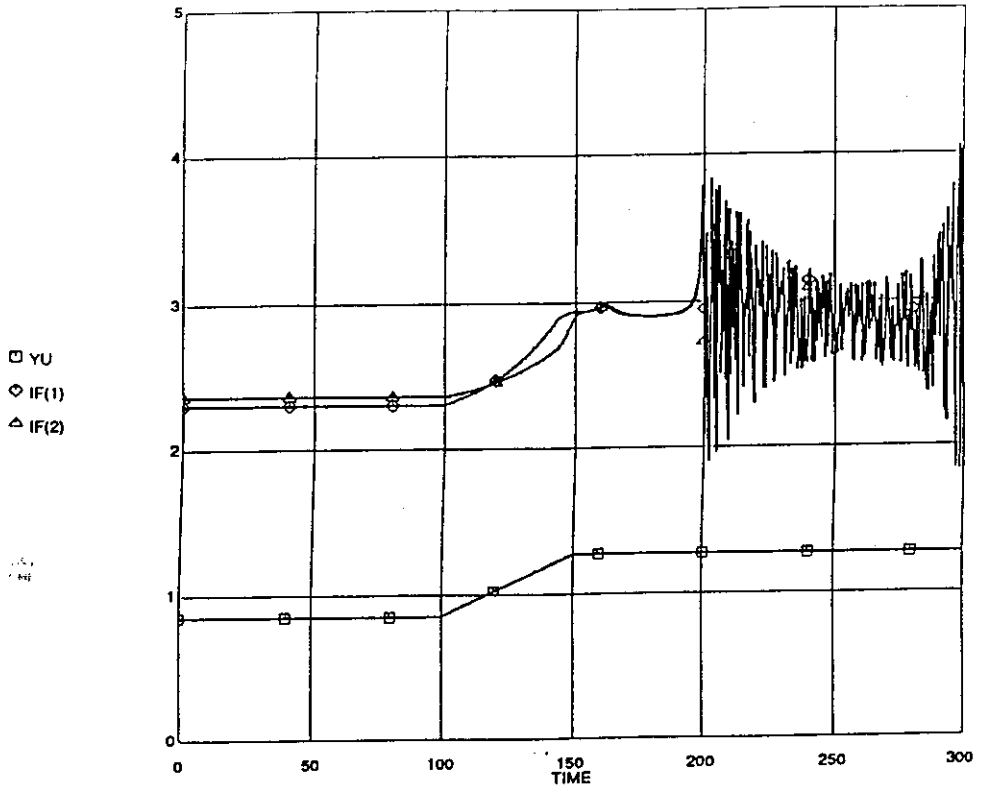

Fig. II-11. Test PLT: Y_u, I_{f1}, I_{f2} transients with $\Delta Y_u = 50\%$.

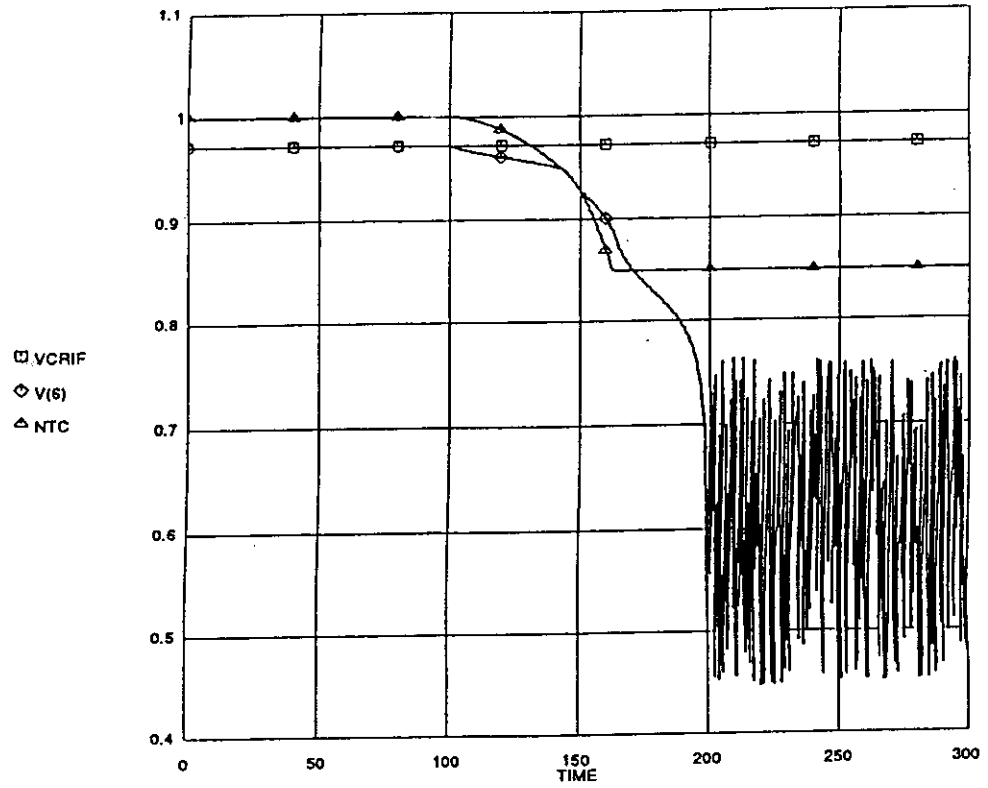

Fig. II-12. Test PLT: V_{cref}, V_6, N_{tc} transients with $\Delta Y_u = 50\%$.

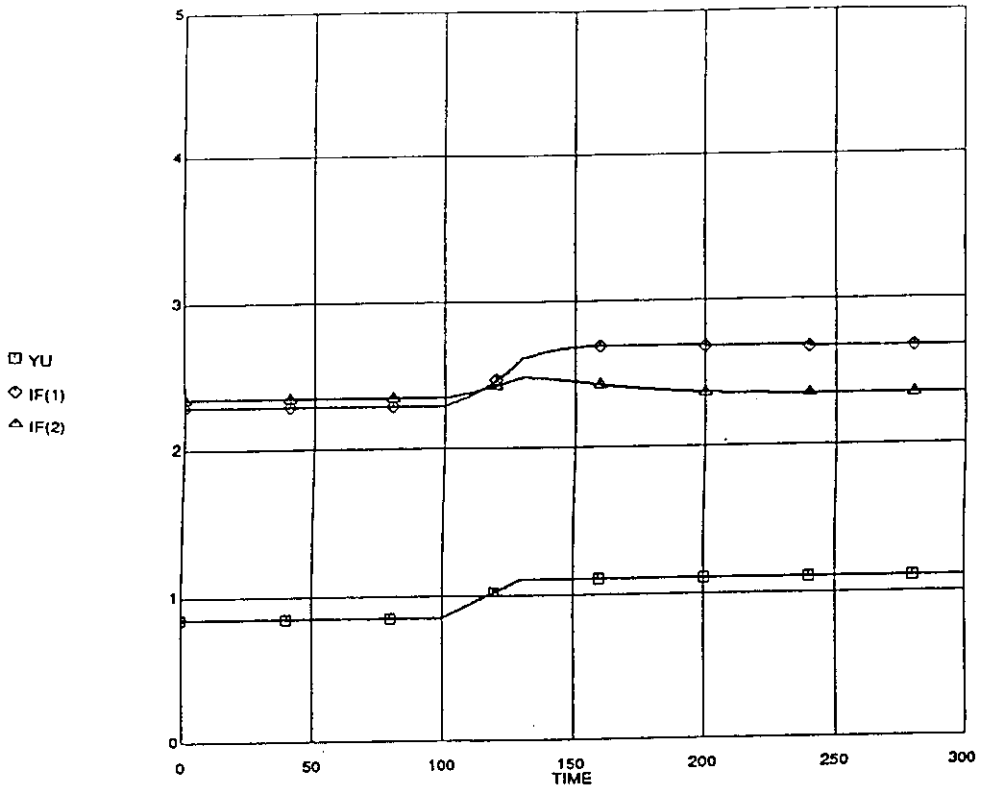

Fig. II-13. Test PLST: Y_u, I_{f1}, I_{f2} transients with $\Delta Y_u = 30\%$.

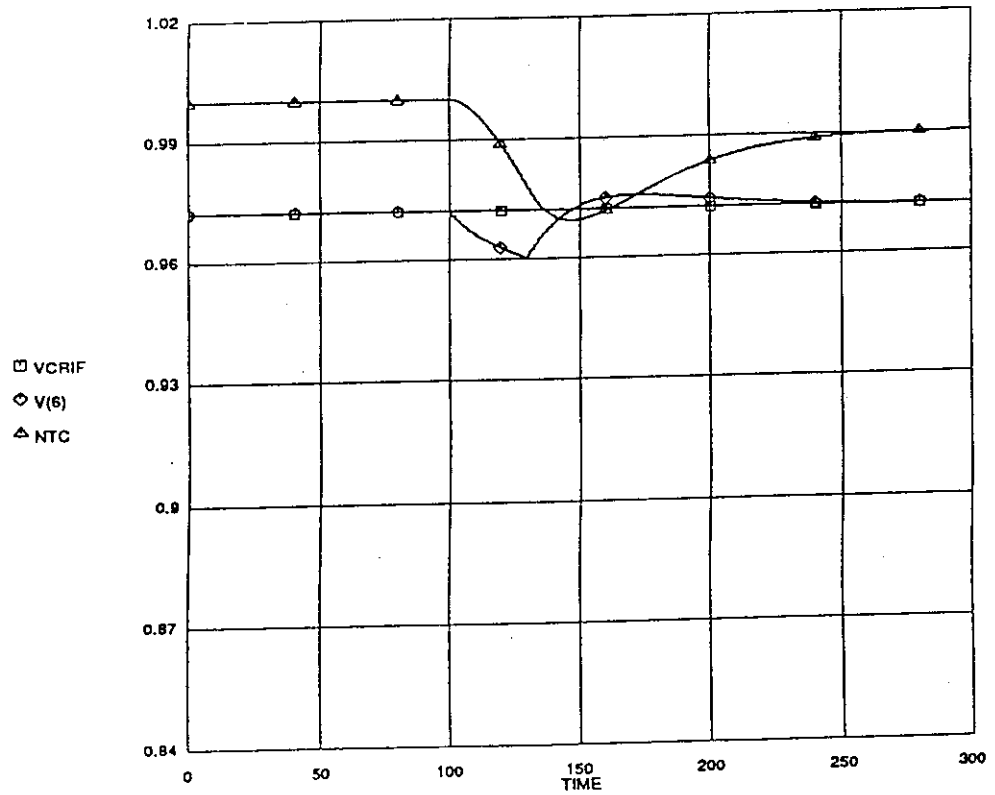

Fig. II-14. Test PLST: V_{cref}, V_6, N_{tc} transients with $\Delta Y_u = 30\%$.

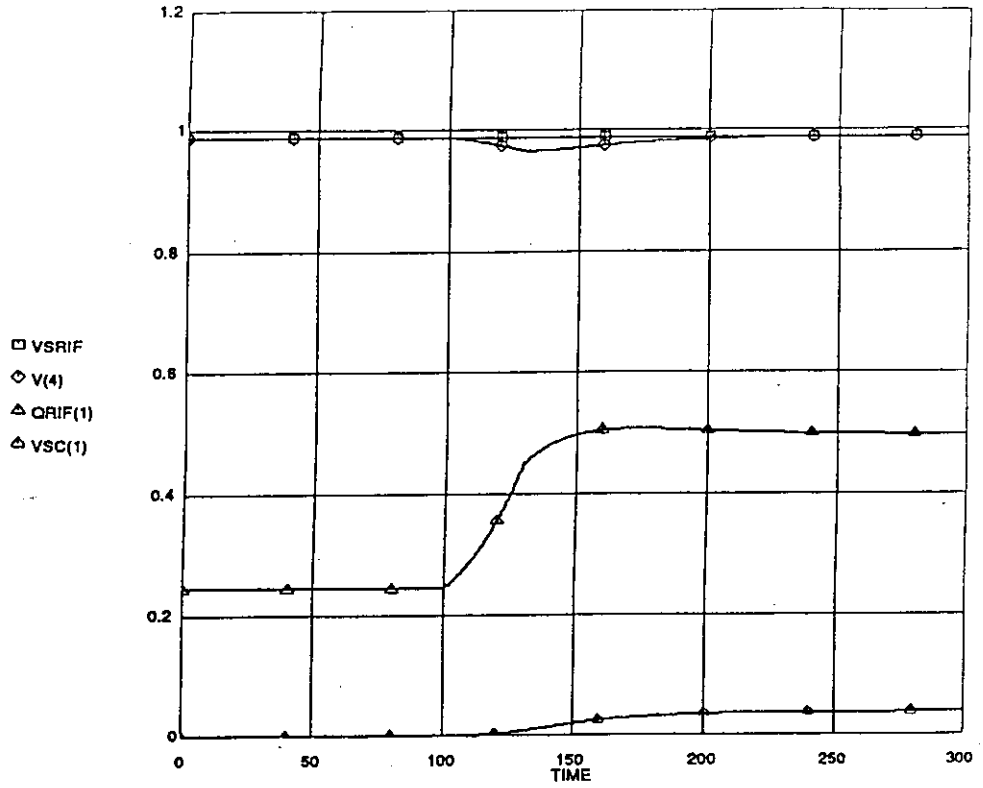

Fig. II-15. Test PLST: V_{sref}, V_4, Q_{ref1}, V_{sc1} transients with ΔY_u = 30%.

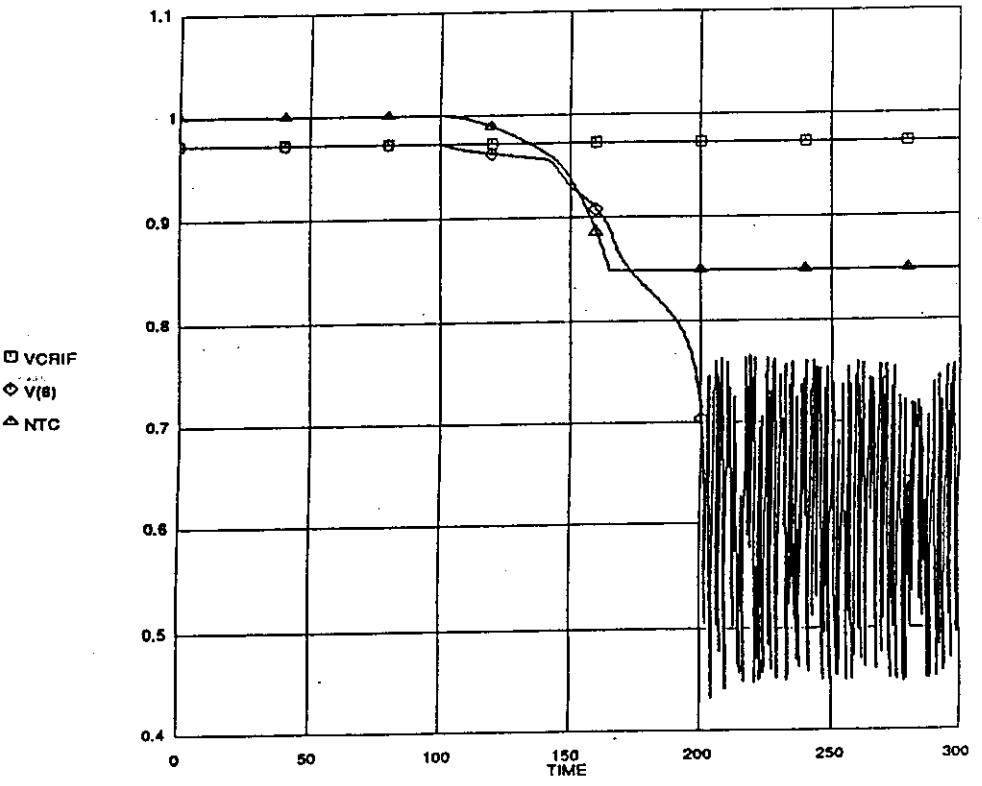

Fig. II-16. Test PLST: V_{cref}, V_6, N_{tc} transients with ΔY_u = 50%.

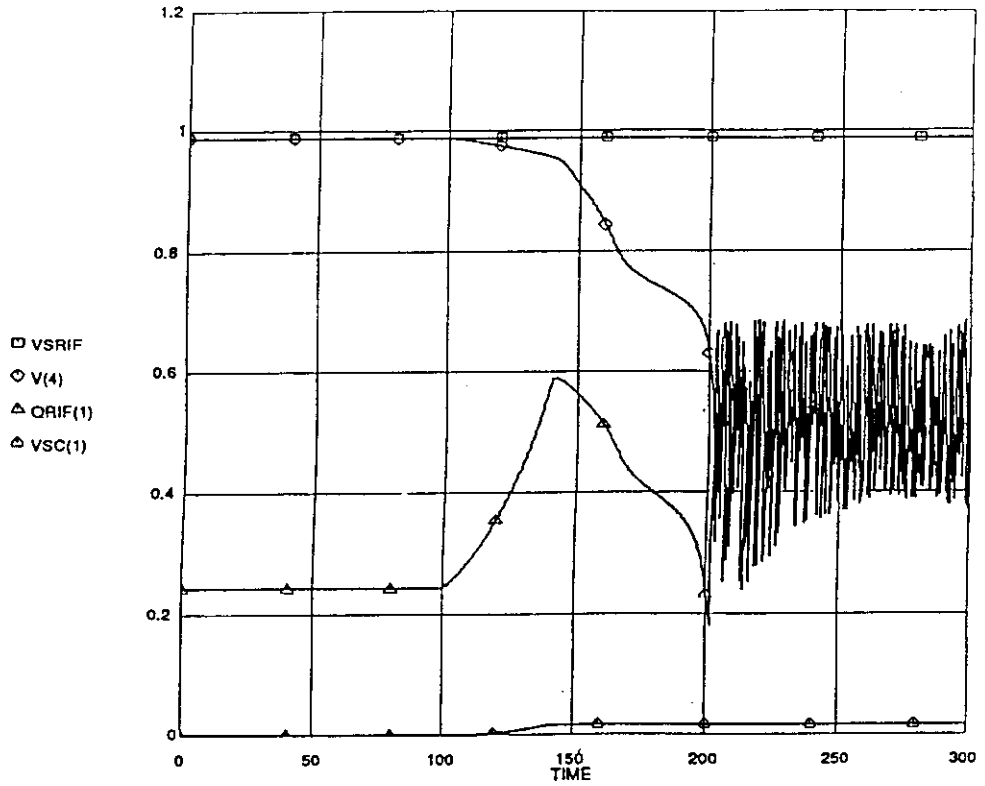

Fig. II-17. Test PLST: V_{sref}, V_4, Q_{ref1}, V_{sc1} transients with $\Delta Y_u = 50\%$.

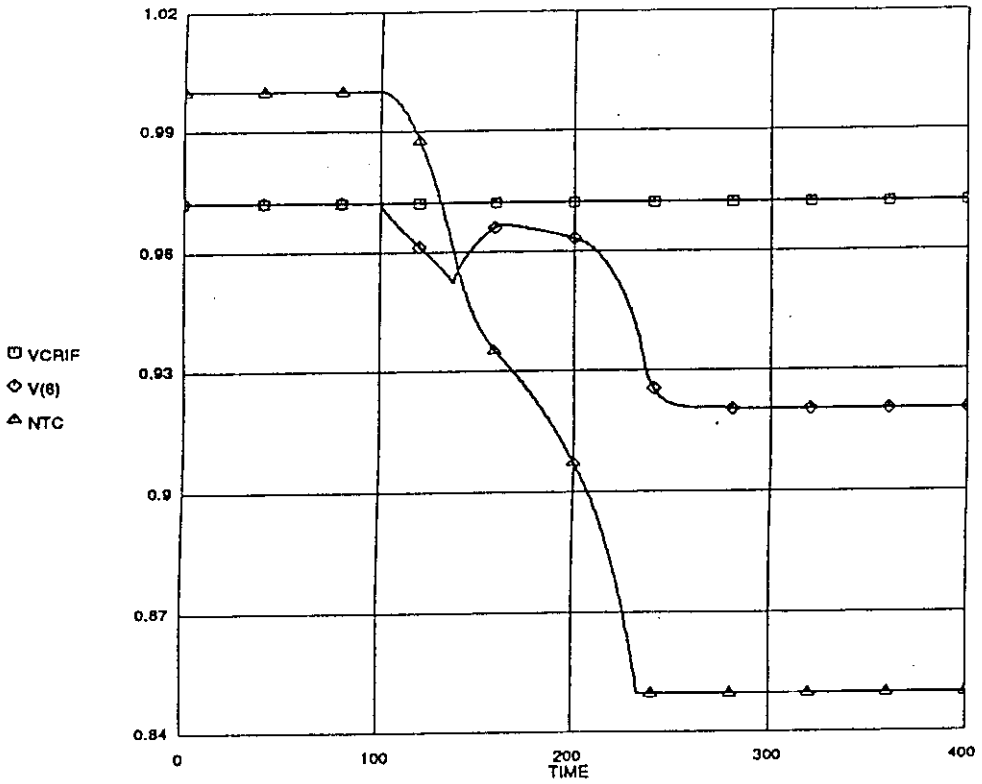

Fig. II-18. Test PLT: V_{cref}, V_6, N_{tc} transients with $\Delta Y_u = 38\%$.

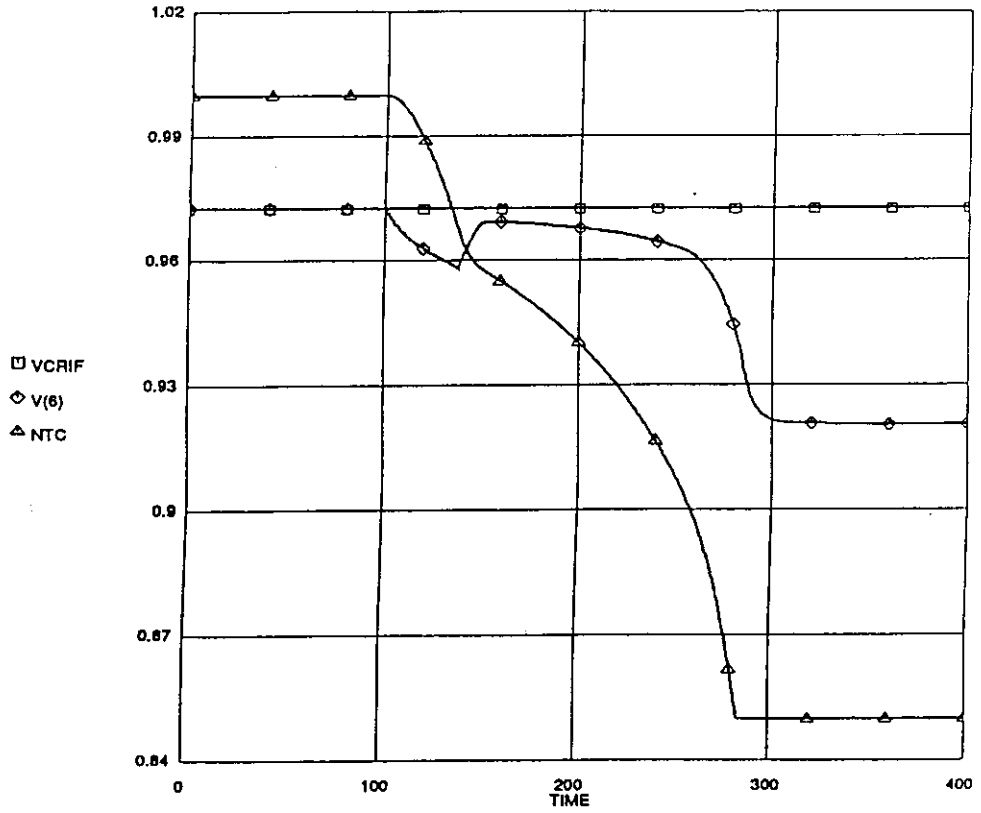

Fig. II-19. Test PLST: V_{cref}, V_6, N_{tc} transients with ΔY_u = 38%.

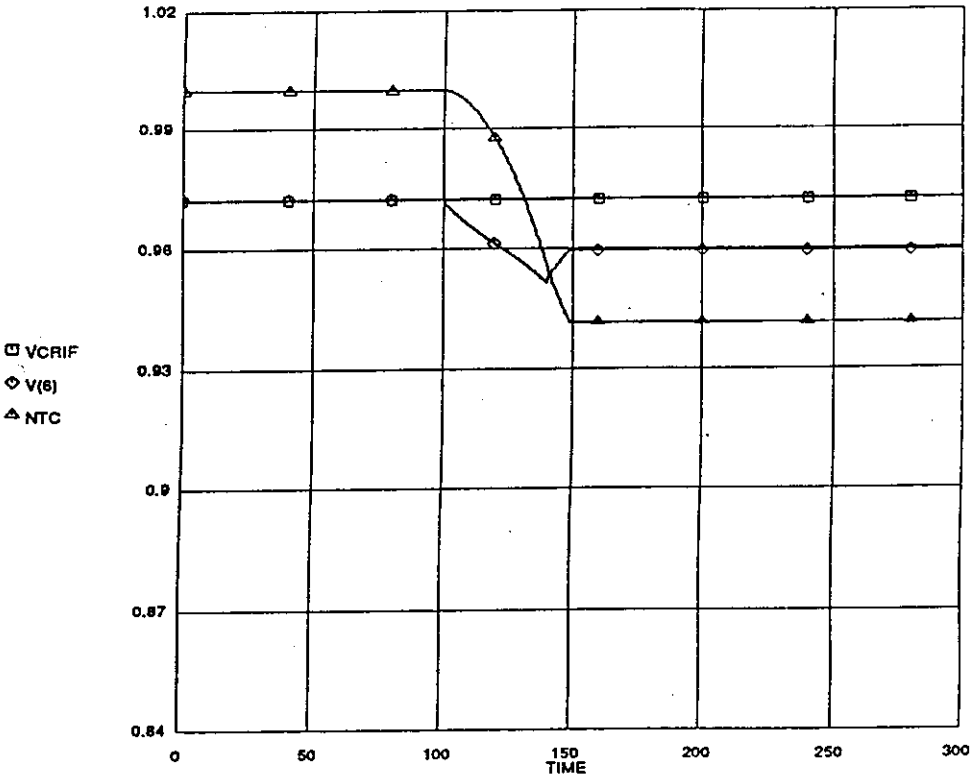

Fig. II-20. Test PLT: V_{cref}, V_6, N_{tc} transients with ΔY_u = 40%, LD = 0 seconds.

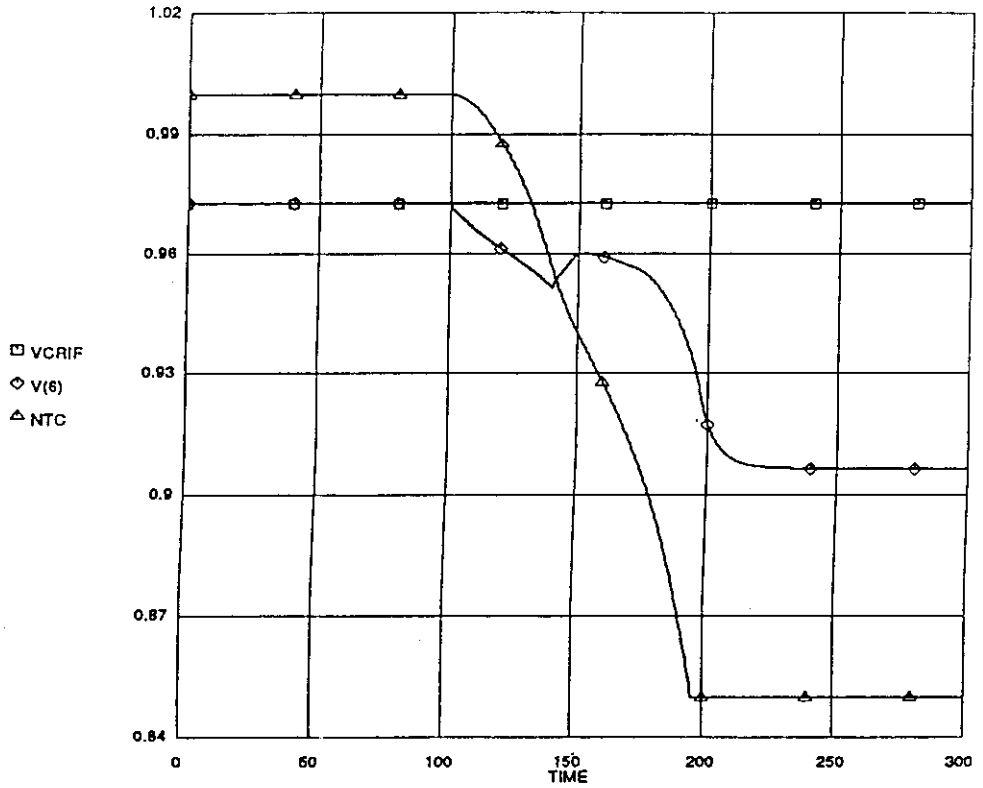

Fig. II-21. Test PLT: V_{cref}, V_6, N_{tc} transients with ΔY_u = 40%, LD = 60 seconds.

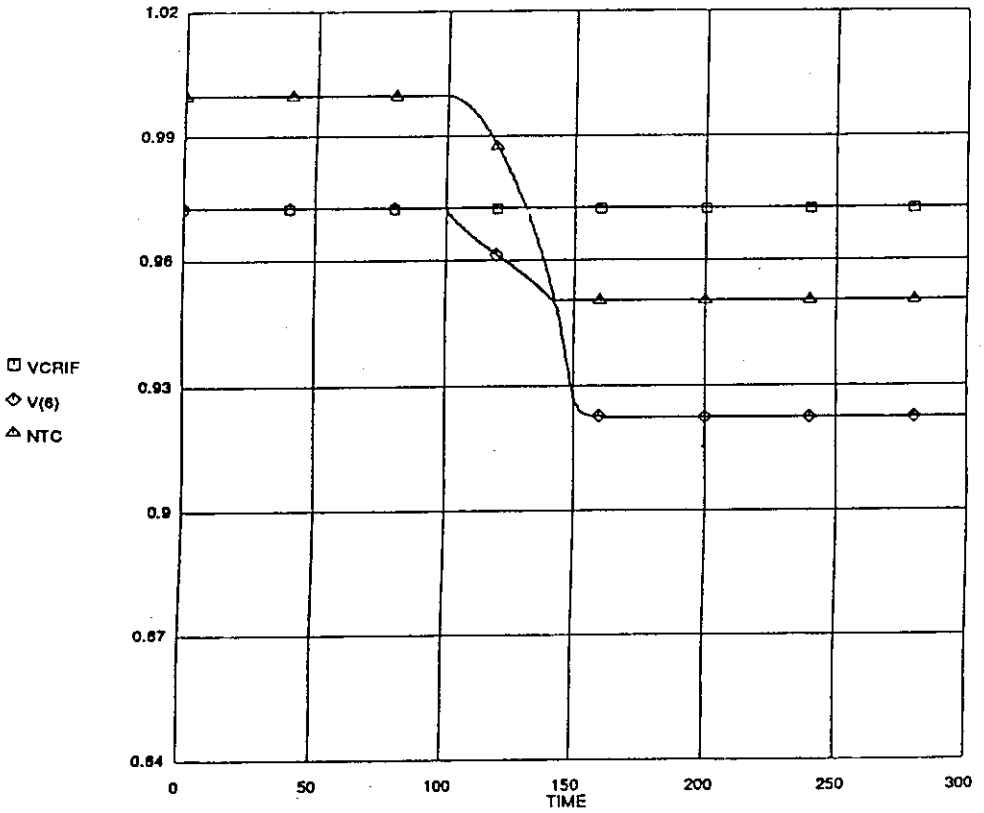

Fig. II-22. Test PLT: V_{cref}, V_6, N_{tc} transients with ΔY_u = 50%, LD = 0 seconds.

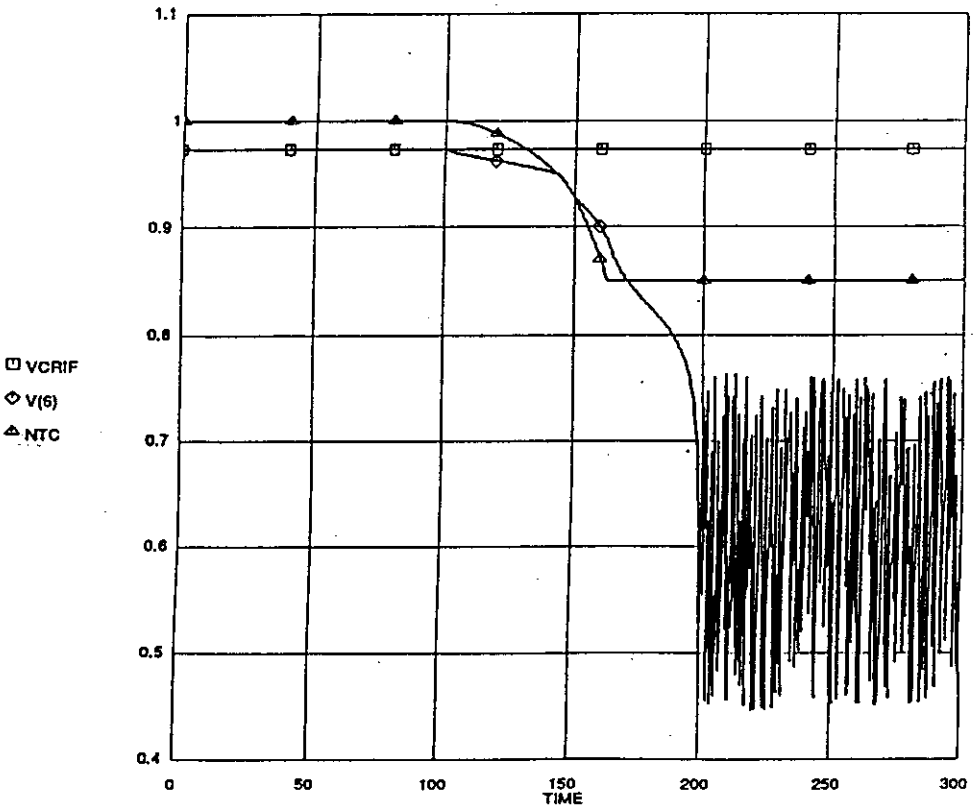

Fig. II-23. Test PLT: V_{cref}, V_6, N_{tc} transients with ΔY_u = 50%, LD = 30 seconds.

Appendix III, Contribution to Chapter 8
Sensitivities of Voltage Stability to System Characteristics, Part 2

J. Y. Leost
Electricité de France

III.1 Test Systems

Three cases are used to describe some voltage phenomena. Case C has been described in [23]; it describes the basics of voltage instability by a simple example. Case D has been described in [23] and [49]; it displays the detrimental influence of automatic LTC which masks the load voltage sensitivity, and shows that transient phenomena can take place during a quasi steady state phase. Case E was presented in [50] and [65]; it is based on a study for the future French "defense plan" set up to reduce the seriousness of incidents which could affect the French power system.

All the simulations of cases C, D and E were done using the EUROSTAG package, jointly developed by Electricité de France and TRACTEBEL ([49] and [50]). The program uses an automatically variable step size integration method, which enables to describe the behavior of the system simultaneously for short-, mid- or long-term dynamics.

III.2 Sensitivity to load characteristics

Case C: Sensitivity to voltage sensitivity exponent. Case C considers an "infinite" bus feeding a reactive load through a purely inductive line. The voltage of this bus is V_o (p.u.), the reactance of the line is X_l (p.u.). The load is represented by the following formula:

$$Q = Q_o \, |V|^a$$

where

Q is the actual reactive power (p.u.);

Q_o is the actual reactive power (p.u.) at V=1.p.u.;

$|V|$ is the modulus of the voltage at the load feeding point;

a is the voltage sensitivity exponent.

Three cases are considered: $a = 0$, $a = 1$ and $a = 2$. So the load is respectively voltage independent, a current sink, or an admittance.

Figure III-1 shows:

- as a function of time, and for $a = 0$, 1, or 2:
  - the load in MVAr
  - the voltage at the load terminals
- the curve V versus Q or a part of it, drawn respectively for $a = 2$, 1, and 0.

On the last curve, the voltage drops to 0.5 p.u., value corresponding to maximum transfer capability of 250 MVAr. This voltage versus reactive power curve is a feature of source (V_o, X_l). With $a = 0$ it is only possible to get the upper

part of it, and with $a = 2$ a greater rate of change would be necessary to get values near $V = 0$.

Case D: Effect of automatic LTC operation. Case D considers a simplified system (Figure III-2) that looks like a part of the 400-kV and 150-kV Belgian systems, as it was some ten years ago, and after tripping a tie line.

The external system is simulated by means of two "infinite" busses. Most loads are fed by 400/150-kV autotransformers and simulated as passive loads behind subtransmission transformers fitted with automatic load tap changers (LTCs). Different regulators, limiters and protective devices are taken into account.

The simulation (Figure III-3) of a hypothetical case starts with the tripping of unit M2, which together with the action of the automatic tap changer, sets the rotor current limiter of unit M1 in action. A bad tuning of this limiter reduces drastically the excitation, provoking the loss of synchronism of the unit M1. After this second unit trips, the voltage at the terminals of machines M3, M4 and M5 becomes too low and they also trip by undervoltage protection. Finally, the rotor protection of M6 is triggered and causes the loss of synchronism of this unit. Then, the voltage in the 150-kV system drops to nearly zero.

Another simulation showed that the introduction of a SVC at station N4 is adequate to avoid this voltage collapse, the M1 generating unit remaining under its rotor current limit.

Case E: Sensitivity to shortage of reactive power. Case E considers the French power system, with some 1100 busses, 2000 lines and transformers, and 100 generators with their controllers; the models include several protective relays, automatically variable LTCs etc. The automatic devices are modelled with the details and the accuracy needed. For instance the generator rotor current limitation, the performances of which may be important not only from the viewpoint of transient and static stability but also during voltage collapse phenomena. One can mention some relays scattered over the network:

- generation unit islanding relay acting on voltage, current or frequency criteria,
- line or transformer overload protection,
- automatic transformer tap changer,
- area islanding protections in case of loss of synchronism (called DRS relays).

A part of the study concerns the voltage collapse due to local reactive power shortages that can lead to the loss of close generation units, aggravating the process. The simulations performed cover the behavior of the system in short-, medium- and long-term dynamics. Hence a great modelling effort, beyond the different automatic devices mentioned above, is adopted; a particular load model incorporates an equivalent admittance behind a transformer with a continually variable transformer ratio automatically tuned. Furthermore all the loads are distributed among areas, the loads within an area being able to vary homothetically in relation with a pilot load. A hand operated remote load-shedding is also added.

In order to study the phenomena associated with the voltage collapse, the

Western part of the French system is examined. The network is weakened by the opening of interconnection links and the unavailability of active and reactive power generating sets. In addition, a rise in the demand at load peak of about 15% within an hour is simulated. Under these extreme conditions, we simulate the loss of a generating plant.

Figure III-4 displays the voltage of a particular substation in this area with (dotted line) or without (solid line) a set of curative measures based on load shedding.

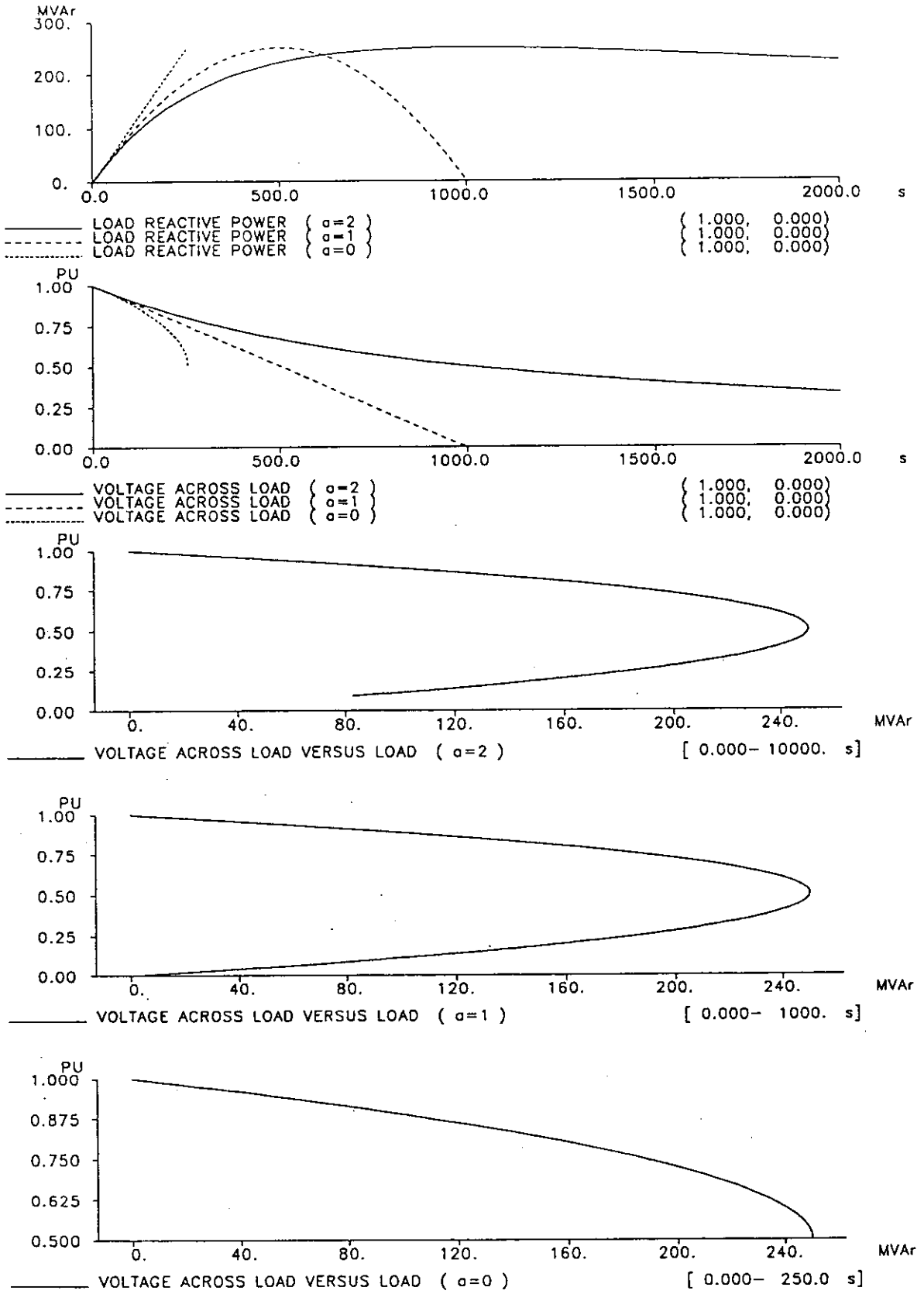

Figure III-1. Sensitivity to voltage sensitivity exponent on a simple system.

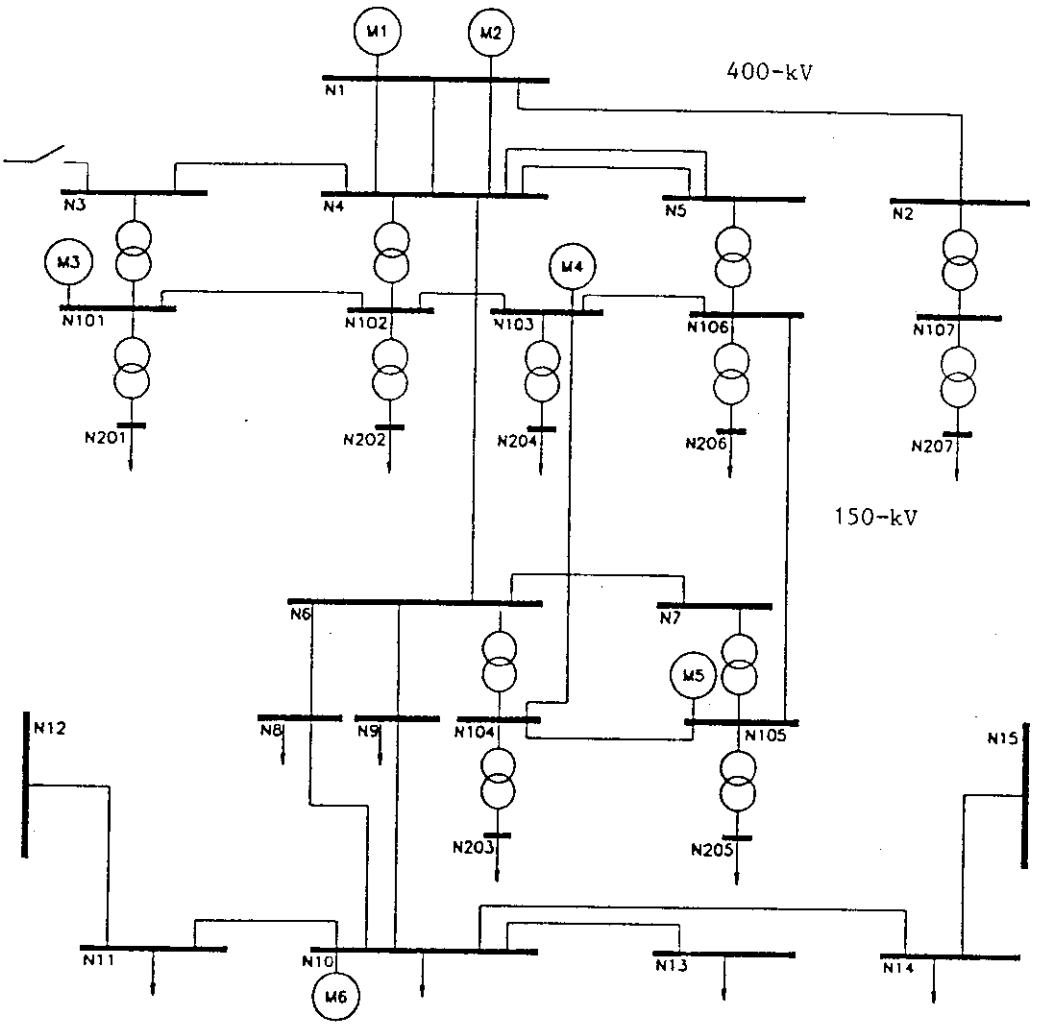

Figure III-2. Simplified representation of the Belgian 400- and 150-kV systems as they were 10 years ago.

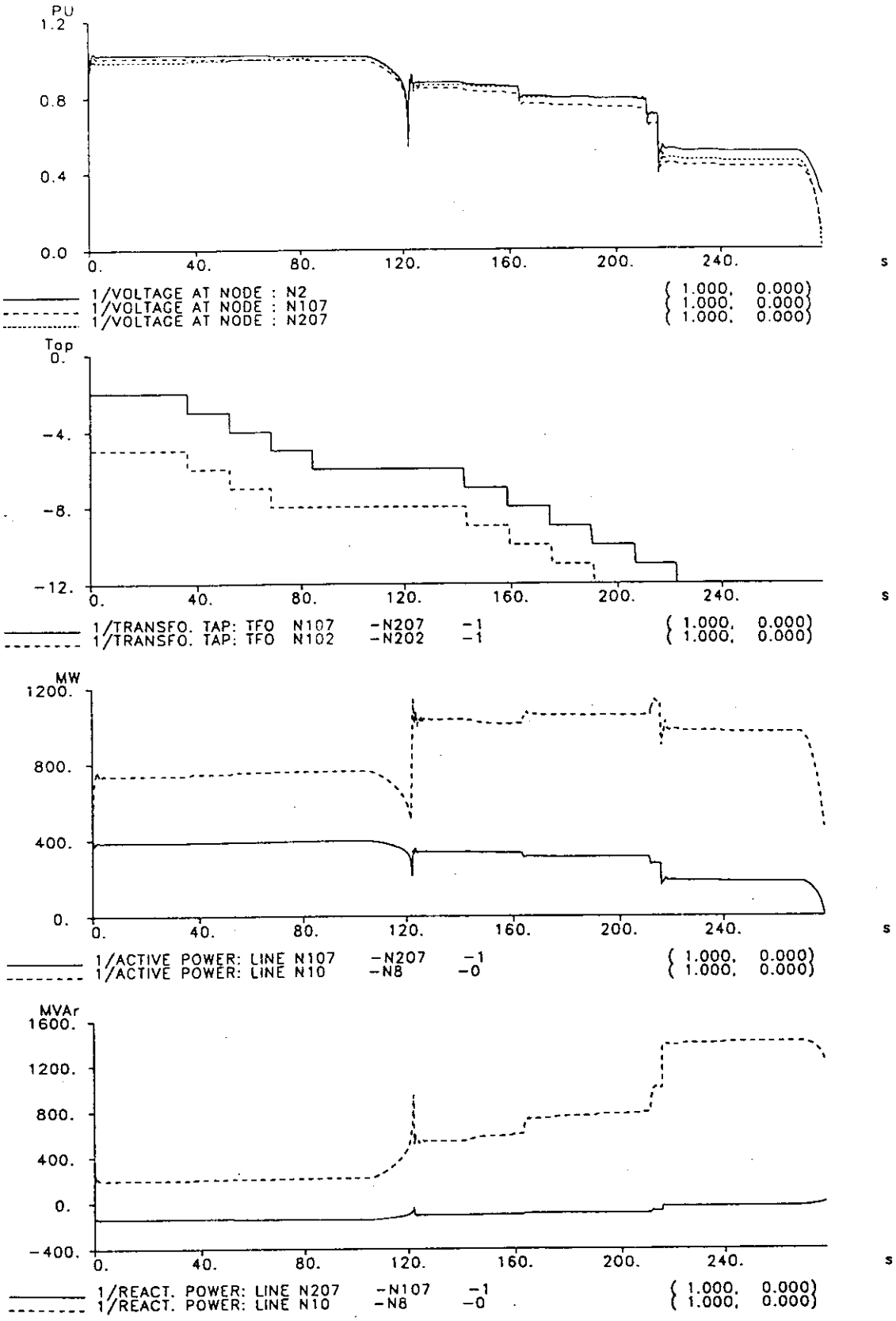

Figure III-3. Voltage, transformer-tap position and imported active power on a transformer and interconnection line, imported reactive power on the same transformer and line (for the system shown in Figure III-2).

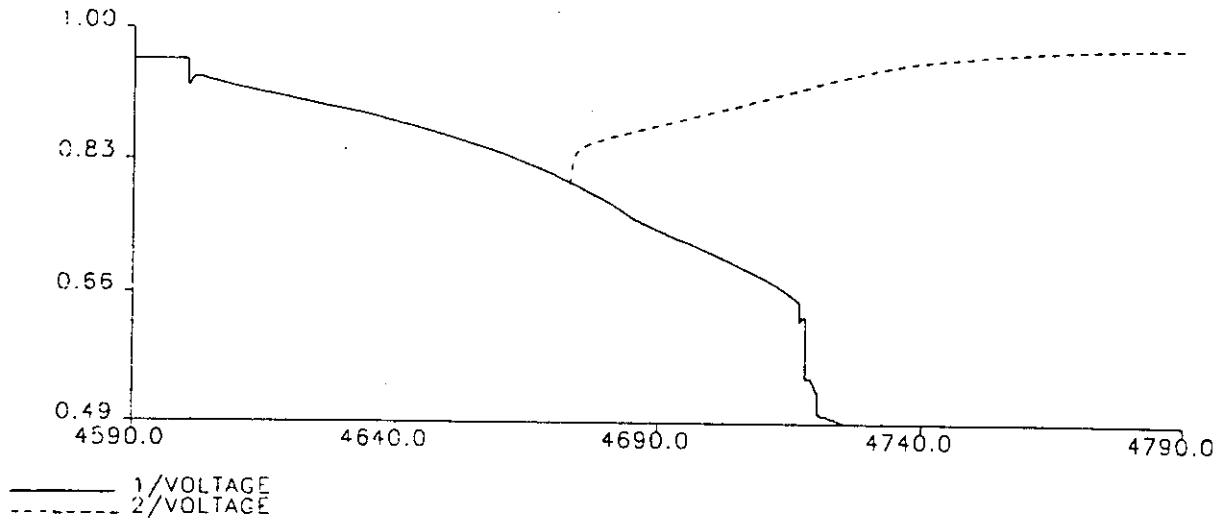

Figure III-4. Simulation on the French system under hypothetical extreme conditions; voltage of a particular bus with (dotted line) or without (solid line) a set of curative measures.

Appendix IV, Contribution to Chapter 8
Effect of Load Representation on the Simulation of Voltage Collapse

C. D. Vournas and N. D. Hatziargyriou
NTU, Athens, Greece

IV.1 Test System

The test system used to demonstrate the effect of load representation on the voltage collapse phenomenon comprises 240 busses, 267 lines, and 30 equivalent generators. This test system has been developed in the Electrical Energy Systems Laboratory of the National Technical University of Athens and is used for dynamic simulation studies. The system is based on a 1993 extrapolation of a Hellenic Power system model, and a pessimistic version of it is used for the subsequent simulations. The interactive Power Systems Simulation Program [1], which is a module of the Graphics Aided Interactive Network Analysis (G.I.N.A.) package developed at NTU is used for subsequent time domain simulations.

IV.2 Sensitivity to Load Characteristics

The disturbance simulated is a 20 MW load switching. Simulation starts at $t = 0$ seconds. The load is switched on at $t = 0.1$ seconds and is switched off at $t = 0.2$ seconds. This is done in order to investigate whether the initial operating point is stable or unstable.

A first order AVR model for all generating units is assumed. The excitation ceilings are included in the simulation.

The dynamic response of the system is a function of the model used for the loads. In order to assess this effect the following cases are examined:

Case A. 100% constant active and reactive power loads, i.e., P = constant, Q = constant.

Case B. 50% of the load is constant active and reactive power loads and 50% is constant admittance loads, i.e.,

$$P = 0.5P_0 + 0.5P_0 (V/V_0)^2$$

$$Q = 0.5Q_0 + 0.5Q_0 (V/V_0)^2$$

where P_0 and Q_0 are the nominal active and reactive power provided in the load data and V_0 is the voltage magnitudes obtained from the initial power flow solution.

Case C. 90% of the load is constant active and reactive power loads and 10% is constant admittance loads.

The response of the system is shown by the time plots of the voltage magnitudes at a weak 150-kV bus, where the voltage at steady state is well below its nominal value.

In Figures IV-1–IV-3, the response of the system for the load representation corresponding to case A, case B, and case C respectively, is shown.

IV.3 Comments

Constant power loads. If the constant power load representation is used, the system exhibits voltage instability, as shown by the response of the system for the minor disturbance mentioned above (20 MW load on and off switching). The voltage response at a weak 150-kV bus is shown in Figure IV-1.

Mixed load representation. If the 50% constant power, 50% constant admittance load representation is used (Figure IV-2), the system does not exhibit voltage problems. In the 90% constant power, 10% constant admittance case (Figure IV-3), the voltage oscillates before reaching its steady state value.

Appendix IV reference

1. C. D. Vournas, N. D. Hatziargyriou, and B. C. Papadias, "Interactive Power System Simulation Program – Application to the Hellenic System," *CIGRE*, paper 38-206, 1990.

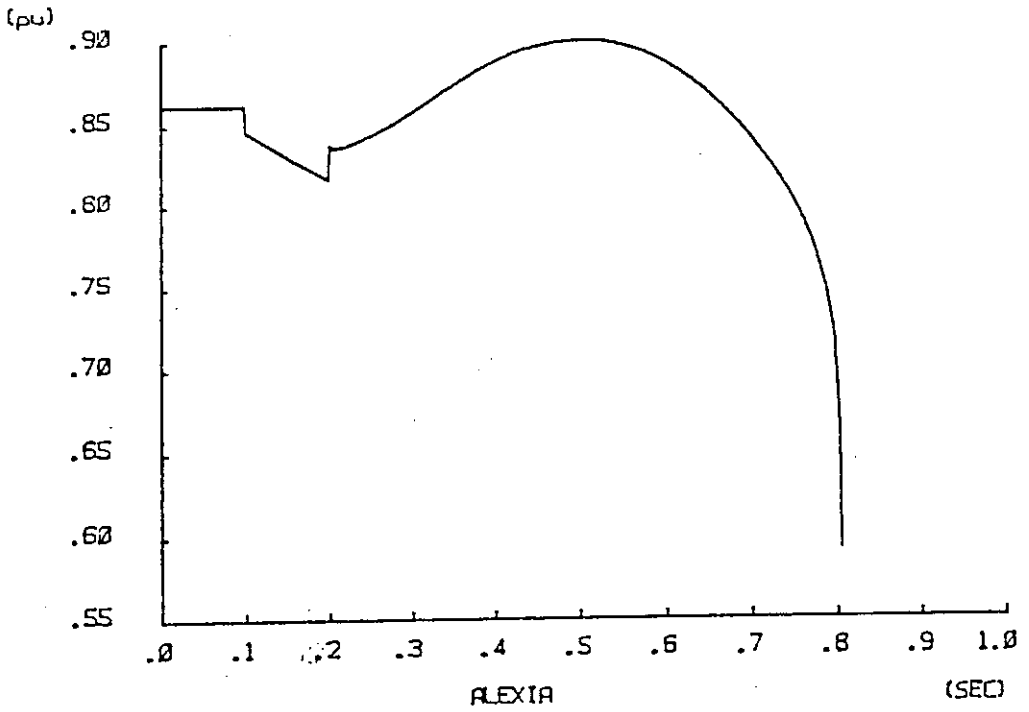

Fig. IV-1. Voltage magnitude for Case A.

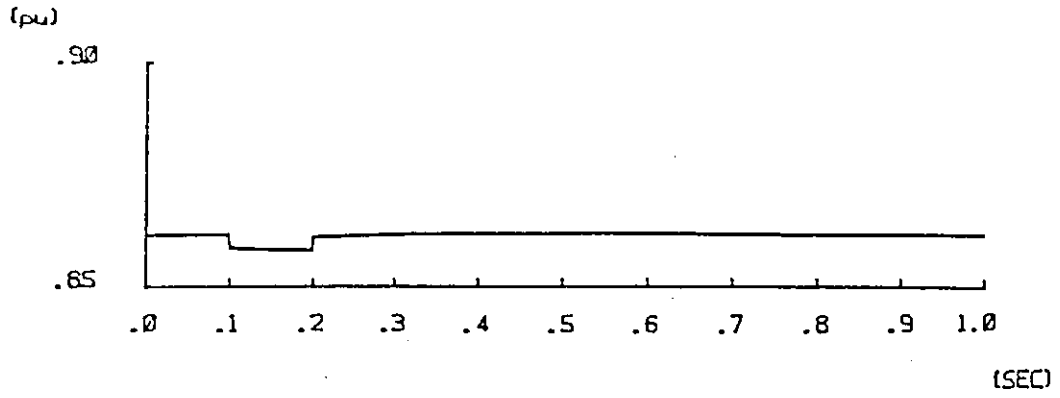

Fig. IV-2. Voltage magnitude for Case B.

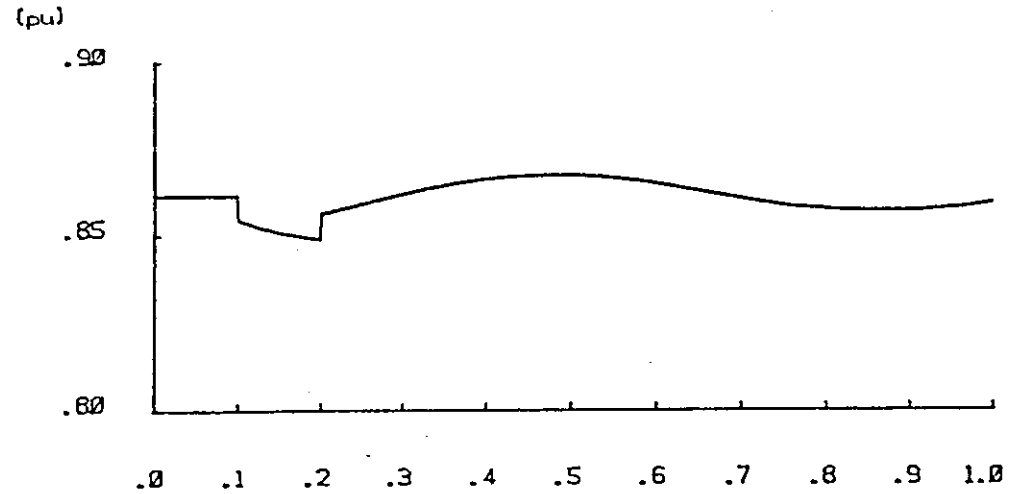

Fig. IV-3. Voltage magnitude for Case C.

Appendix V, Contribution to Chapter 8
Sensitivity to Undervoltage Load Shedding and Generator Line Drop Compensation

C. W. Taylor
Bonneville Power Administration, USA

Bonneville Power Administration identified cold weather-related voltage stability problems in 1988. The voltage stability problems are greatest in the Puget Sound (Seattle-Tacoma) area of the Pacific Northwest, but problems also exist to the north in the Vancouver, British Columbia area, and to the south in the Portland, Oregon area. The problems involve very heavily loaded transmission lines connecting generation east of the Cascade Mountains with west-side load areas.

Two of the most effective solutions adopted were undervoltage load shedding and generator line drop (transformer drop) compensation.

V.1 Puget Sound Area Undervoltage Load Shedding

BPA and four other Puget Sound area utilities implemented a undervoltage load shedding program in December 1991. The load shedding program trips up to 1800 MW of load in three steps of 5% each. The program is as follows:

- 5% of area load shed at voltage 10% below lowest normal voltage—3.5 second time delay.
- 5% of area load shed at voltage 8% below lowest normal voltage—5 second time delay.
- 5% of area load shed at voltage 8% below lowest normal voltage—8 second time delay.

The "lowest normal voltage" is the voltage measured at the particular substation during very cold weather in February 1989 and December 1990. In some cases this voltage is about 0.95 pu of 115-kV nominal voltage.

Because much of the load is highly voltage sensitive (e.g., electric space heating), the load shedding time delays are not critical.

References 9 and 65 provide details of the microprocessor-based undervoltage relay installations. Undervoltage load shedding is being extended to the Portland, Oregon load area.

V.2 Methods for Very Large Scale Simulation

BPA and other Puget Sound area utilities prepared "superbase" cases for power flow and dynamic simulation of voltage stability. The cases include expanded subtransmission representation of the Puget Sound area, the Vancouver, British Columbia area, and the western Oregon area (about 2750 busses).

Using the superbase power flow cases, Puget Sound area voltage stability is evaluated by two minute, very large scale dynamic simulations. The simulated system comprises 4960 busses, 8898 branches, 411 generators (fully represented with excitation and prime mover equipment modeling), 573 induction motors (third order models), 719 under-load tap changing (LTC) transformers (discrete taps with limits and deadband), 729 thermostatically-controlled

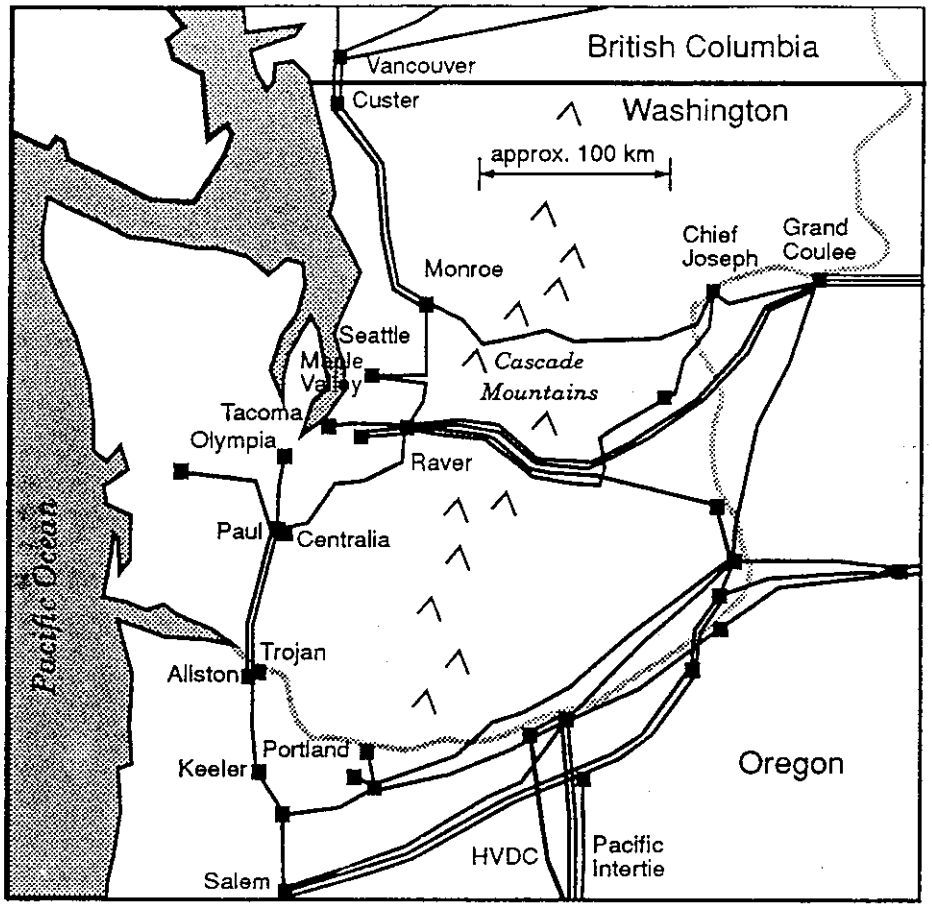

Fig. V-1. Pacific Northwest 500-kV transmission system.

loads. Seven major generators have overexcitation limiters modeled, and two important generators have installed line drop compensation represented. About 50 undervoltage load shedding relays, which may trip either loads or lines with tapped loads, are represented. Extra-heavy loads (one-in-twenty year cold weather conditions) are represented for the 1992–93 winter season.

The computer program used is the EPRI/Ontario Hydro Extended Transient Midterm Stability Program (ETMSP 3.0). The EPRI LOADSYN computer program [44] was used to facilitate load modeling for both power flow and dynamic simulation.

Figure V-1 shows the Puget Sound 500-kV network. The major load-area power plants are the Centralia coal-fired plant (two 811 MVA units) and the 1280 MVA Trojan nuclear plant. Major power plants east of the Cascade Mountains include Chief Joseph and Grand Coulee hydro plants on the Columbia River.

V.3 Simulation of a Major Outage

Referring to Figure V-1, the disturbance simulated is outage of the high capacity, series-compensated, double-circuit Grand Coulee–Raver 500-kV line loaded at 2866 MW. This severe disturbance is outside planning criteria for the extra-heavy load conditions represented.

Case without load shedding. For a case without load shedding, Figure V-2 shows selected 500-kV voltages. The initial synchronizing swings, followed by voltage decay due to tap changing and thermostatic controls, are evident. The case is stable but, at the end of the simulation, 500-kV voltages are about 0.86 per unit or 430-kV (normal voltage levels are 535–545 kV). The voltage drop is over 20%. Most load tap changing transformers regulating load voltage reach their boost limit, and many thermostatically controlled loads are limited to their maximum value (assumed to be 120% of initial value). The Trojan, Centralia, Chief Joseph, and Grand Coulee power plants have field current limiting enforced.

Much of the load is resistive electric space heating. Because of the favorable load characteristics, the system stabilizes with partial voltage collapse. System performance, however, is clearly unacceptable. There is great risk of a blackout caused by power plant or transmission line tripping because of the low voltage, high current conditions. With field current limiting on major generators, there are no remaining reactive power reserves. Furthermore, low generator terminal voltage (because of field current limiting) results in stator current overloads; overload elimination (automatic or manual) would be by reducing power plant output or by tripping the generator, either of which could end in a blackout.

Case with load shedding. Figure V-3 shows corresponding 500-kV voltages with installed undervoltage load shedding modeled. The amount of undervoltage load shedding is 686 MW and 187 MVAr. The minimum 500-kV voltage is now 0.96 pu or 480 kV (about 10% drop). For the same case, Figure V-4 shows some unregulated 115-kV bus voltages. Again, most LTC transformers reach their boost limits and eleven of the thermostatically controlled loads reach their maximum value. Regulated (load) side voltages are about 10% higher. The increases in voltage which can be seen on the plots are due to twelve blocks of load shedding.

About 1100 MW of load shedding remains unused, and provides protection for possible undesirable protective relaying of generators or transmission lines. In the simulation world, the unused undervoltage load shedding provides "protection" against modelling shortcomings.

Figure V-5 shows field current at important generators. After time delay, field current limiting is enforced at the Trojan, Chief J5, Chief J2 and Coulee 51 generators. Centralia is near its maximum field current, but load shedding has prevented significant overload during the simulation duration.

Effect of generator line drop compensation. Sensitivity cases showed that generator line drop compensation installed at the Centralia power plant and the Grand Coulee Third power plant significantly reduced the amount of undervoltage load shedding. Both power plants connect to 500-kV transmission, and compensation in both cases is 50% of the step-up transformer. For the outage described, the line drop compensation reduced load shedding from 1040 MW to 689 MW. Final voltage levels were similar for both cases.

V.4 Conclusions

Undervoltage load shedding is an effective (i.e., cost-effective) means to prevent voltage collapse. It is low cost, and can be made dependable and secure by design. The local, decentralized control means that single failures are not a

problem.

Undervoltage load shedding removes the burden on operators to make rapid decisions to prevent voltage collapse. More risk can be taken in system operation. Note, however, that follow-up operator action is necessary to restore voltages to normal levels.

For all cases, the system is *stable*—even without load shedding. Simple power flow simulation with constant power loads would indicate voltage collapse, even for much less severe disturbances.

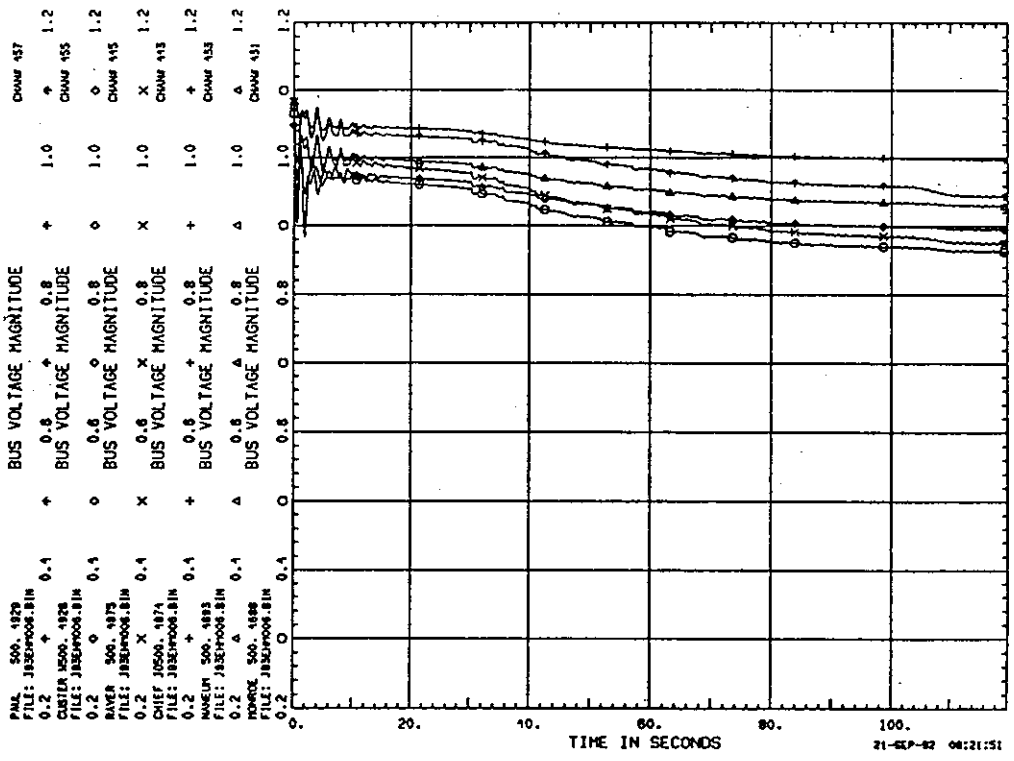

Fig. V-2. 500-kV voltages for Grand Coulee–Raver 500-kV double circuit line outage without load shedding.

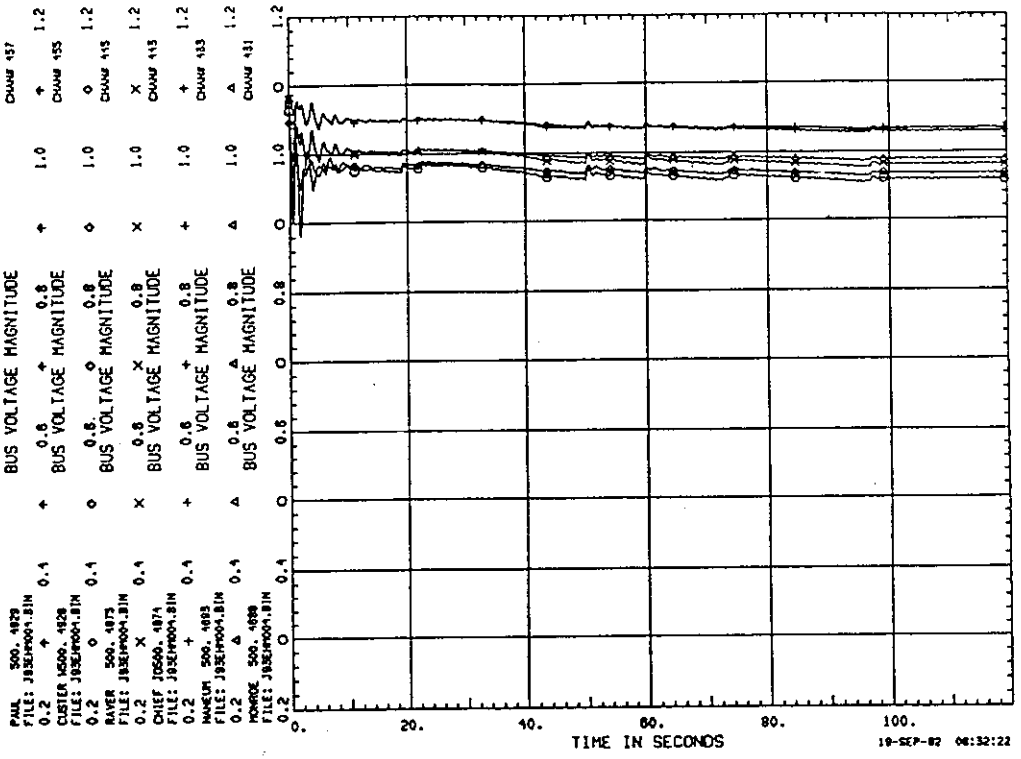

Fig. V-3. 500-kV voltages for Grand Coulee–Raver 500-kV double circuit line outage with load shedding.

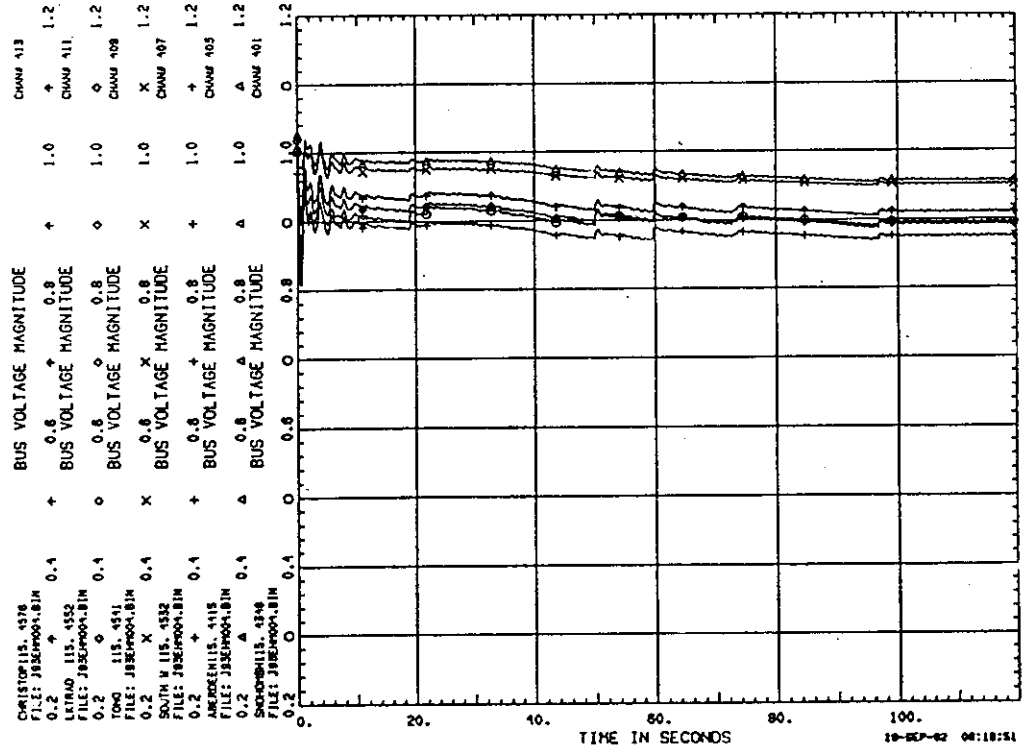

Fig. V-4. 115-kV voltages for Grand Coulee–Raver 500-kV double circuit line outage with load shedding.

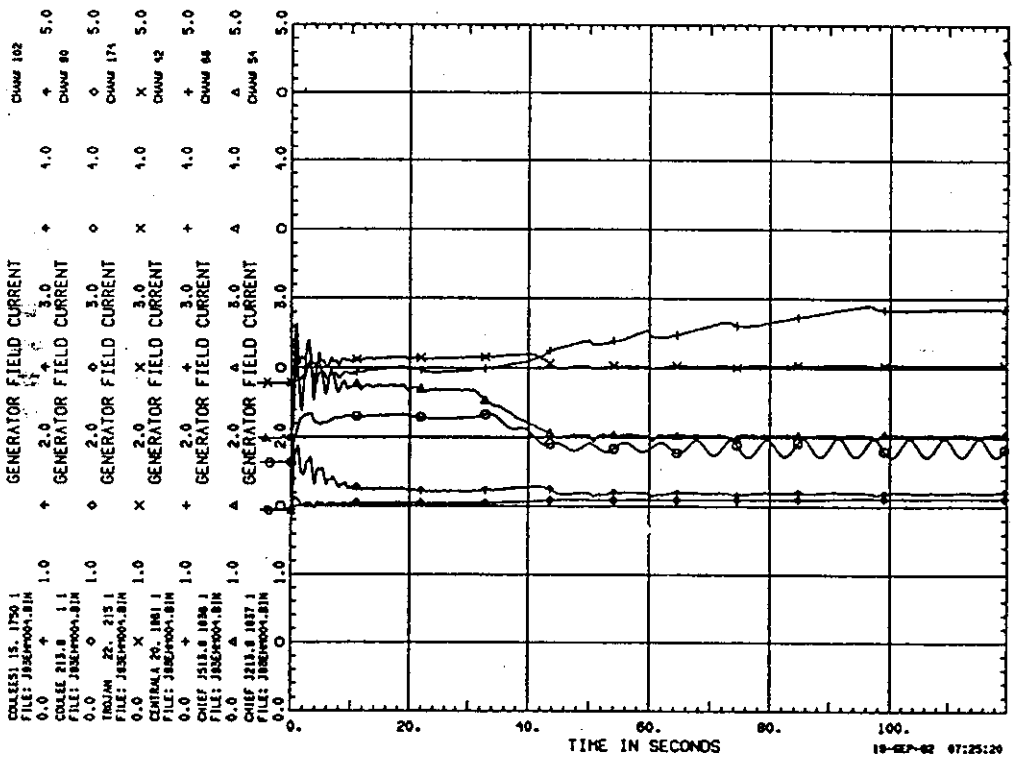

Fig. V-5. Field currents of important generators for Grand Coulee–Raver 500-kV double circuit line outage with load shedding.

Appendix VI, Contribution to Chapter 8
Voltage Stability in Weak Power Systems

F. Aboytes
C.F.E. Mexico

Voltage collapse is a problem directly related to the structure of a system. Therefore, when the structure is weak it is common to observe voltage control problems and voltage instability cases.

A weak power system is characterized by a high sensitivity to changes in active and reactive nodal injections. Generally it is longitudinal, with few lines between major generation and load centers. Usually the system is radial and large distances are involved. As a result, many load nodes are far away from voltage controlled points, and critical operating problems arise when contingencies occur in the system. Table VI-1 presents sensitivity indicators (MVAr/kV) that show the weakness of nodes in a typical longitudinal system. It should be observed the range of reactive injections required to change 1 kV at different voltage levels.

Table VI-1 Sensitivity Indicators (MVAr/kV)

Nodes, 400-kV	SI	Nodes, 230-kV	SI	Nodes, 138-kV	SI
DMT	33	REA	18	MAF	11
LUT	45	CDA	7	LUN	6
EVG	13	LAS	11	MTM	9
TLA	29	AIM	9	YER	12
ORF	12	IRN	5	REA	10

The mechanism of voltage instability has been presented in the main report. However, it is important to stress at this point that in weak power systems usually the phenomenon is very fast (seconds), and once again this fact is related to system structure and load behavior. In a robust system, reactive power changes, due to a changes in load or contingencies, are provided by nearby generators; since in a robust system electrical distances to voltage controlled points are small, this effort (response) is shared by several units.

On the other hand, in a weak system there are few generators to supply the reactive power required by the contingency, and usually the electrical distance to these units is substantial. The result are large voltage deviations, and the possibility of voltage collapse as reactive power is transported from remote sources.

The main difference between the cases presented is that in a robust system the problem is more related to limits and controls of reactive sources, and critical cases arise when limits are enforced. Whereas in weak systems a large voltage deviation is produced by the initial reactive power flow, here voltage instability is very fast and dependent on the load behavior at reduced voltage.

The problem is best appreciated when contingencies are considered. In a robust system the outage of a line or a generator does not appreciably change the distance to voltage controlled points, whereas in a weak system significant changes are obtained when a line is out of service (as normally few lines are available) or when voltage support is lost. In a weak system electrical distances to voltage controlled nodes need to be updated as topology and generation patterns are modified. A drastic change in electrical distance, due to contingencies, makes the system weaker and the speed of voltage collapse phenomenon may increase.

The analysis of particular cases can be performed based on sensitivity indicators, as in Table VI-1, where the effect of contingencies is reflected. The indicators show the effect as nodes become weaker.

The analysis of the radial system shown in Figure VI-1, where a load is supplied through a transmission system of two parallel lines, is an example of common situations found in several areas of a weak system.

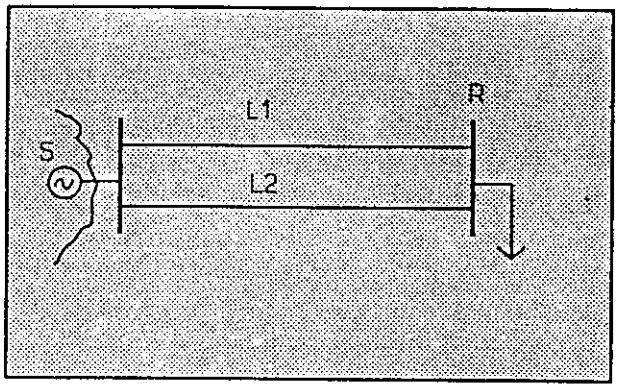

Fig. VI-1. Typical configuration in longitudinal systems.

For the case shown in Figure VI-1, the outage of a line leaves only one line supplying the load; this increases the electrical distance from node R to voltage controlled nodes (S). In this case impedances of lines L1 and L2 are most important in distance calculations.

Conventional *P–V* characteristics can be used to obtain maximum transmission limits for voltage collapse under different system conditions. For a 230-kV system (290 km) with lines L1 and L2 connected, load modelled as constant power with unity power factor, the transmission limit is 320 MW. When power factor is changed to 0.85 lagging, the limit is reduced to 200 MW. For the case with only one line in service, transmission limit is 100 MW. *P–V* characteristics for these cases are shown in Figures VI-2 to VI-4. In the figures the effect of voltage magnitude at the sending end, V_s, is included.

Results show a substantial change in transmission limit as topology and load modelling change. This suggest that preventive measures must be taken to avoid an instability condition. When different load modelling is considered, the transmission limit is modified and it is also common to obtain a substantial

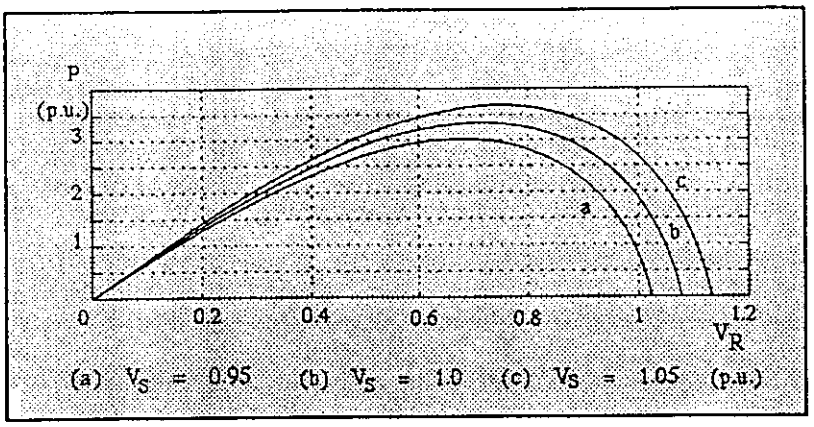

Figure VI-2. *P–V* characteristic for test system (Figure VI-1). Load model: constant power with unity power factor.

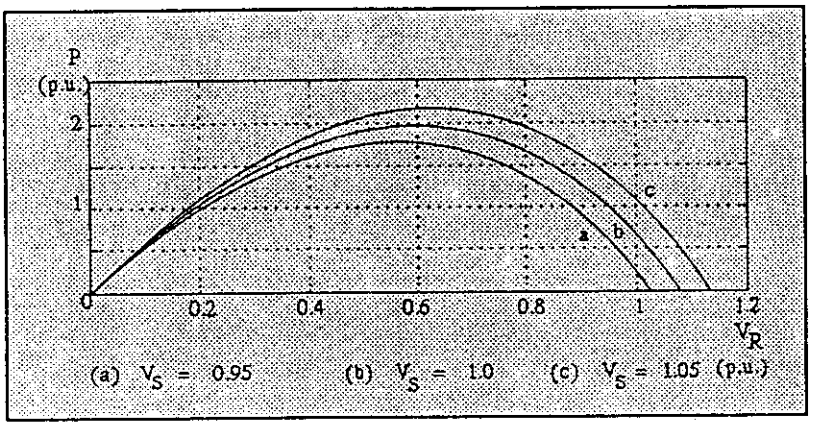

Figure VI-3. *P–V* characteristic for test system (Figure VI-1). Load model: constant power with 0.85 power factor.

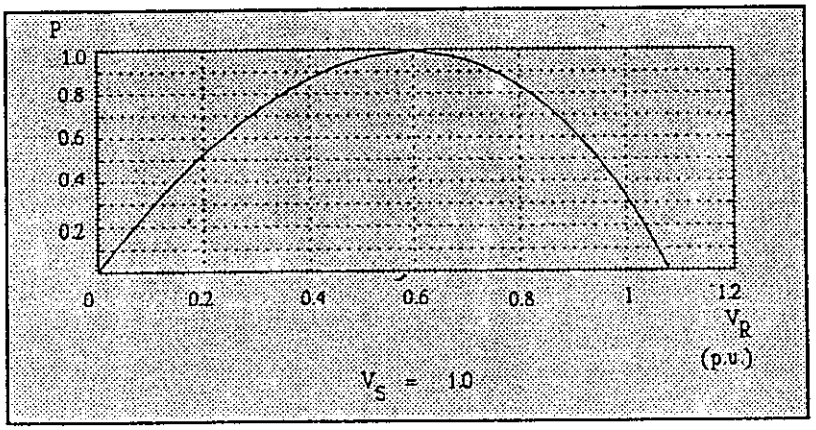

Figure VI-4. *P–V* characteristic for test system with one line out (Figure VI-1). Load model: constant power with 0.85 power factor.

change when topology is altered.

In a more general case, load nodes are connected to several reactive power sources; therefore an equivalent representation is required to obtain electrical distances to voltage controlled points. The main difference with the simple case of Figure VI-1 is that now the problem could be a mixture of synchronous and voltage instability phenomena. In a longitudinal system (Figure VI-5) few reactive power sources need to be considered due to the radial structure.

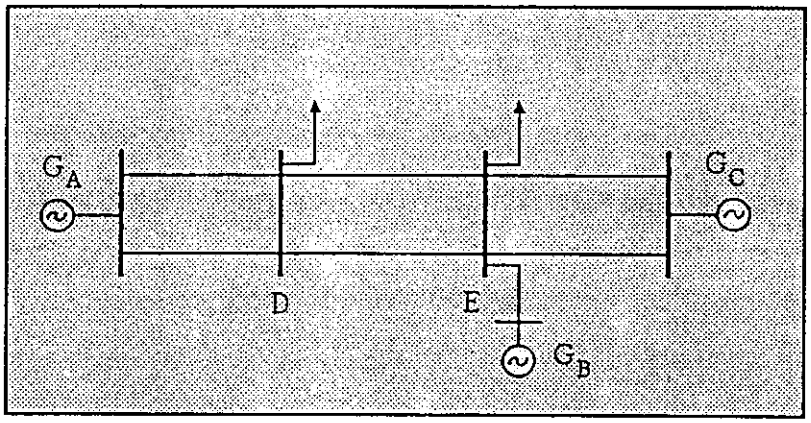

Figure VI-5. Longitudinal system with several reactive power sources.

Voltage control in any point in the system (Figure VI-5) will be dependent on the equivalent impedances to reactive sources (G_A, G_B, G_C). Figure VI-6 shows the equivalent reactive model for node D.

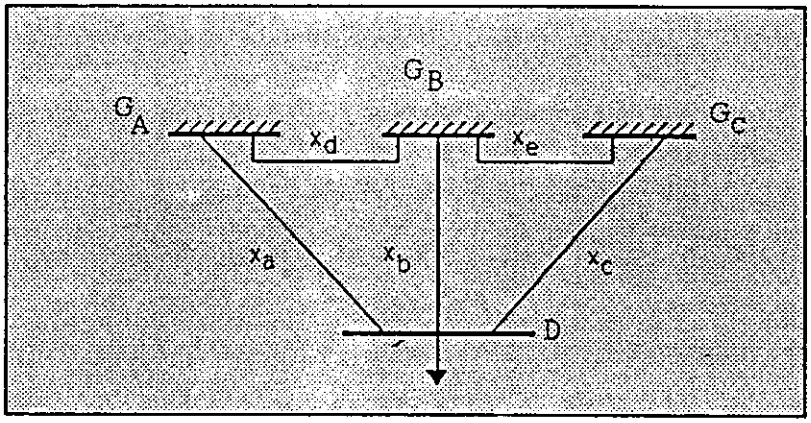

Figure VI-6. Equivalent distance to voltage controlled points.

Figure VI-7 shows the response of a weak system to contingencies in areas where voltage support is weak. In this case voltage collapse develops in the first second after the perturbation. Analysis of the response shows that real and

reactive power flows produced by the contingency causes the decline of voltage up to the point of instability. Critical cases can be caused by single outages of lines and generators, or by faults with delayed clearing.

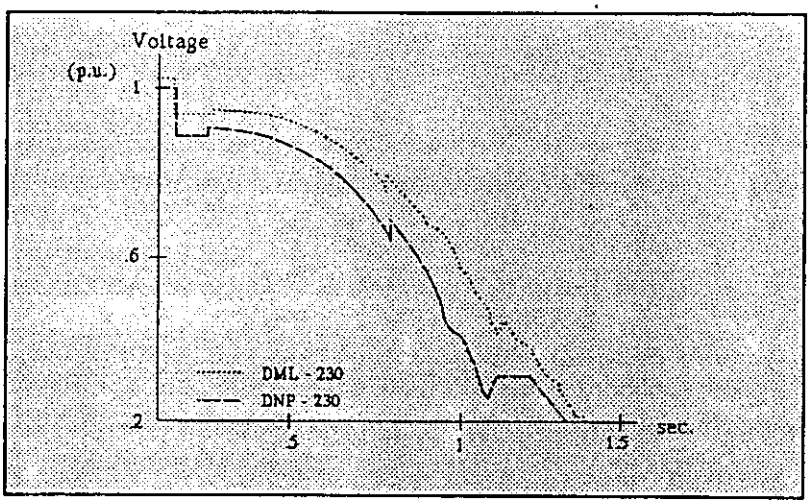

Figure VI-7. Voltage instability in a longitudinal system.

Appendix VI References

1. F. Aboytes, *Reactive Power-Voltage Control in Electrical Power Systems*, CFE, 1991, Book (in Spanish).
2. F. Aboytes, "Voltage Stability in Weak Power Systems," IEEE, RVP-92-SIS-05, pp. 32-40, Acapulco Gro., Mexico, 1992 (in Spanish).

Appendix VII, Contribution to Chapter 8
Sensitivity of Voltage Stability to HVDC Control System Characteristics

A. E. Hammad
NOK, Baden, Switzerland

In this appendix a simplified ac/dc test system is used to demonstrate the sensitivity of transient ac voltage stability to HVDC control system modes and parameters. The simulation results show how the HVDC scheme can force the ac system to a transient voltage instability condition and how to avoid such a condition by adopting a suitable HVDC control strategy.

The test system, partially shown in Figure VII-1, incorporates HVDC transmission connected to two identical ac system equivalents at rectifier and inverter stations. The ac equivalents have a short circuit capacity of 2.5 times the rated dc transmission power. AC filters and shunt capacitors (60% rating) are used for reactive power compensation at both dc terminals.

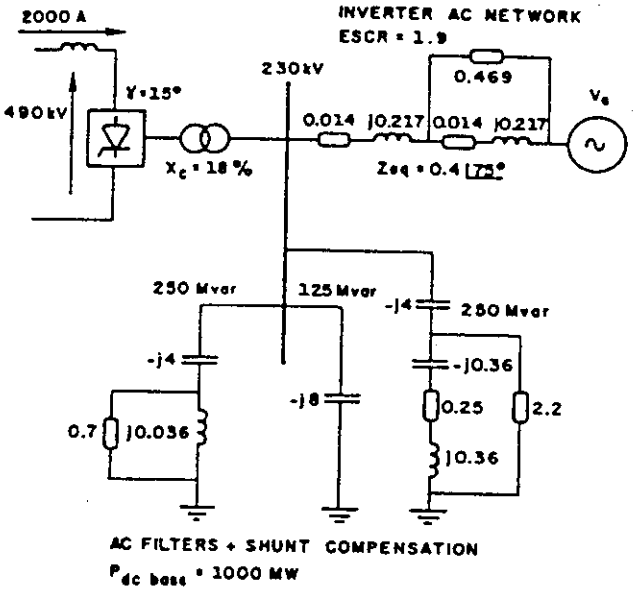

Fig. VII-1. One terminal of studied ac/dc system/

AC system equivalent system impedance values and operating conditions of the HVDC scheme (one per unit power, constant power control at rectifier and constant minimum extinction angle, γ_{min} at inverter) are chosen such that the initial operating point is very close to the critical stability value determined by the voltage stability factor, VSF, shown on Figure VII-2. The VSF index, as defined in reference 35, is the incremental ac voltage variation at the commutating busbar due to a small reactive power change at a given power level. The point of transient voltage instability is identified by the crossing of the VSF from a positive (stable) to a negative (unstable) value. The VSF index include

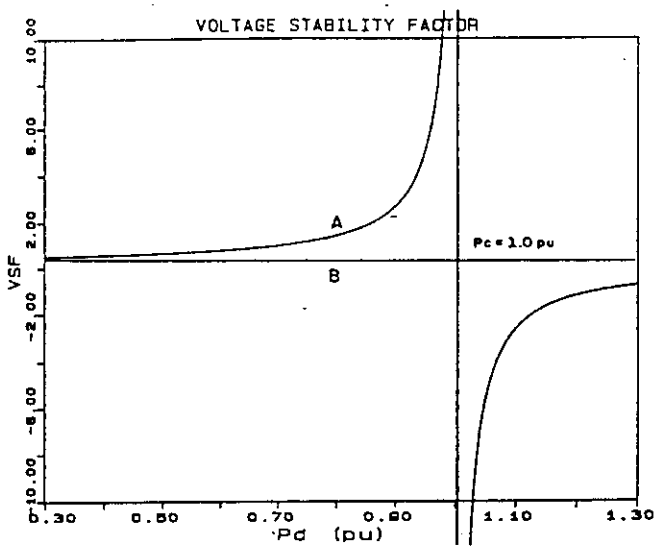

Fig. VII-2. Voltage Stability Factor for ac.dc system. Curve A: inverter with γ_{min} control. Curve B: inverter with V_d control.

the effects of all system components existing at the ac/dc interconnection (converters, converter transformers, ac network, filters, shunt compensation, etc.) as well as the HVDC control system mode and parameters. These effects are expressed in terms of incremental Q/V dynamic characteristics of each system component. In simple terms, the VSF equals the inverse of the summation of all $\Delta Q/\Delta V$ dynamic characteristics.

Figure VII-3 depicts the $\Delta Q/\Delta V$ dynamic characteristics for:

(A) HVDC scheme with rectifier operating with power control and inverter operating with γ_{min} control;

(B) same as (A) but rectifier operating with dc voltage control;

(C) same as (A) but rectifier operating with current control;

(D) AC system including filters and shunt capacitors.

In Figure VII-3 note that control mode (A) corresponds to a negative contribution to voltage stability whereas modes (B) and (C) improve it, particularly mode (B).

Curve A in Figure VII-2 is the result of characteristics (A) and (D) in Figure VII-3, and curve B is the result of characteristics (B) and (D).

Time simulation of the test system are used to further demonstrate the effect of various HVDC control schemes on the transient ac voltage stability phenomena. A 20% power order step is applied (t = 0.62 seconds) to the HVDC controller input. Figure VII-4 shows the system response when the HVDC controls correspond to mode (A) above.

In Figure VII-4, although the dc power increases to a maximum value (t = 0.66 seconds) a voltage collapse process follows with the dc current further

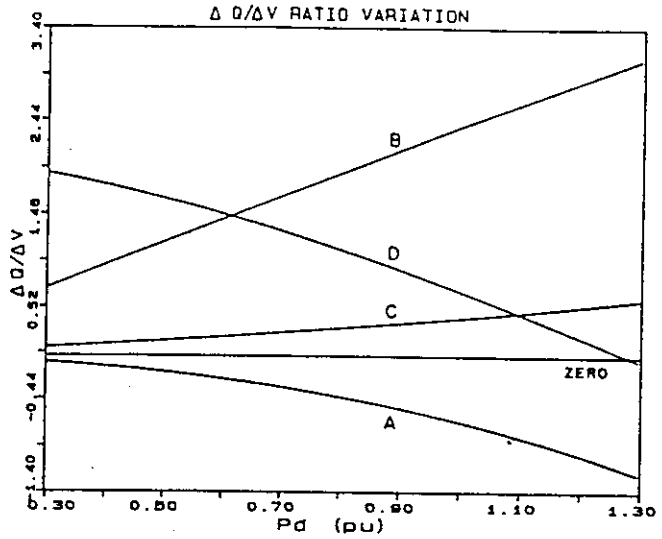

Fig. VII-3. Incremental Q/V dynamic characteristics. (A): rectifier P_d, inverter γ_{min} controls. (B): rectifier P_d, inverter V_d controls. (C): rectifier I_d, inverter γ_{min} controls. (D): ac system including shunt compensation.

increasing due to the action of the power controller. Commutation failure results on account of the system reaching an unacceptable operating condition.

If the HVDC controller is provided with a dc current limiter, the voltage collapse process ceases when such a limiter is activated as shown in Figure VII-5. At such condition, the dc system operates in a mode similar to (C) above, i.e., switches from power to current control mode which is slightly more stable. Note that the ac/dc system in this case operates in a rather deteriorated condition. An action provoked by a voltage-dependent current order limiter control would produce a similar result.

One solution to completely avoid voltage instability in this case is to enforce the ac system infeed at the HVDC inverter terminal by increasing the short circuit capacity, e.g., by ac line addition or employing synchronous condensers or by adding static VAr compensators. Another solution is to adapt a non-classical HVDC control strategy, such as (B) above. In both solutions additional costs are involved. However, in many practical cases the economics favor the latter solution.

Figure VII-6 shows the system response for the same disturbance as in Figures VII-4 and VII-5, but with a dc voltage control mode (B) at the HVDC inverter terminal. Note how the system operates stably with a higher dc power transfer level

A similar transient voltage instability condition arises when attempting to recover the dc power fast following a severe ac system disturbance as shown in Figure VII-7 for control strategy (A). To avoid voltage collapse, the dc power recovery is delayed as shown in Figure VII-8a. Adopting the control strategy (B), however, enables a fast and stable recovery as shown in Figure VII-8b.

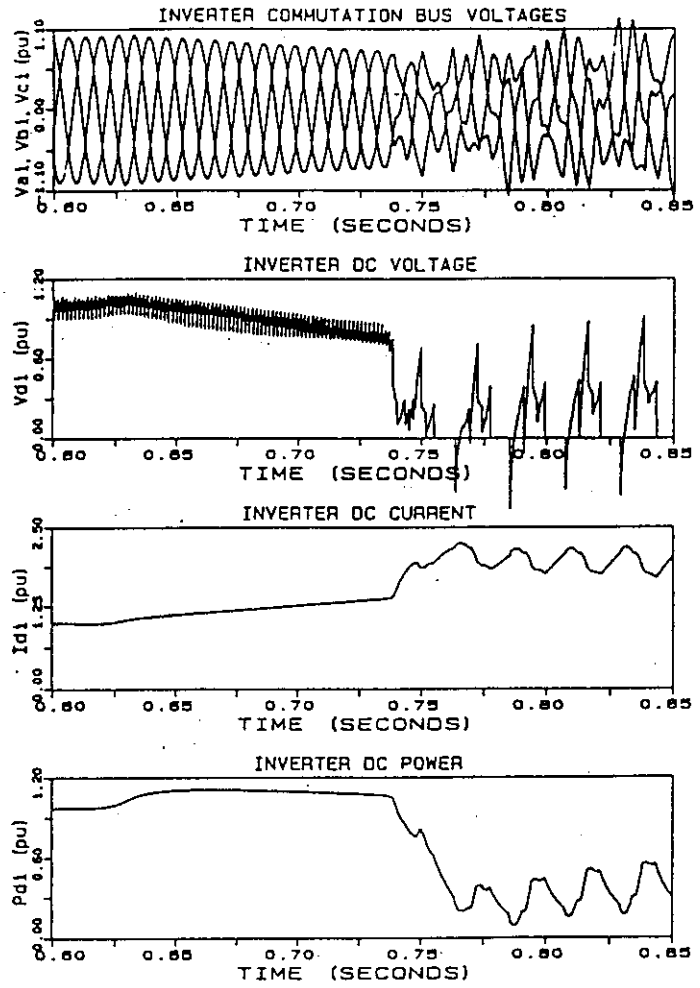

Fig. VII-4. Response for 20% power order step. HVDC with control mode (A).

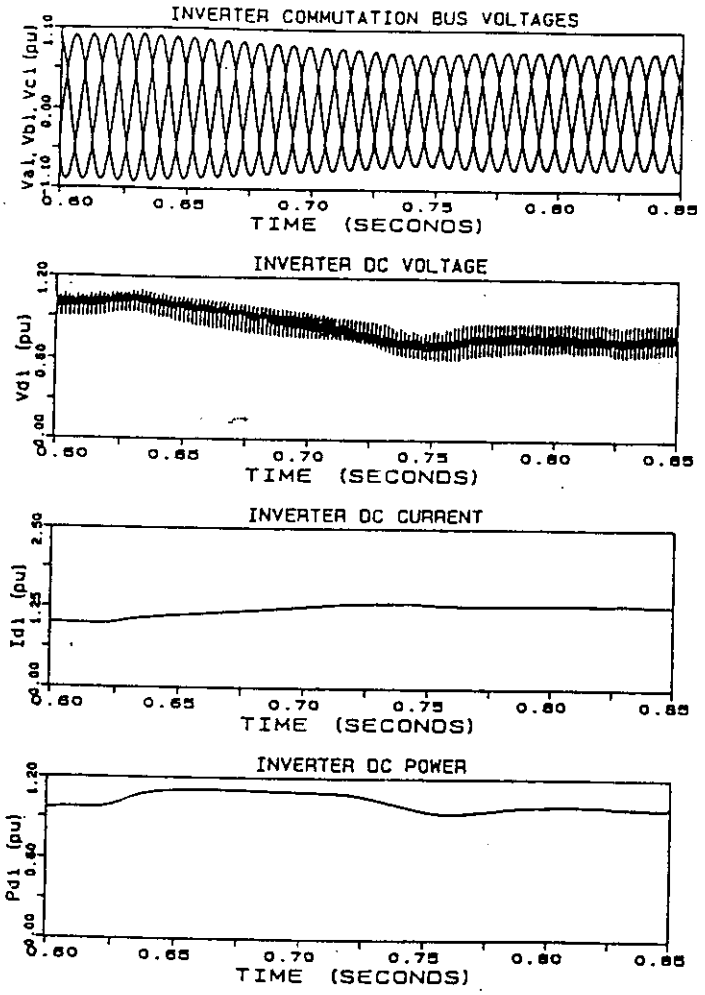

Fig. VII-5 Response for 20% power order step. HVDC with control mode (C).

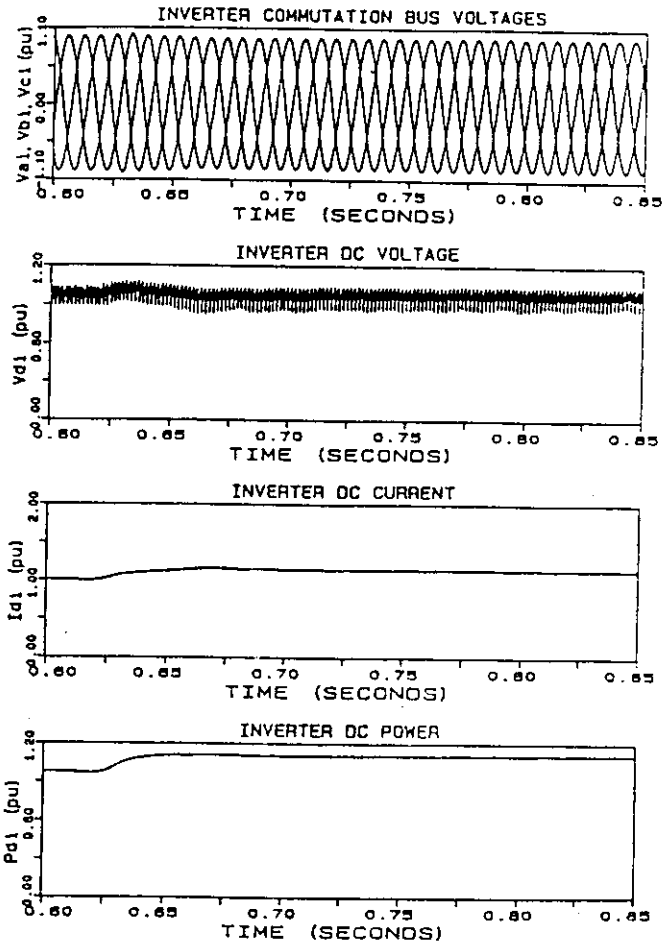

Fig. VII-6. Response for 20% power order step HVDC with control mode (B).

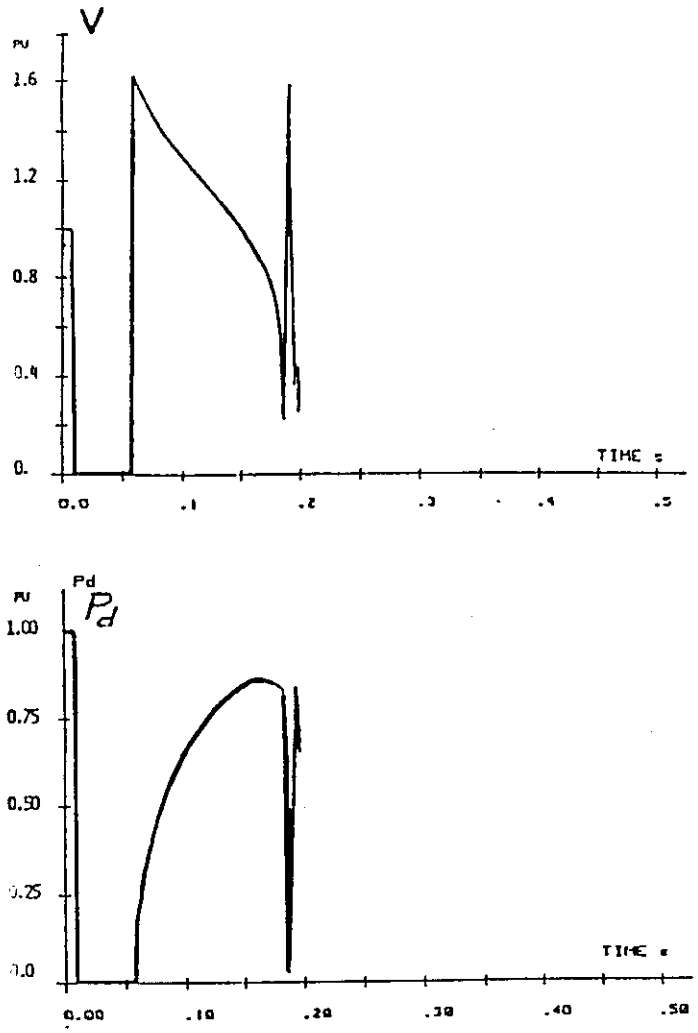

Fig. VII-7. HVDC recovery with control mode (A). Fast recovery time

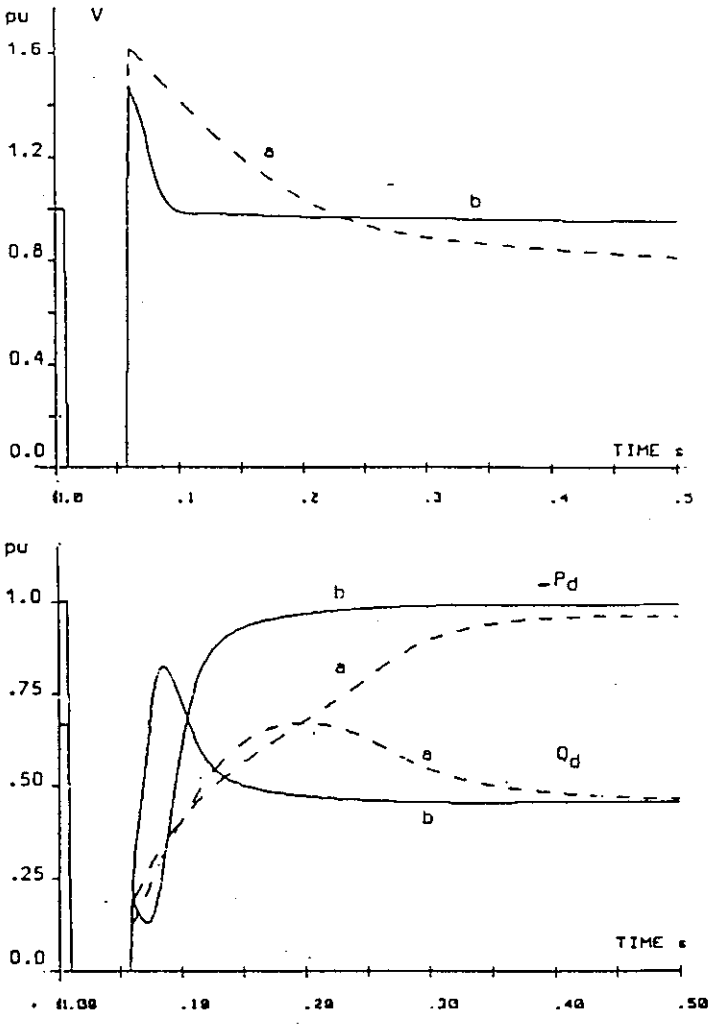

Fig. VII-8. HVDC recovery. Curve a: with control mode (A), delayed recovery. Curve b: with control mode (B), fast recovery.

Appendix VIII, Voltage Collapse Incidents

Table VIII-1—Voltage Collapse Incidents

Date	*Location*	*Time Frame*	*References*
11/30/86	SE Brazil, Paraguay	2 seconds	4, 5
5/17/85	South Florida	4 seconds	1, 3
8/22/87	West Tennessee	10 seconds	6, 7
12/27/83	Sweden	50 seconds	1, 2
9/22/77	Jacksonville, Florida	few minutes	8
9/2/82	Florida	1–3 minutes	9, 10
11/26/82	Florida	1–3 minutes	9, 10
12/28/82	Florida	1–3 minutes	9, 10
12/30/82	Florida	2 minutes	9, 10
12/9/65	Brittany, France	?	11
11/10/76	Brittany, France	?	11
8/4/82	Belgium	4.5 minutes	12
1/12/87	Western France	4–6 minutes	1, 20
7/23/87	Tokyo	20 minutes	1
12/19/78	France	26 minutes	1, 11, 14
8/22/70	Japan	30 minutes	19

Table VIII-2—Voltage Incidents Without Collapse

Date	*Location*	*Time Frame*	*References*
5/21/83	Northern California	2 minutes	1, 15
5/20/86	England	5 minutes	16
9/22/70	U.S., New York state	several hours	1, 17
7/20/87	U.S., Illinois and Indiana	hours	6
6/11/84	Northeast U.S.	hours	18

Appendix VIII references

1. IEEE Committee Report, *Voltage Stability of Power Systems: Concepts, Analytical Tools, and Industry Experience*, IEEE/PES 90TH0358-2-PWR, 1990.
2. K. Walve, "Modeling of Power System Components at Severe Disturbances," *CIGRE* paper 38-18, 1986.
3. D. McInnis, "South Florida Blackout," unpublished Florida Power & Light report.
4. IEEE Committee Report, "HVDC Controls for System Dynamic Performance," *IEEE Transactions on Power Systems*, Vol. 6, pp. 743–752, May 1991.
5. H. Arakaki, J. C. Lopes, and A. A. S. Praca, "Itaipu HVDC Transmission System—Analysis of Control System and Protection Performance after Two Years of Operation," paper SP-25, *Proceedings of 1st Symposium of Specialists in Electric Operational Planning*, Rio de Janeiro, August 17–21, 1987.

Describes disturbance on November 30, 1986. After several ac system outages,

the São Roque inverter ac voltage dropped instantaneously to 0.85 pu for several seconds. Repetitive commutation failures occurred and dc power control increased dc current which increased converter reactive consumption. A complete dc system shutdown and an ac breakup resulted. Over 1,200 MW of load was shed. This and other disturbances led to several dc control changes.

6. North American Electric Reliability Council, *1987 System Disturbances*, July 1988
7. G. C. Bullock, "Cascading Voltage Collapse in West Tennessee, August 22, 1987," *Proceeding of 17th Annual Western Protective Relay Conference*, Spokane, Washington, October 1990.

Describes a 78-cycle phase-to-phase arcing 115-kV bus fault in Memphis, Tennessee that resulted in 161-kV and 500-kV system voltages between 75% and 82% of normal for about 10 seconds after fault clearing. The prolonged voltage depression was because of heavy reactive requirements of motor loads. Zone 3 relays operated and cascading resulted. Load loss was 1265 MW.

8. W. R. Lachs, IEEE Voltage Instability Task Force correspondence, October 18, 1985.

Describes and analyses a series of voltage collapses in Jacksonville, Florida on September 22, 1977. The collapses involved unit trips, field current limiting, manual load shedding, and other phenomena.

9. North American Electric Reliability Council, *Review of Selected Major Bulk Power System Disturbances in North America—1982.*
10. IEEE Committee Report, "VAR Management—Problem Recognition and Control," *IEEE Transactions on Power Apparatus and Systems*, vol. PAS-103, no. 8, pp. 2108–2116, August 1984.

Describes disturbances in Florida on September 2, 1982, November 26, 1982, December 28, 1982 and December 30, 1982. All disturbances were initiated by loss of large generator units in central or southern Florida. Because of the increased imports, voltages deteriorated, with separations after one to three minutes. The islanding was followed by underfrequency load shedding of about 2000 MW. These disturbances led to installation of shunt reactor and shunt capacitor switching by voltage relays at several 230-kV substations.

11. C. Barbier and J-P Barret, "Analysis of Phenomena of Voltage Collapse on a Transmission System," *Revue Generale de l'electricite*, vol. 89, October 1980, pp. 672-690.
12. A. J. Calvaer and E. Van Geert, "Quasi Steady State Synchronous Machine Linearization Around an Operating Point and Application," *IEEE Transactions on Power Apparatus and Systems*, vol. PAS-103, no. 6, pp. 1466–1479, June 1984.
13. A. Cheimanoff and C. Curroyer, "The Power Failure of December 19, 1978," *Revue Generale de l'electricite*, vol. 89, April 1980, pp. 280–320.
14. J. A. Casazza, Interim Report on the French Blackout of December 19, 1978, DOE report, February 8, 1979.
15. R. H. Vierra, "Reactive Power and Voltage Control in Western System," presented at IEEE/PES summer meeting, Vancouver, July 16, 1985.

Discusses incident on May 21, 1983 when voltages along Pacific AC Intertie were severely depressed about two minutes after a Pacific HVDC Intertie bipolar outage (1286 MW). The initial Pacific AC Intertie loading was 2240 MW and the lowest voltage was 385-kV at Vaca-Dixon 500-kV substation. The low volt-

age caused tripping of pumps at various aqueduct stations.

16. M. G. Dwek, CIGRE Study Committee 38 discussion, 1988.

Describes near voltage collapse in England on May 20, 1986. During a thunderstorm six 400-kV circuits were lost within one minute. Voltage decayed progressively over a five minute period, with 352 kV recorded at the lowest point. Within 5 minutes, 1000 MW of gas turbines were brought on line to restore voltages. Predictions were that voltage collapse should have resulted—speculation is that interaction of tap changers with different timer settings slowed the voltage decay, allowing time for operator action.

17. General Electric Company, *Long-Term Power System Dynamics*, Phase III, EPRI Final Report EL-983, May 1982.

Describes voltage declines and fluctuations across New York state over several hours on September 22, 1970. At 1545, voltage at a 345-kV bus was 318 kV—when voltage fell another 6 kV, operators shed 200 MW of load.

18. North American Electric Reliability Council, *1984 System Disturbances*, p. 24.

Describes low voltages in Northeast United States on June 11, 1984. Cause was combination of abnormally high loads, planned outages, and forced outages. Despite voltage reductions and use of available shunt capacitors, the west-to-east transfers in PJM and NYPP imports from Canada had to be reduced to keep within voltage and reactive precontingency limits.

19. T. Nagao, "Voltage Collapse at Load Ends of Power Systems," *Electrical Engineering in Japan*, vol. 95, no. 4, 1975.

20. Y. Harmand, et al., "Analysis of a Voltage Collapse Incident and Proposal for a Time-Based Hierarchical Containment Scheme," *CIGRE* paper 38/39-02, 1990.

Le CIGRÉ a apporté le plus grand soin à la réalisation de cette brochure thématique numérique afin de vous fournir une information complète et fiable.

Cependant, le CIGRÉ ne pourra en aucun cas être tenu responsable des préjudices ou dommages de quelque nature que ce soit pouvant résulter d'une mauvaise utilisation des informations contenues dans cette brochure.

Publié par le CIGRÉ
21, rue d'Artois
FR-75 008 PARIS
Tél. : +33 1 53 89 12 90
Fax : +33 1 53 89 12 99

The greatest care has been taken by CIGRE to produce this digital technical brochure so as to provide you with full and reliable information.

However, CIGRE could in any case be held responsible for any damage resulting from any misuse of the information contained therein.

Published by CIGRE
21, rue d'Artois
FR-75 008 PARIS
Tel : +33 1 53 89 12 90
Fax : +33 1 53 89 12 99